Temporal and Longitudinal Extent of Surface Coal Mining Influences on Water Quality and Benthic Macroinvertebrate Communities in Central Appalachian Headwater Streams

Thomas Raymond Cianciolo

Thesis submitted to the faculty of the Virginia Polytechnic Institute and State University in partial fulfillment of the requirements for the degree of

Master of Science

In

Forest Resources and Environmental Conservation

Daniel L. McLaughlin

Stephen H. Schoenholtz

Carl E. Zipper

David J. Soucek

May 7th, 2019

Blacksburg, VA

Keywords: surface coal mining, salinity, benthic macroinvertebrates, trace elements, specific conductance, bioaccumulation, selenium

Temporal and Longitudinal Extent of Surface Coal Mining Influences on Water Quality and Benthic Macroinvertebrate Communities in Central Appalachian Headwater Streams

Thomas Raymond Cianciolo

Abstract (Academic)

Increased loading of dissolved ions (salinization) and trace elements from surface coal mining is a common alteration to headwater streams in the central Appalachian region. However, temporal and spatial trends of water quality and associated influences on biota in these stream systems have not been well-studied. To address this research need, I analyzed temporal trends in specific conductance, ion matrix, and benthic macroinvertebrate communities in 24 headwater streams, including 19 influenced by surface mining, from 2011-2019. There was limited evidence of recovery of water chemistry or macroinvertebrate communities in these streams, indicating lasting impacts from surface coal mining. Among benthic macroinvertebrates, Ephemeroptera and the scraper functional feeding group were most-impacted by chronic salinization in study streams. In addition, I analyzed spatial patterns of water chemistry in a subset of these streams using synoptic sampling of multiple constituents under baseflow and highflow conditions. Study results indicate that water chemistry is spatially dynamic and can be influenced by both groundwater dilution and inputs from tributaries. Lastly, I investigated patterns in selenium bioaccumulation across and within streams, from particulate matter to top trophic levels (i.e. fish and salamanders). I found that benthic macroinvertebrates had the highest concentrations of selenium in these ecosystems, with lower concentrations in salamander and fish species. However, there was limited evidence of longitudinal trends in bioaccumulation dynamics downstream of mining impacts. Collectively, this work indicates long-term (ca. decades) coal-mining influences but also highlights future research needs to better understand downstream impacts to water quality and biotic communities.

Temporal and Longitudinal Extent of Surface Coal Mining Influences on Water Quality and Benthic Macroinvertebrate Communities in Central Appalachian Headwater Streams

Thomas Raymond Cianciolo

Abstract (public)

Surface coal mining affects water quality in central Appalachian headwater streams. However, long-term and downstream patterns of impacted water quality and potential effects on aquatic life have not been well-studied. To address this research need, I analyzed trends in water quality parameters and aquatic insect communities in 24 headwater streams from 2011-2019. There was limited evidence of recovery of water chemistry or aquatic life in these streams, indicating lasting impacts from surface coal mining. Certain aquatic insects including Ephemeroptera (mayflies) appear to be more impacted than others by long-term altered water quality. In addition to trends over time, I also analyzed downstream variation in water chemistry in a subset of these streams under baseflow conditions and after a rain event. Results indicate that water chemistry can vary greatly within a stream network and is influenced by tributary inputs and dilution from groundwater. Concentrations of the trace element selenium can also be elevated as a result of surface mining. This is of environmental concern because selenium can biomagnify, where concentrations increase in organisms higher in the food chain and can cause toxic effects. Here, I investigated selenium bioaccumulation patterns across organisms in the food chain and with distance downstream across six headwater streams. I found that aquatic insects had the highest concentrations of selenium, with lower concentrations in salamanders and fish. This work indicates that surface coal mining has long-term (ca. decades) effects on headwater streams, but also points to future research to better understand downstream impacts to water quality and aquatic life.

ACKNOWLEDGEMENTS

When I first started at Virginia Tech two years I ago, I had no idea where it might take me. I'm so glad it took me to the coalfields of southwestern VA and southern WV. I had the unique opportunity of experiencing a new part of the country, improving my research skills in the field and in the lab, and meeting lots of amazing people along the way. I could not have completed this thesis without the help of countless people whom I try to thank below.

First of all, I would like to thank my co-advisors Stephen Schoenholtz and Daniel McLaughlin for taking me on as a student and for mentoring me along my journey. I could not have asked for a better pair of advisors and I will miss our weekly meetings. Special thanks for reading my thesis more times than I did and providing thoughtful, in-depth comments and suggestions. I could not have done the research I did without the two of you guiding me along the way! Thanks also to Carl Zipper and Dave Soucek for being outstanding committee members who always made an effort to see what I was up to. I look forward to working with you in the future!

Of course, none of this work would have been possible without the dedication of Tony Timpano who found the study sites and trained me both in the lab and the field. It has been a pleasure building off the research you started, and I would like to thank you for letting me part of it. I will miss our long conversations in the F-150 driving across the coalfield. Thanks for showing me the best restaurants in the coalfield including Asia café in Norton, VA and "The Hat" in Grundy, VA. I would also like to thank Kriddie Whitmore for laying the foundation for my selenium bioaccumulation research. I'm so thankful that I did not have to develop all the laboratory methods that I know you spent months working on. Thanks also for helping me in the field this past summer!

A large part of why I loved the field work aspect of my research were the incredible people who volunteered their time to help and learn alongside me. Special thanks to my family members (Paul, Owen, Mom, & Dad) who drove up from Knoxville, TN on several occasions to help me. Thanks to all the others who helped me despite thunderstorms, snow, stinging nettle, and horrible roads: Rachel Pence, Tony Timpano, Stephen Schoenholtz, Daniel McLaughlin, Liz Sharp, Ary James, Cassidy Quistorff, Mira Chaplin, Jack Ferrell, and Ferry Buchanan.

Collecting field samples is an important part of my research but without the assistance and expertise of many people in the lab, I would not have had any data to analyze. Dave Mitchem deserves a big thank you for showing me how to use the microwave digestion unit, acid-wash dishes, and stay safe working in the lab. Thank you, McAlister Council-Troche, for letting me freeze dry all my samples and developing a selenium speciation method. Lastly, I would like to thank Zenah Orndorff for spending countless hours at the ICP-MS running all my samples.

Lastly, I would like to thank my wife Cassidy for supporting me throughout my time at Virginia Tech. We went through some big life changes over the past two years and your love and encouragement were unwavering despite living apart for a year and the stresses of organizing a wedding. Thanks for being my best friend, true companion, and fellow Hokie.

TABLE OF CONTENTS

LIST OF FIGURES

LIST OF TABLES

CHAPTER 1 – INTRODUCTION

BACKGROUND

Surface coal mining activities are a major driver of land-use change in the central Appalachian coalfield region of the U.S. (Sayler 2008), which is a well-documented terrestrial and aquatic biodiversity hotspot in North America (Stein et al. 2000). To date, roughly 5,900 km^2 (3.5%) of forestland in central Appalachia has been converted to surface-mining with an annual increase of approximately 87 km^2 yr^{-1} (Pericak et al. 2018). Surface mining activities in central Appalachia generally start with deforestation followed by exposure of buried coal seams by removing overlaying bedrock layers using explosives and earth-moving equipment (USEPA 2011). Until recently, the waste rock, or overburden, produced during this process was often deposited in adjacent valleys. Consequently, headwater streams can be buried under tens to hundreds of meters of waste rock. The once-buried overburden, now brought near the surface and exposed to air and water, rapidly weathers increasing loading of dissolved ions to headwater streams. In addition to water chemistry impacts, surface mining also affects hydrology of headwater streams, often causing higher average baseflows and increased peak discharge during storm events compared to reference conditions (Bernhardt and Palmer 2011). Consequently, surface-mining can strongly influence water quality and biological communities in headwater streams draining these impacted areas (USEPA 2011). Moreover, surface mining impacts to the chemistry of headwater streams and resultant negative effects on benthic macroinvertebrates can persist long after the mining activities terminate (Evans et al. 2014, Pond et al. 2014, Timpano et al. 2018b), highlighting the need for research addressing the long-term effects of altered headwater stream chemistry on aquatic biota.

SALINITY

Surface coal mining is a major contributor to increased concentrations of dissolved inorganic salts (i.e. salinity) in headwater streams in central Appalachia because of accelerated weathering of deposited overburden (Griffith et al. 2012). A characteristic of the predominant geology in the central Appalachian coalfield is initial oxidation of pyrite that often produces acids being rapidly neutralized by carbonates and other minerals, resulting in alkaline (pH >7) drainage waters (Clark et a. 2018). This alkaline drainage is enriched in dissolved major ions dominated by sulfate (SO_4^{2-}), bicarbonate (HCO_3^-), calcium (Ca^{2+}), and magnesium (Mg^{2+}) (Palmer 2010, Pond et al. 2008, Timpano et al. 2015). Consequently, total dissolved solids (TDS) and its commonly measured surrogate, specific conductance (SC), are elevated in surface mining-influenced streams compared to reference conditions. Previous work has shown sustained increases in salinity for decades following mining activities (Evans et al. 2014, Pond et al. 2014). In addition, there can be substantial variation in water chemistry within headwater stream networks and over shorter time scales (Timpano et al. 2018a, Johnson et al. 2019). For example, highflow conditions can access new sources of dissolved ions, while also increasing dilution from tributaries and groundwater (Zimmer et al. 2013). A more common pattern,

however, is short-term dilution under high flows, seasonal dilution during cold-weather months, and relatively high concentrations during lower-flow conditions of the late summer and early fall (Timpano et al. 2018a). In addition, biogeochemical transformations (e.g. changing redox conditions) can also influence concentrations of certain constituents (Tiwari et al. 2017). As a result, water quality downstream of mined areas is highly dynamic over time and space, highlighting a research need to better understand both long-term and downstream impacts of surface coal mining (Johnson et al. 2019).

BENTHIC MACROINVERTEBRATES

It is well-documented that increased concentrations of dissolved ions have negative impacts on condition of aquatic biota in headwater streams influenced by surface mines (Merricks et al. 2007; Pond et al. 2008, 2014; Boehme et al. 2016, Timpano et al. 2015, 2018b). Specifically, benthic macroinvertebrates have been used to assess such negative impacts because of their important ecological role in nutrient cycling and as a food source (Wallace and Webster 1996), as well as their integration of time-varying water chemistry and habitat conditions (Barbour et al. 1999). Such assessments of benthic macroinvertebrate community structure in streams with elevated salinity have shown reduced taxonomic richness and communities shifted to more tolerant taxa (Pond et al. 2008, 2014, Timpano et al. 2018b). Much of this loss in diversity comes from the relatively high sensitivity of Ephemeroptera (mayflies) and the scraper functional feeding group to elevated salinity (Merricks et al. 2007, Pond et al. 2008, 2014, Timpano et al. 2018b). However, it is likely that water chemistry in surface mining-influenced streams will change over time as overburden continues to weather (Clark et al. 2018), as could the relationship between benthic macroinvertebrates and measured water quality. These potential recovery dynamics are largely unknown, highlighting the need for a long-term, coupled study of SC and attendant response of benthic macroinvertebrate communities.

SELENIUM

Elevated levels of the trace element selenium (Se) have been found in streams influenced by surface mining in the central Appalachian coalfield (EPA 2011). Although Se contributes minimally to TDS, this trace element can bioaccumulate in the aquatic food chain (USEPA 2016) with toxic effects, particularly to egg-laying aquatic vertebrates (Young et al. 2010). Selenium is a naturally occurring trace element in the sedimentary rocks underlying central Appalachia, where it can substitute for sulfur in pyrite (Tuttle et al. 2009) and organic sulfur in coal layers (Coleman et al. 1993). Selenium is released to the water column as oxyanions (i.e. selenate and selenite) when weathering overburden is oxidized (Lussier et al. 2003). Water-column Se can be stored in stream particulate matter (e.g. biofilm and leaf detritus) or utilized by primary producers (Luoma and Presser 2009). Benthic macroinvertebrates can further biomagnify Se when they consume primary producers or particulate matter (Whitmore et al. 2018), with likely, but less observed, continued biomagnification into higher trophic levels (i.e. fish and salamanders). Site-specific factors such as water residence time, speciation of Se, and characteristics of biotic communities can influence uptake of Se. Despite the known risk of

elevated Se to aquatic systems, there has been little research conducted to study transport of Se from its origin below mined areas to downstream waters or the degree to which it bioaccumulates in top trophic levels of headwater streams (Presser 2013).

NEED FOR STUDY

Surface coal mining has been shown to impact water chemistry and aquatic life negatively in headwater streams in the central Appalachian coalfield region. Despite the known consequences of surface-mining, there is a gap in our understanding of the temporal and spatial impacts of this land disturbance on receiving downstream waters. A long-term field study addressing recovery of headwater streams and more detailed spatial analysis in field sites is needed to improve our understanding of surface mining impacts while also informing regulation and management.

OBJECTIVES

In this thesis, I assess temporal and spatial impacts of surface coal mining on headwater streams in the central Appalachian coalfield. Chapter 2 addresses two primary objectives by evaluating: 1) long-term temporal trends in water chemistry and benthic macroinvertebrate communities, and 2) spatial and flow-driven variability of water chemistry. Chapter 3 assesses within- and across-site variation in Se bioaccumulation from water column to fish in a subset of the streams studied in Chapter 2. Chapter 4 provides a summary and conclusions for my work.

LITERATURE CITED

Barbour, M. T., Gerritsen, J., Snyder, B. D., & Stribling, J. B. (1999). *Rapid bioassessment protocols for use in streams and wadeable rivers: periphyton, benthic macroinvertebrates and fish* (2nd ed., p. 339). Washington, DC: US Environmental Protection Agency, Office of Water.

Bernhardt, E. S., & Palmer, M. A. (2011). The environmental costs of mountaintop mining valley fill operations for aquatic ecosystems of the Central Appalachians. *Annals of the New york Academy of Sciences*, *1223*(1), 39-57.

Boehme, E. A., Zipper, C. E., Schoenholtz, S. H., Soucek, D. J., & Timpano, A. J. (2016). Temporal dynamics of benthic macroinvertebrate communities and their response to elevated specific conductance in Appalachian coalfield headwater streams. *Ecological Indicators*, *64*, 171-180.

Clark, E. V., Daniels, W. L., Zipper, C. E., & Eriksson, K. (2018). Mineralogical influences on water quality from weathering of surface coal mine spoils. *Applied Geochemistry*, *91*, 97-106.

Coleman, L., Bragg, L. J., & Finkelman, R. B. (1993). Distribution and mode of occurrence of selenium in US coals. *Environmental Geochemistry and Health*, *15*(4), 215-227.

Evans, D. M., Zipper, C. E., Donovan, P. F., & Daniels, W. L. (2014). Long-term trends of specific conductance in waters discharged by coal-mine valley fills in central Appalachia, USA. *Journal of the American Water Resources Association*, *50*(6), 1449-1460.

Johnson, B., Smith, E., Ackerman, J. W., Dye, S., Polinsky, R., Somerville, E., ... & D'Amico, E. (2019). Spatial Convergence in Major Dissolved Ion Concentrations and Implications of Headwater Mining for Downstream Water Quality. *Journal of the American Water Resources Association* , 55(1), 247-258.

Luoma, S. N., & Presser, T. S. (2009). Emerging opportunities in management of selenium contamination. *Environmental Science & Technology*, 43(22), 8483-8487.

Lussier, C., Veiga, V., & Baldwin, S. (2003). The geochemistry of selenium associated with coal waste in the Elk River Valley, Canada. *Environmental Geology*, *44*(8), 905-913.

Merricks, T. C., Cherry, D. S., Zipper, C. E., Currie, R. J., & Valenti, T. W. (2007). Coal-mine hollow fill and settling pond influences on headwater streams in southern West Virginia, USA. *Environmental Monitoring and Assessment*, *129*(1-3), 359-378.

Palmer, M. A., Bernhardt, E. S., Schlesinger, W. H., Eshleman, K. N., Foufoula-Georgiou, E., Hendryx, M. S., ... & White, P. S. (2010). Mountaintop mining consequences. *Science*, *327*(5962), 148-149.

Pericak, A. A., Thomas, C. J., Kroodsma, D. A., Wasson, M. F., Ross, M. R., Clinton, N. E., ... & Amos, J. F. (2018). Mapping the yearly extent of surface coal mining in Central Appalachia using Landsat and Google Earth Engine. *PloS one*, *13*(7), e0197758.

Pond, G. J., Passmore, M. E., Borsuk, F. A., Reynolds, L., & Rose, C. J. (2008). Downstream effects of mountaintop coal mining: comparing biological conditions using family-and genus-level macroinvertebrate bioassessment tools. *Journal of the North American Benthological Society*, *27*(3), 717-737.

Pond, G. J., Passmore, M. E., Pointon, N. D., Felbinger, J. K., Walker, C. A., Krock, K. J., ... & Nash, W. L. (2014). Long-term impacts on macroinvertebrates downstream of reclaimed mountaintop mining valley fills in central Appalachia. *Environmental management*, *54*(4), 919-933.

Presser, T. S. (2013). *Selenium in Ecosystems Within the Mountaintop Coal Mining and Valley-fill Region of Southern West Virginia: Assessment and Ecosystem-scale Modeling*. US Department of the Interior, US Geological Survey. Professional paper 1803.

Sayler, K. L. (2008). Land cover trends: central Appalachians. US Department of the Interior. *US Geological Survey, Washington*.

Stein, B. A., Kutner, L. S., & Adams, J. S. (Eds.). (2000). *Precious heritage: the status of biodiversity in the United States*. Oxford University Press.

Timpano, A. J., Schoenholtz, S. H., Soucek, D. J., & Zipper, C. E. (2015). Salinity as a limiting factor for biological condition in Mining-Influenced central Appalachian headwater streams. *Journal of the American Water Resources Association*, *51*(1), 240-250.

Timpano, A. J., Zipper, C. E., Soucek, D. J., & Schoenholtz, S. H. (2018a). Seasonal pattern of anthropogenic salinization in temperate forested headwater streams. *Water Research*, *133*, 8-18.

Timpano, A. J., Schoenholtz, S. H., Soucek, D. J., & Zipper, C. E. (2018b). Benthic macroinvertebrate community response to salinization in headwater streams in Appalachia USA over multiple years. *Ecological Indicators*, *91*, 645-656.

Tiwari, T., Buffam, I., Sponseller, R. A., & Laudon, H. (2017). Inferring scale-dependent processes influencing stream water biogeochemistry from headwater to sea. *Limnology and Oceanography*, *62*(S1), S58-S70.

Tuttle, M. L., Breit, G. N., & Goldhaber, M. B. (2009). Weathering of the New Albany Shale, Kentucky: II. Redistribution of minor and trace elements. *Applied Geochemistry*, *24*(8), 1565-1578.

USEPA (United States Environmental Protection Agency). 2011. The Effects of Mountaintop Mines and Valley Fills on Aquatic Ecosystems of the Central Appalachian Coalfields. Office of Research and Development, National Center for Environmental Assessment, Washington, DC. EPA/600/R-09/138F.

USEPA (Environmental Protection Agency). 2016. Aquatic Life Ambient Water Quality Criterion for Selenium – Freshwater. https://www.epa.gov/wqc/aquatic-life- criterion-selenium

Wallace, J. B., & Webster, J. R. (1996). The role of macroinvertebrates in stream ecosystem function. *Annual Review of Entomology*, *41*(1), 115-139.

Whitmore, K. M., Schoenholtz, S. H., Soucek, D. J., Hopkins, W. A., & Zipper, C. E. (2018). Selenium dynamics in headwater streams of the central Appalachian coalfield. *Environmental Toxicology and Chemistry*, *37*(10), 2714-2726.

Young T. F., K. Finley, W. J. Adams, J. Besser, W. D. Hopkins, D. Jolley, E. McNaughton, T. S. Presser, D. P. Shaw, J. Unrine. 2010. What You Need to Know about Selenium. In: Chapman PM, Adams JB, Brooks ML et al (eds) Ecological Assessment of Selenium in the Aquatic Environment. CRC Press, Boca Raton, pp 7-46.

Zimmer, M. A., Bailey, S. W., McGuire, K. J., & Bullen, T. D. (2013). Fine scale variations of surface water chemistry in an ephemeral to perennial drainage network. *Hydrological Processes*, *27*(24), 3438-3451.

CHAPTER 2 – SPATIOTEMPORAL TRENDS IN WATER CHEMISTRY AND BENTHIC MACROINVERTEBRATES OF HEADWATER STREAMS INFLUENCED BY SURFACE COAL MINING IN CENTRAL APPALACHIA

INTRODUCTION

Increased concentrations of dissolved inorganic salts (i.e. salinity) in freshwater streams is a global problem resulting from various forms of anthropogenic land use, including resource extraction, urbanization, and agriculture (Kaushal et al. 2018). Salinization of streams threatens biodiversity and ecosystem function with additional impacts to human health and infrastructure (Cañedo-Argüelles et al. 2016). For example, anthropogenic salinization of freshwater has been linked to altered fish assemblages (Higgins and Wilde 2005), shifts in macroinvertebrate community structure and trait composition (Szöcs et al. 2014), and reduced reproductive success and survivability in freshwater mussels (Blakeslee et al. 2013, Beggel and Geist 2015). In the central Appalachian coalfield, surface-mining activity is a major contributor to increased salinity in headwater streams (Griffith et al. 2012). Increased loading of dissolved ions in streams draining mined areas is persistent over time (Evans et al. 2014) and distance downstream (Johnson et al. 2019), highlighting the need for long-term study of salinity and associated impacts to biological communities in these systems downstream of mining activities.

In central Appalachia, approximately 3.5% (5,900 km^2) of the land area has been impacted from surface mining (Pericak et al. 2018), with documented effects to water chemistry of headwater streams (Palmer et al. 2010). Surface mining activities expose buried coal seams by removing overlaying layers of bedrock using explosives and earth-moving equipment (USEPA 2011a). Waste rock, or overburden, is deposited into the adjacent valleys of headwater streams, effectively burying stream channels under tens to hundreds of meters of waste rock (USEPA 2011a). This deposited overburden is exposed to air and water, accelerating natural weathering processes and increasing loading of dissolved ions to headwater streams. In central Appalachia, the acids produced by pyrite oxidation are often buffered by neutralizers released from dissolution of carbonates and other associated minerals, resulting in drainage waters that are often alkaline (Clark et al. 2018). Resultant alkaline drainage that flows out of impacted areas is enriched in major ions including sulfate (SO_4^{2-}), bicarbonate (HCO_3^-), calcium (Ca^{2+}), and magnesium (Mg^{2+}) and has elevated pH, total dissolved solids (TDS), and specific conductance (SC) (Palmer 2010, Pond et al. 2008, Timpano et al. 2015).

Numerous studies have documented that elevated salinity, often measured in the field as SC, impacts benthic macroinvertebrate communities in streams draining mined areas in the central Appalachia coalfield (Boehme et al. 2016; Merricks et al. 2007; Pond et al. 2008, Timpano et al. 2015, 2018b). Streams with elevated salinity have reduced taxon richness and community structure shifted to more-tolerant taxa (Pond et al. 2008, Timpano et al. 2018b). Sensitive taxa including *Ephemeroptera* (mayflies) can be absent in streams with high salinity (Merricks et al.

2007). Moreover, the scraper functional feeding group has been documented to have lower richness and abundance in streams with elevated SC compared to reference streams (Pond et al. 2014, Timpano et al. 2018b). Loss of benthic macroinvertebrate taxa and specific functional feeding groups is ecologically important because of their significant role in decomposition and nutrient cycling, as well as being an important food source for higher trophic levels (Wallace and Webster 1996).

Because of their functional role in aquatic ecosystems, benthic macroinvertebrates are useful indicators of water quality conditions and thus stream impairment (Wallace and Webster 1996). The U.S. EPA's Rapid Bioassessment Protocols (RBPs) are used for assessing physical habitat, water quality, and biological stream conditions (Barbour et al. 1999) and rely heavily on a suite of metrics that characterize benthic macroinvertebrate communities. Central Appalachian states commonly use such RBPs and associated evaluations of benthic macroinvertebrate community structure to assess water quality under the Clean Water Act, which regulates water quality in surface mining-influenced streams. Example state-specific RBPs include the Virginia Stream Condition Index (VSCI) and the West Virginia Stream Condition Index (WVSCI) (Burton and Gerritsen 2003, Gerritsen et al. 2000, respectively). Benthic macroinvertebrates are used in such RBPs because they are easy to sample in the field and integrate time-varying water chemistry and habitat conditions (Barbour et al. 1999). Further, benthic macroinvertebrates vary in sensitivity to SC and dissolved ion composition (Barbour et al. 1999) and thus can indicate effects of altered water chemistry from mining impacts. However, improved quantification of associations between measured water chemistry and responses in benthic macroinvertebrate community structure is needed to inform regulatory standards for headwater streams in the central Appalachian region (Timpano et al. 2015, Boehme et al. 2016).

As weathering of mine spoils in closed and reclaimed coal mines continues with time, it is likely that water chemistry in affected headwater streams will change (Clark et al. 2018) as could its impact on aquatic biota (Pond et al. 2014). Streams that receive discharge from mined areas can be impacted by elevated SC long after termination of mining and restoration activities, with likely sustained effects to benthic macroinvertebrate communities. Evans et al. (2014) monitored SC across a chronosequence of 127 streams that ranged from 1 to 23 years since establishment of valley fills and modelled recovery time to attain relatively low TDS levels (SC <500 µs/cm) as 19.6 years after closure of mining and revegetation. Daniels et al. (2016) conducted laboratory leaching tests of mine spoils and found gradual decline of SC over time, but hypothesized recovery time on the scale of decades. Neither Evans et al. (2014) nor Daniels et al. (2016) documented TDS decline to the <200 µs/cm conditions that characterize relatively undisturbed streams of this region. However, long-term monitoring studies are needed to continuously measure SC over a range of sites in the central Appalachian coalfield to better understand temporal trends in water chemistry following surface mining activities. Further, to my knowledge, there are few long-term studies of how biotic response may change with time

since mining operations (see Pond et al. 2014), highlighting the need for long-term, coupled study of SC and attendant response of benthic macroinvertebrate communities.

The ion matrix that constitutes salinity of surface mining-influenced headwater streams may also vary spatially across the stream network and with flow conditions. Such spatiotemporal variation in water chemistry can be influenced by several processes, including dilution, constituent source activation, and biogeochemical transformations (Zimmer et al. 2013, Tiwari et al. 2017). For example, major ions leached from waste overburden (e.g. SO_4^{2-}, Ca^{2+}, sodium (Na^{+}), and Mg^{2+}) are largely conservative, with water column concentrations declining with distance downstream in response to inputs of more-dilute groundwater (Johnson et al. 2019). However, other elements, such as iron (Fe) and manganese (Mn), can respond to changing redox conditions (e.g., valley fill pond, wetland establishment). These processes also can vary with differing flow conditions and stream attributes (Temnerud and Bishop 2005), as can different constituent sources (Paybins 2003). Effects of continued weathering can also alter both the ion matrix and the conductivity of leachate waters (Clark et al. 2018b). Consequently, downstream water quality can be highly dynamic over time and across site conditions, highlighting a research need to better understand downstream impacts of surface mining (Johnson et al. 2019).

In this study, I continued to build upon a rich long-term dataset of 30-minute, continuous SC data and seasonal sampling of benthic macroinvertebrates and water chemistry across 24 headwater streams in central Appalachia. My objectives were to assess long-term temporal trends in SC, ion matrix, and benthic macroinvertebrate community metrics. I also used high spatial-resolution sampling across three of these streams to assess spatial- and flow-driven variability of water chemistry within small-watershed (<1.5 km^2) headwater streams influenced by surface mining.

METHODS

Site Selection

The 24 study headwater streams are located in the coalfield region of southwestern VA and southern WV (Figure 2-1). These streams were identified to meet rigorous criteria for water chemistry and habitat quality and to isolate TDS as a stressor to aquatic life (Table 2-1; Timpano 2015). Of the 24 study streams, 19 are test streams influenced by surface coal mining. The other five are reference streams within relatively undisturbed, forested watersheds. Both reference and test sites have comparable riparian and in-stream habitat conditions and have been selected such that other potential stressors such as excessive sedimentation, channelization, extreme pH, and low dissolved oxygen are minimized within a 100 m sample reach. A subset of three of the 19 test streams was identified for high-resolution spatial sampling of multiple water chemistry constituents (Figure 2-1). These streams were identified to have land access permission throughout the entire watershed and to have a watershed area <1.5 km^2 (Table 2-2).

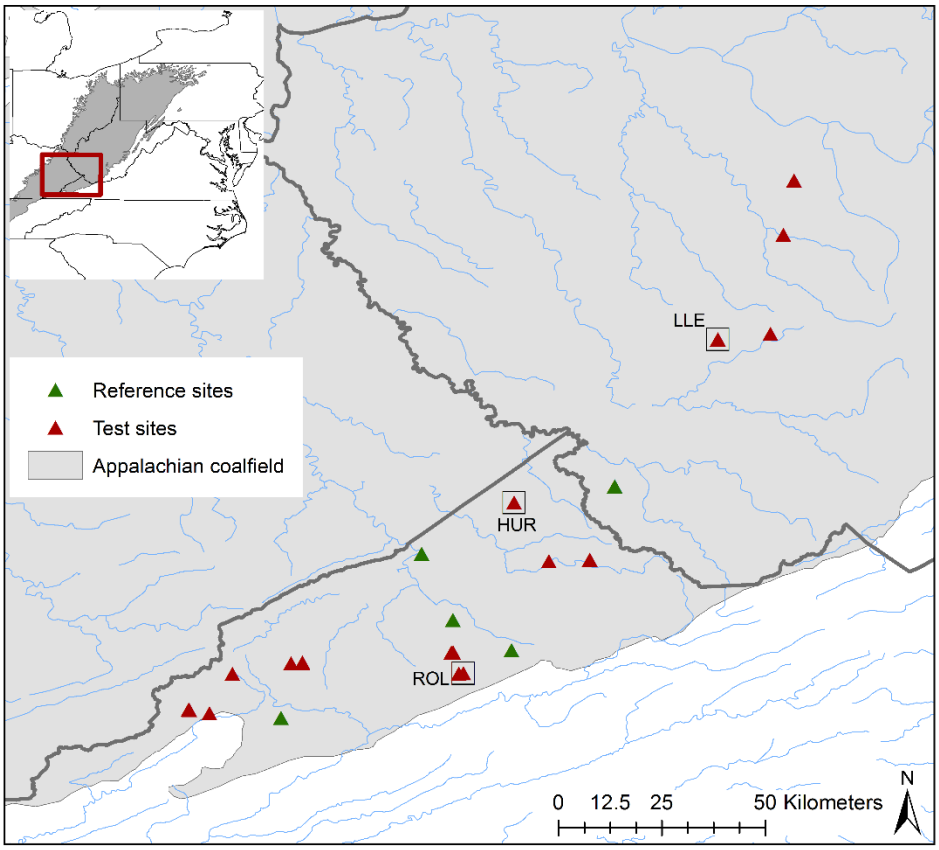

Figure 2-2-1: Location of 24 study streams in the coalfield region (shaded gray area) of southern WV and southwestern VA. Five are reference sites (green triangles) and 19 are test sites influenced by surface mining (red triangles). The selected subset of three test streams for high-resolution spatial sampling are within the black square outlines.

Table 2-2-1: Abiotic criteria for selection of reference and test streams (Timpano 2015).

Parameter or condition (units or range)	Selection Criterion[1]
Dissolved oxygen (mg/L)	≥ 6.0
pH	≥ 6.0 & ≤ 9.0
Epifaunal substrate score (0-20)[2]	≥ 11
Channel alteration score (0-20)[2]	≥11
Sediment deposition score (0-20)[2]	≥ 11
Bank disuprtive pressure score (0-20)[2]	≥ 11
Riparian vegetation zone width score, per bank (0-10)[2]	≥ 6
Total RBP habitat score (0-200)[2]	≥ 140
Residental land use immediately upstream	none

[1]Parameters and numeric selection criteria from Burton and Gerristen (2003). [2]RBP habitat, high gradient streams (Barbour et al. 1999).

Table 2-2: Watershed characteristics for three Appalachian headwater streams selected for high-resolution sampling.

Site ID	annual mean SC (µs/cm)	watershed area (km^2)	%watershed mined[1]
LLE	562	0.67	11
HUR	383	1.49	21
ROL	625	1.33	30

[1] %watershed mined between 1980-2016 calculated using a time series of leaf-on clear sky Landsat satellite images and techniques utilized by Li et al. (2015).

Data Collection – Temporal Trends in SC, Ion Matrix, and Benthic Macroinvertebrates

Water Chemistry

In situ SC and stream temperature were measured every 30 minutes between 2011 and 2018 using automated dataloggers (HOBO Freshwater Conductivity Data Logger, model U24-001, Onset Computer Corp., Bourne, Massachusetts) installed within the 100-m stream reach comprising each study site. Seasonal (i.e. spring and fall) water chemistry monitoring included standard *in situ* measures of water temperature, SC, and pH via a calibrated handheld multi-probe meter (YSI Professional Plus –YSI, Inc., Yellow Springs, Ohio, USA).

Seasonal (i.e. spring and fall) grab samples were also collected to assess the ionic composition of streamwater. Water was collected in a clean, plastic bucket below a riffle within the 100-m study reach of each stream where stream water was vertically mixed. Water was drawn into a sterile 60-ml syringe and pushed through a 0.45 µm pore filter into pre-labeled sterile polyethylene water chemistry sample bags. Filtered streamwater was collected in separate 100 ml aliquots for analysis of TDS and alkalinity and in separate 50-ml aliquots for analysis of trace elements/cations and anions. Approximately six drops of 1+1 concentrated ultrapure nitric acid was added to the cation sample to lower the pH below 2 (UESPA 1996). Samples were stored in a cooler on ice and transported to the lab where they were stored at 4^{o}C until analysis.

Samples were analyzed for TDS by evaporating 50 ml of sample water for test sites and 100 ml of sample water for reference sites in a drying oven at 180^{o}C (USEPA 1971). Total Alkalinity was measured by titration of a field-filtered water sample with a prepared standard acid using a potentiometric auto-titrator (TitraLab 865, Radiometer Analytical, Lyon, France) (APHA 2005). Calculations of HCO_3^- and CO_3^{2-} were made from Total Alkalinity and pH measurements (APHA 2005). Samples were analyzed for major cations (Ca^{2+}, Mg^{2+}, K^+, Na^+) and dissolved trace elements (B, Al, Cr, Cu, Co, Fe, Ni, Mo, Cd, Ba, Pb, Mn, Se, Zn) using an ICP-MS. (Thermo iCAP-RQ) (UESPA 1996). An ion chromatograph (Dionex ICS 3000) was used to measure concentrations of chloride (Cl^-) and SO_4^{2-}.

Benthic Macroinvertebrate Community Structure

Benthic macroinvertebrates were sampled in study streams using the semi-quantitative, single habitat (riffle-run) method established by the Virginia Department of Environmental Quality (VDEQ 2008). Approximately six, 1-meter riffles throughout each 100-m study reach were sampled using a 0.3m-wide D-frame kicknet with 500-µm mesh size to achieve a sample area of 2 m^2. Sampled riffles were representative of reach hydrology and had sufficient water velocity to wash dislodged benthic macroinvertebrates into the kicknet. A single composite sample was made from the six riffle kicks in each stream and preserved in 95% ethanol. Samples were returned to the lab for sorting and identification.

In the laboratory, composite macroinvertebrate samples were washed with water and cleaned to remove sediment, leaf material, and detritus. Each cleaned sample was evenly spread on a gridded tray for sub-sampling. Semi-quantitative composite samples were sub-sampled following the EPA Rapid Bioassessment Protocol (Barbour et al. 1999), and Virginia Department of Environmental Quality standard operating procedures (VDEQ 2008). Random sub-samples contained a specimen-count of 200 (±20%) individuals and were stored in labeled vials until identification. Sub-sampled individuals were identified to the genus level using standard keys except individuals in family Chironomidae and subclass Oligochaeta, which were identified at those levels.

Data Collection – Spatial Patterns in Water Chemistry

The downstream boundary of the three stream reaches selected for detailed spatial assessment of water chemistry variation was defined as the *in-situ* SC datalogger location used for the long-term study. Each of the three selected streams was sampled twice (Table 2-3), once after a rain event under highflow conditions and again after a period of no rain under baseflow conditions. During each sampling event, samples were collected every 100 m along the stream mainstem moving up the watershed from the *in-situ* SC datalogger location. When a tributary was reached, samples were taken in the main channel directly above and below the tributary as well within tributary. At each sample location, *in situ* measures of water temperature, SC, and pH were made via a calibrated handheld multi-probe meter (YSI Professional Plus –YSI, Inc., Yellow Springs, Ohio, USA). Grab samples of streamwater were also taken to assess ionic composition. When sufficient stream velocity was present, a water sample was collected in a clean, plastic bucket below a riffle where streamwater had been vertically mixed. Water was then drawn into a sterile 60-ml syringe and pushed through a 0.45 µm pore filter into pre-labeled sterile polyethylene water chemistry sample bags. When sufficient stream velocity was not present (e.g., at the upper reaches of tributaries), water was drawn from the stream channel directly into a 60-ml sterile syringe. Filtered streamwater was collected in a 100 ml aliquot for analysis of alkalinity and in separate 50-ml aliquots for analysis of trace elements/cations and anions. Approximately six drops of 1+1 concentrated ultrapure nitric acid was added to the cation sample to lower the pH below 2 (UESPA 1996). Samples were stored in a cooler on ice and transported to the lab where they were stored at 4^{o}C until analysis.

Samples were analyzed for Total Alkalinity by titration of a field-filtered water sample with a prepared standard acid using a potentiometric auto-titrator (TitraLab 865, Radiometer Analytical, Lyon, France) (APHA 2005) . Calculations of HCO_3^- and CO_3^{2-} concentrations were made from Total Alkalinity and pH measurements (APHA 2005). Samples were analyzed for major cations (Ca^{2+}, Mg^{2+}, K^+, Na^+) and dissolved trace elements (B, Al, Cr, Cu, Co, Fe, Ni, Mo, Cd, Ba, Pb, Mn, Se, Zn) using an ICP-MS (Thermo iCAP-RQ) (USEPA 1996). An ion chromatograph (Dionex ICS 3000) was used to measure concentrations of Cl^- and SO_4^{2-}.

Table 2-3: Sampling dates and antecedent precipitation for spatial sampling events at three headwater streams influenced by surface mining.

Site ID	Date sampled	flow type	4-day precipitation (in)[1]
ROL	6/6/2018	base	0.08
ROL	6/27/2018	high	1.33
LLE	12/6/2018	base	0.26
LLE	11/10/2018	high	0.93
HUR	3/14/2019	base	0.18
HUR	11/16/2018	high	1.7

[1] Data combined from Daily Summary Observations produced by the National Oceanic and Atmospheric Administration (NOAA)

Data Analysis – Temporal Trends in SC, Ion Matrix, and Benthic Macroinvertebrates

To investigate temporal trends in salinity, weekly mean SC values were calculated for all 24 study streams using 30-minute continuous SC data (Timpano et al. 2017). A seasonal Kendall analysis was conducted on these weekly means to assess temporal trends (Helsel and Hirsch 2002, Timpano et al. 2017). This non-parametric analysis is commonly used for water quality time series and accounts for seasonal variability while being resistant to data gaps. An analysis of seven different linear trend techniques using 11 years of biweekly environmental data found the seasonal Kendall analysis to have the highest power while also maintaining its alpha value (Hess et al. 2001). The seasonal Kendall test produces a non-parametric correlation coefficient (tau) and associated P-value. The tau value ranges from -1 to +1, indicating the correlation strength and direction, where a positive tau specifies an increasing trend. A Theil-Sen slope analysis was then used to analyze the magnitude of trends when significant, based on the seasonal Kendall analysis (Timpano et al. 2017). The Theil-Sen slope analysis is a nonparametric test that is insensitive to outliers and tests the relationship between two variables (Helsel and Hirsch 2002), in this case SC and time. The output slope is the median value of slopes calculated between all pairs of sample points.

Ionic composition of streamwater was evaluated using both an anion and cation matrix indicator on a millimolar (mmol) basis (Timpano et al. 2017). Ratio of sulfate to bicarbonate (SO_4:HCO_3) was chosen as the anion indicator because laboratory studies have shown that sulfate is the dominant anion early in the leaching process of mine spoils and slowly decreases in concentration with repeated leaching events (Orndorff et al. 2015; Daniels et al. 2016). In contrast, concentration of bicarbonate slowly increases with repeated leaching events (Orndorff et al. 2015; Daniels et al. 2016). Ratio of calcium to magnesium (Ca:Mg) was chosen as a cation matrix indicator because previous work has observed reduced Ca:Mg ratio in test streams influenced by surface coal mining relative to reference streams (Clark et al. 2018, Timpano et al. 2017). Differences in these cation and anion matrix indicators between reference and test streams were analyzed for site-type effect with study site defined as a random variable. Trends were analyzed using mixed models (RStudio, Boston, MA) with ion ratios as the dependent variable and year (numeric) and season (categorical) as independent variables. P-values < 0.05 indicated a significant effect by year and thus a significant temporal trend.

Temporal trends in biological conditions were evaluated using eight metrics describing benthic macroinvertebrate structure (Barbour et al. 1999) (Table 2-4). Each of the selected metrics has been shown to respond negatively to increasing SC (Timpano et al. 2018b); they include measures of taxonomic richness, community composition, and functional feeding groups. I used spearman correlation to validate the relationship between salinity and the selected biological metrics. Correlations between SC measured at the time of sampling and biological metrics across all 24 study streams were made each year (2011-2018) for both fall and spring sampling seasons. Temporal trends in biological metrics were analyzed using mixed models (RStudio, Boston, MA) with metrics as the dependent variable and year (numeric) and season (categorical) as independent variables (Timpano et al. 2017). P-values < 0.05 indicated a significant effect by year thus a significant temporal trend.

Data Analysis – Spatial Patterns in Water Chemistry

Maps of spatial variation in SC were made for each stream network and each sampling event using ESRI's ArcGIS, GPS coordinates recorded in the field, and mining layers produced by Pericak et al. (2018). Under baseflow and highflow, relative concentrations of major ions and trace elements compared to stream origin concentrations were plotted against distance downstream (Table C-1). Differences in discharge between highflow and baseflow were not directly measured in the field; however, decreased SC can be used as a surrogate for higher flow in these headwater streams (Timpano et al. 2018a). Effect of the highflow event on water chemistry was analyzed by calculating percent difference in constituent concentrations between highflow and baseflow and plotting those differences with distance downstream. Separate graphs were made for major ions and trace elements. These multiple ways of presenting spatial water chemistry illustrated effects of longitudinal trends, tributary inputs,

and variable flow conditions on water quality variation in these surface mining-influenced headwater streams.

RESULTS

Temporal Trends in SC, Ion Matrix, and Benthic Macroinvertebrates

Specific Conductance

I found some increasing and decreasing temporal trends in SC among the five reference and 19 test streams (Figure 2-2, Appendix A, Table B-1). However, ten study streams showed no significant trends in SC (Table B-1). Four of the five reference streams had statistically significant trends in SC, with increasing trends in two sites and decreasing trends in two sites. However, the magnitude of these trends was small, ranging from -3.31 µs/cm yr^{-1} (-2.60% yr^{-1}) to 0.60 µs/cm yr^{-1} (1.74% yr^{-1}). Of the 19 surface mining-influenced test streams, two had increasing SC, eight had decreasing SC, and the remaining nine test streams exhibited no trend. For the ten test sites with observed SC trends, the magnitude of temporal change was greater than reference streams, ranging from -30.22 µs/cm yr^{-1} (-4.4% yr^{-1}) to 42.90 µs/cm yr^{-1} (9.8% yr^{-1}). The mean rate of change for SC at test sites with declining trends was -2.2% of mean SC yr^{-1} with a range of -0.6% to -4.4% yr^{-1}. The adjacent watersheds of FRY and RFF were the only two test streams showing increasing trends in SC (1.1% yr^{-1} and 9.8% yr^{-1}, respectively). Both of these streams received surface mining activity within the study period (2011-2015): 0.8% of watershed area for FRY and 20.8% of the watershed area for RFF. However, six other test streams had recent mining, four of which had decreasing trends in SC. Recent watershed disturbance by mining in streams with decreasing SC ranged from 0.5% to 2.4% of watershed area.

Ion Matrix

Ratios of SO_4:HCO_3 were higher in test streams (1.77 $\pm$ 0.07 SE) than reference streams (0.37 $\pm$ 0.03 SE) (p-value = 0.018) (Figure 2-3). The Ca:Mg ratio was higher in reference streams (1.63 $\pm$ 0.06 SE) than test streams (1.13 $\pm$ 0.02 SE) (p-value = 0.015). Mixed models with year (numeric) and season (categorical) as independent variables resulted in 12 of the 19 test streams with significant decreasing trends in the SO_4:HCO_3 ratio (Table B-1), whereas there were no significant trends in reference sites. Only nine of the 24 total streams (7 test, 2 reference) had significant trends in Ca:Mg ratio, all of which were negative (Table B-1).

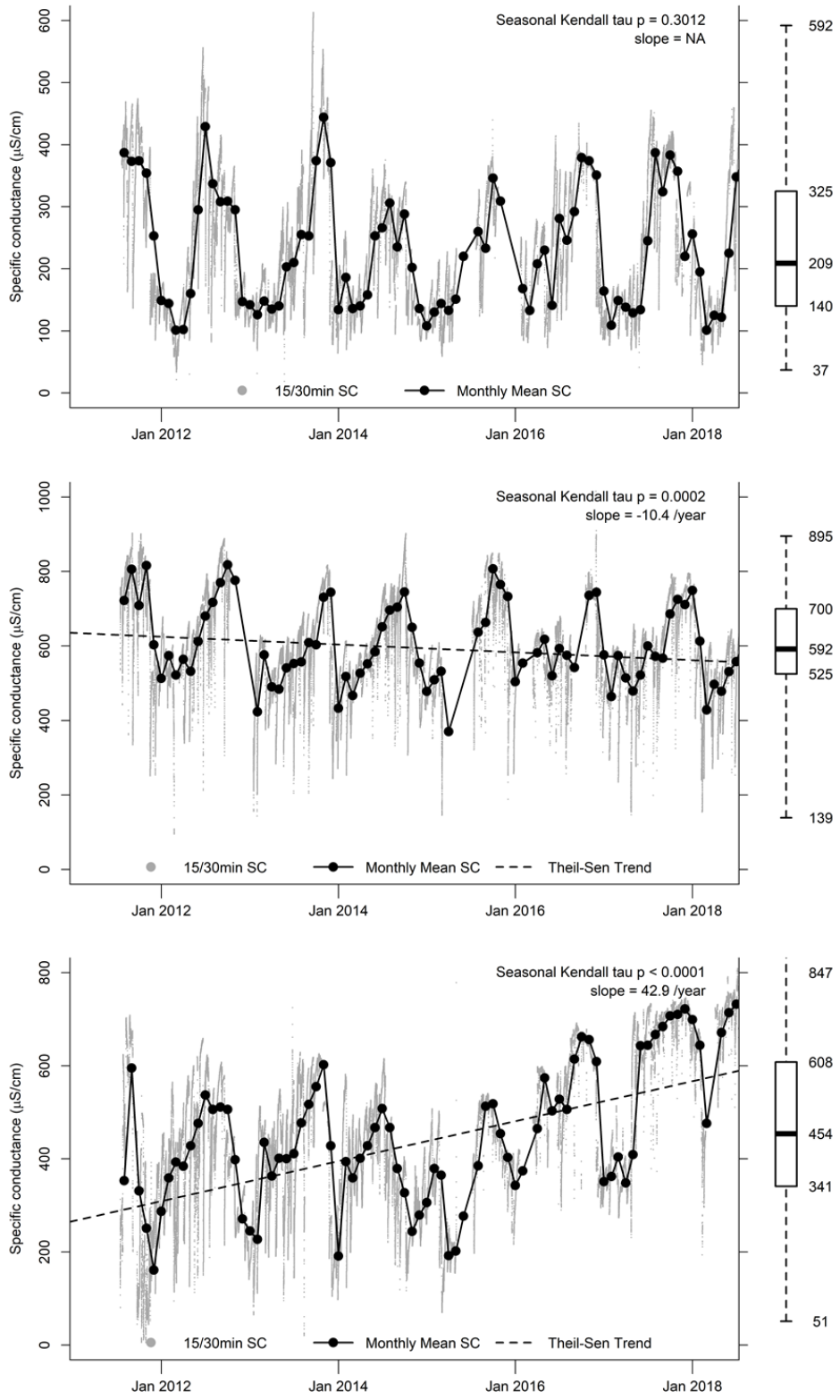

Figure 2-2: Example trends in specific conductance (SC) across 24 streams during the study period (2011-2018). No change in SC (top). Decreasing trend in SC (middle). Increasing trend in SC (bottom).

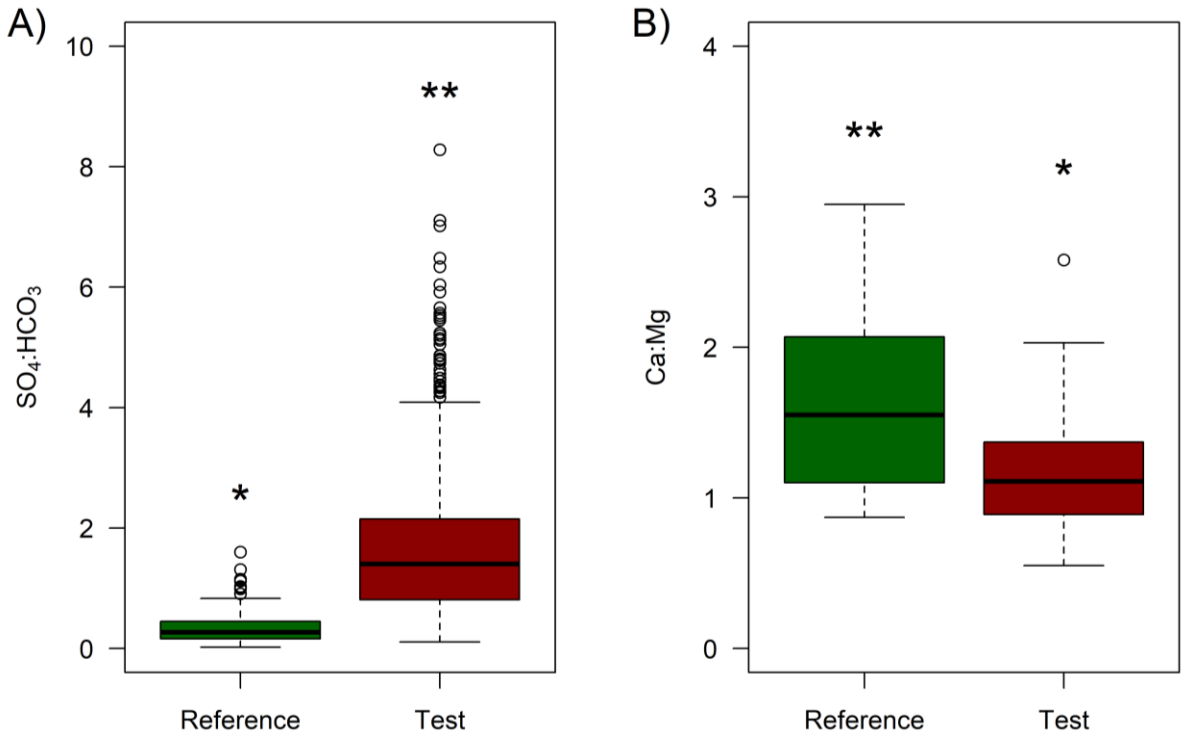

Figure 2-3: Ion matrix in five reference streams and 19 test streams in the central Appalachian coalfield from 2011-2018. **A)** mmol ratio of SO_4:HCO_3 in reference and test streams, and **B)** mmol ratio of Ca:Mg in reference and test streams. For each panel, difference in the number of asterisks denote significant difference based on a linear mixed-effects model with study site defined as a random variable, alpha =0.05.

Benthic Macroinvertebrates

I used spearman correlations to test my prediction that the selected biological metrics would decrease with increasing salinity. During spring seasonal sampling across all years, there was a highly significant (p-value <0.01) negative correlation between SC measured at the time of sampling and the selected biological metrics (Table 2-4). Correlations were not as strong in the fall for scraper richness or Shannon diversity. In fall of 2012 and 2013, there was no significant relationship between SC and scraper richness. In fall 2013, there was no significant relationship between SC and Shannon diversity. The test stream RFF was excluded from all analyses of benthic macroinvertebrate communities because of removal of the riparian buffer and increased sedimentation observed after Fall 2017.

Temporal trends in biological metrics were analyzed using mixed models, with few observed significant trends. Reference streams only had two significant trends in biological metrics over the study period (one positive trend in richness and one decreasing trend in scraper richness; Table B-1). Test streams had a total of 14 positive trends and five negative trends over the five-

year span of study. Shannon diversity had the most trends across sites with four positive trends found at test streams. Scraper richness had no positive trends and one negative trend.

Table 2-4: Spearman correlations between specific conductance and selected benthic macroinvertebrate metrics across 23 study headwater streams in the central Appalachian coalfield using seasonal fall and spring sampling during five years.

	Fall					Spring				
Metric	**2011**	**2012**	**2013**	**2015**	**2017**	**2012**	**2013**	**2014**	**2016**	**2018**
Richness	-0.75*	-0.51*	-0.78*	-0.56*	-0.77*	-0.75*	-0.76*	-0.72*	-0.66*	-0.74*
EPT** richness	-0.80*	-0.62*	-0.71*	-0.59*	-0.71*	-0.81*	-0.81*	-0.81*	-0.82*	-0.76*
Ephemeroptera richness	-0.80*	-0.76*	-0.79*	-0.82*	-0.80*	-0.87*	-0.88*	-0.83*	-0.93*	-0.80*
Ephemeroptera richness less Beatidae	-0.84*	-0.73*	-0.75*	-0.81*	-0.80*	-0.86*	-0.88*	-0.88*	-0.88*	-0.77*
%Ephemeroptera less Beatidae	-0.85*	-0.74*	-0.76*	-0.83*	-0.83*	-0.84*	-0.89*	-0.90*	-0.89*	-0.78*
scraper richness	-0.61*	-0.39	-0.33	-0.53*	-0.69*	-0.71*	-0.59*	-0.74*	-0.74*	-0.73*
Shannon diversity	-0.61*	-0.41	-0.55*	-0.55*	-0.60*	-0.61*	-0.67*	-0.76*	-0.71*	-0.67*
% Ephemeroptera	-0.73*	-0.79*	-0.76*	-0.84*	-0.78*	-0.69*	-0.87*	-0.86*	-0.83*	-0.84*

*P-value <0.05, **EPT- calculated as the total number of distinct taxa from three orders of macroinvertebrates: 1) Ephemeroptera (mayflies), 2) Plecoptera (stoneflies), and 3) Trichoptera (caddisflies).

Across the 18 test streams, negative trends in SC (i.e. improving water quality) corresponded with few positive trends in biological metric scores (Figures 2-4, 2-5). For community-level metrics (richness, scraper richness, EPT richness, and Shannon diversity), there were five positive trends and one negative trend observed in streams with decreasing SC (Figure 2-4). Test streams with no change in SC showed some change in community-level metrics, with three positive trends and no negative trends. The one stream with increasing SC did not have any trends in community-level metrics.

The four metrics that exclusively measure Ephemeroptera taxa (%Ephemeroptera less Baetidae, %Ephemeroptera, Ephemeroptera richness, and Ephemeroptera richness less Baetidae) (Figure 2-5) showed less response to negative trends in SC compared to the community-level metrics (Figure 2-4). For these four Ephemeroptera-specific metrics, all eight test streams with decreasing SC had no significant trends in metric scores. However, test streams with no temporal trends in SC showed some changes in Ephemeroptera metrics with six positive and three negative trends. As observed for community-level metrics, the one stream with increasing SC did not have any trends in Ephemeroptera metrics.

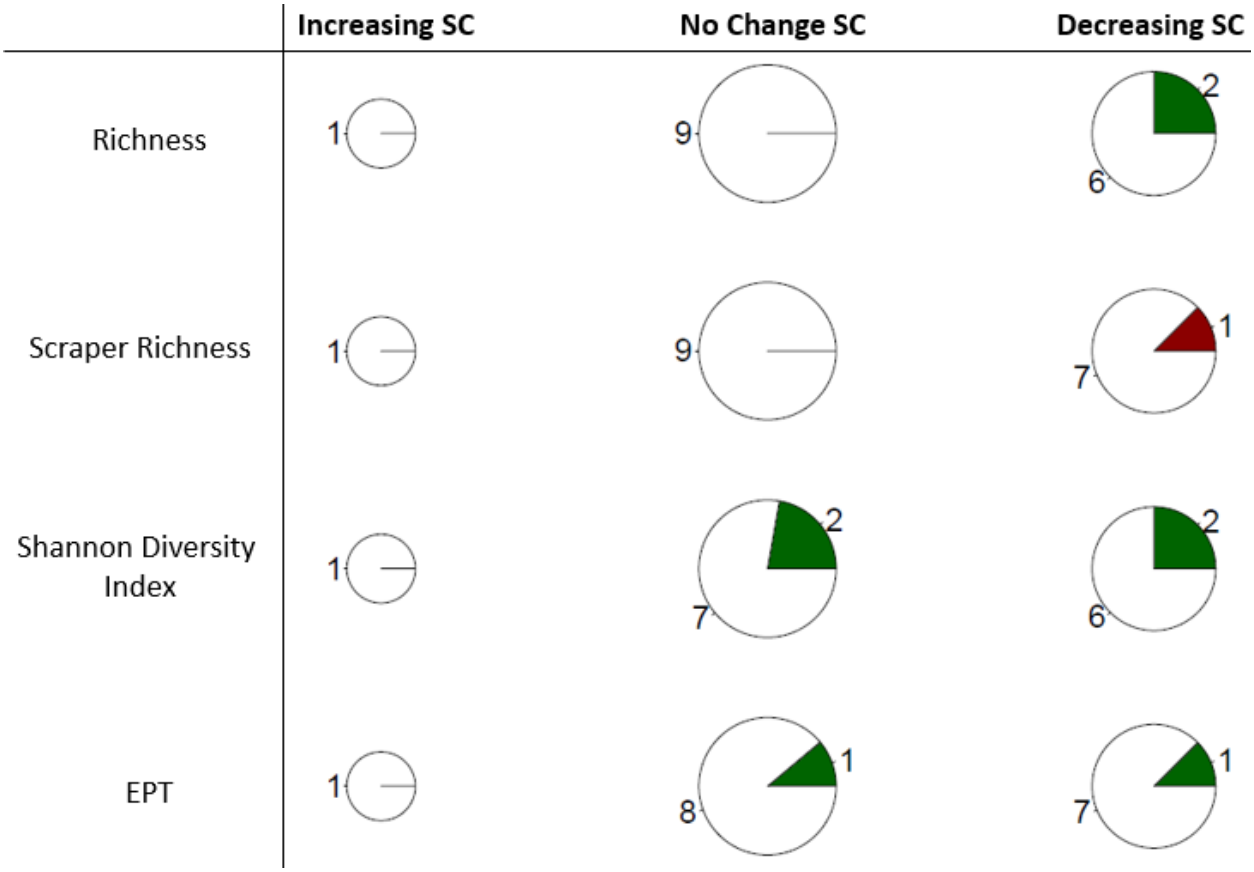

Figure 2-4: Temporal trends in specific conductance (SC) and benthic macroinvertebrate community metrics that include non-Ephemeroptera taxa in 18 test streams influenced by surface mining in the central Appalachian coalfield. Size of pie charts represent number of streams with SC trends (1-positive, 9-no change, 8-decreasing). White denotes proportion of streams with no change in listed biological metrics, green denotes positive trend in listed biological metric, and red denotes negative trend in listed biological metric.

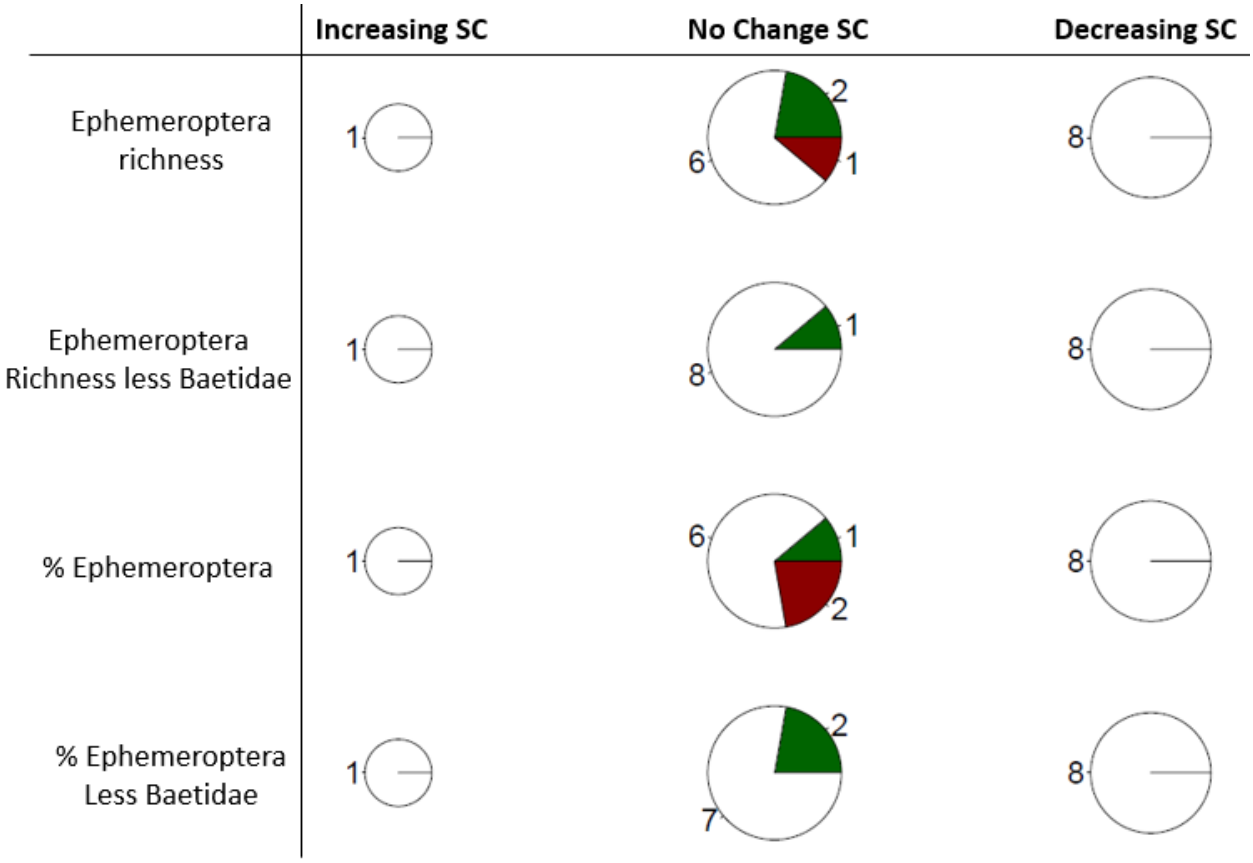

Figure 2-5: Temporal trends in specific conductance (SC) and benthic macroinvertebrate community metrics based exclusively on Ephemeroptera in 18 test streams influenced by surface mining in the central Appalachian coalfield. Size of pie charts represent number of streams with SC trends (1-positive, 9-no change, 8-decreasing). White denotes proportion of streams with no change in listed biological metrics, green denotes positive trend in listed biological metric, and red denotes negative trend in listed biological metric.

Spatial Patterns in Water Chemistry

HUR

Stream network length was the same in HUR between baseflow and highflow sampling events (Figure 2-6a-b). At the bottom of the sampled stream network, SC was 335 µs/cm under baseflow compared to 232 µs/cm under highflow, suggestive of flow differences during these periods. Under baseflow, SC was influenced by tributary inputs. Tributaries 3 and 4 added water dilute in SC, resulting in lower SC values in the mainstem after confluences with these tributaries. However, tributary 5, which is proximate to the valley fill in this watershed, had the highest SC (732 µs/cm) and contributed to a 49% increase in SC in the mainstem under baseflow conditions (Figure 2-6c). Because of increased SC from this tributary, SC was 16% greater at the most downstream sampled location (at the *in-situ* datalogger) than the stream origin. However, major ions did not always follow the spatial pattern observed for SC. For

example, tributary 3, although more dilute in SC than the mainstem, had increased concentrations of Mg, Cl, and SO_4 (Figure C-1). The high-SC tributary 5 enriched Mg, SO_4, and Ca in the mainstem while further diluting Na. Tributaries had less of an effect on the concentrations of trace elements. All trace elements except for Mn, Fe, and Ba showed patterns of dilution with distance downstream from stream origin (Figure C-2).

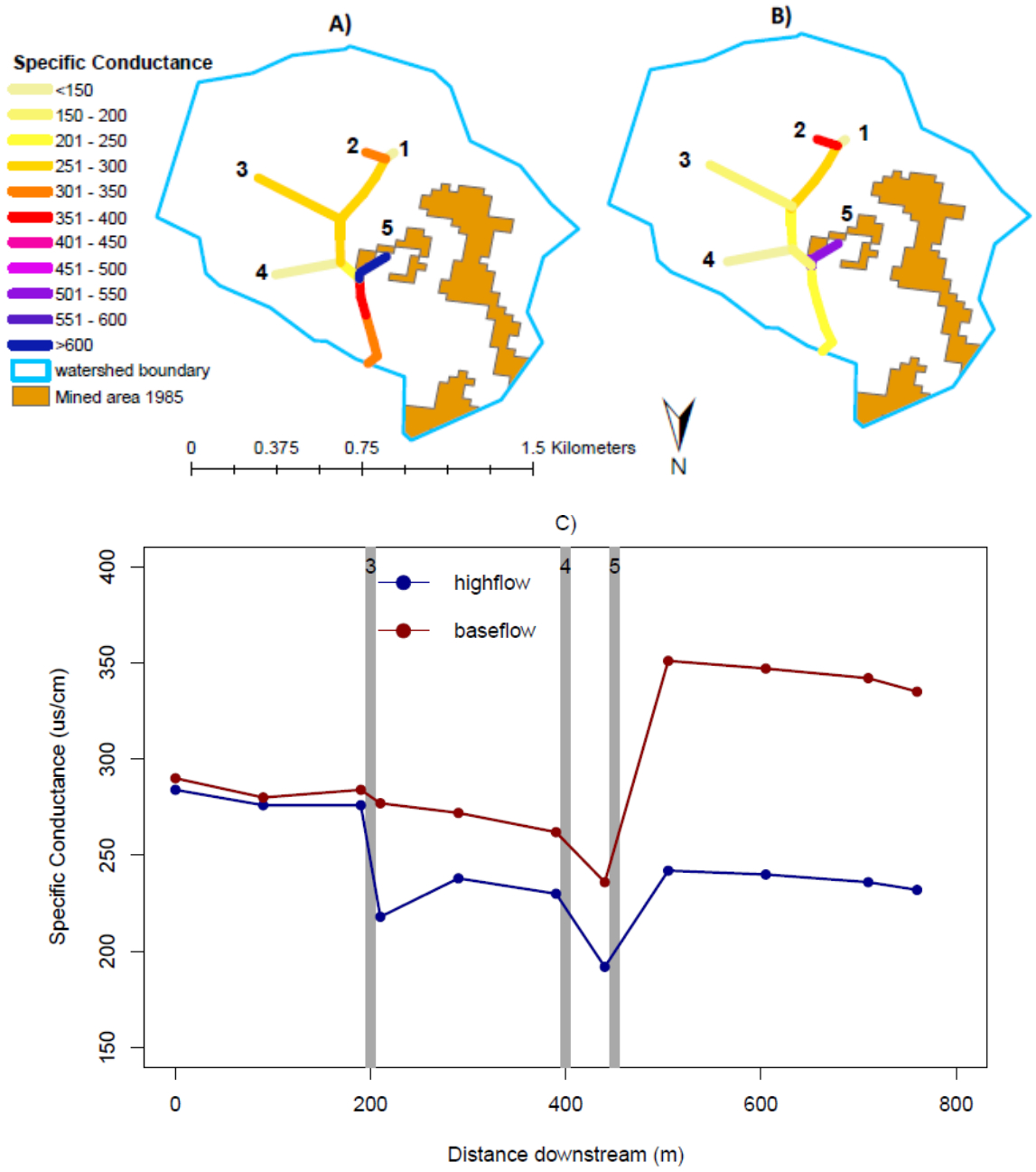

Figure 2-6: Spatial maps of specific conductance (SC) under **(A)** baseflow and **(B)** highflow conditions for Hurricane Branch, VA. **(C)** Specific conductance with distance downstream under baseflow and highflow. Tributaries are marked with gray-shaded lines and labeled with numbers corresponding to location in figures **(A)** and **(B)**.

During highflow conditions, there was more dilution in SC with distance downstream compared to baseflow conditions (Figure 2-6c). However, in the furthest upstream part of the stream network, tributary 2 had slightly higher SC under highflow indicating source activation (384 µs/cm at highflow vs. 331 µs/cm at baseflow) (Figure 2-6b). Note that tributary 2 is not shown in Figure 2-6c, which begins below the confluence of tributaries 1 and 2. Consequently, at upstream sample locations, SC was nearly identical to baseflow conditions before substantial dilution from tributaries 3 and 4 (Figure 2-6c). Tributary 5 still contributed water with elevated SC but its effect on mainstem SC was less than at baseflow, contributing to a 26% increase in SC. Unlike baseflow, SC was 18% less at the downstream sample location compared to the stream origin. All major ions, except for Mg and Cl, generally decreased in concentrations with distance downstream under highflow (Figure C-1). Spatial patterns of individual major ion enrichment and dilution in tributaries were similar under baseflow and highflow. Similarly, trace elements generally showed similar patterns of downstream dilution as observed during baseflow conditions (Figure C-2).

Comparing concentrations between flow conditions demonstrated that highflow generally resulted in lower major ion concentrations compared to baseflow (Figure C-1). Chloride was the one exception to this trend with increased concentrations under highflow at every sample location. The relative dilution of most major ions under highflow increased with distance downstream. In contrast, relative concentrations of trace elements were more variable (Figure C-2). Strontium and Ba had spatial patterns similar to major ions with concentrations becoming increasingly dilute with highflow, whereas other elements (i.e. B, Mn, Fe, and Zn) were consistently enriched compared to baseflow conditions. Manganese showed the most enrichment being approximately two times higher in concentration at the downstream sampling location under highflow compared to baseflow conditions.

LLE

Stream network length was the same in LLE across baseflow and highflow sampling events (Figure 2-7a-b). Specific conductance measured at the bottom of the sampled stream network was 280 µs/cm under baseflow and 209 µs/cm under highflow. Similar to SC patterns in HUR, SC was influenced by tributary inputs in LLE under baseflow conditions (Figure 2-7c). Tributary 2 reduced SC by half in the mainstem, whereas tributaries 3 and 4 both increased SC in the mainstem. Tributary 4, although the shortest tributary, had the highest SC of any part of the stream network and increased SC in the mainstem by 42% under baseflow conditions. In the absence of tributaries, SC generally decreased with distance downstream. The overall decrease in SC under baseflow conditions did not necessarily correspond to dilution in major ion concentrations. For example, Na was enriched throughout the stream network as a result of increased contributions from all tributaries (Figure C-3). Bicarbonate was also enriched at the bottom of the stream network compared to the origin as a result of high inputs from tributary 4. Trace elements were more variable in concentration across the stream network compared to major ions (Figure C-4). Tributary 3 contributed elevated Al and Mn concentrations to the

mainstem, which remained enriched at the bottom of the sampled stream network. Tributary 4 had a similar effect on Sr concentrations.

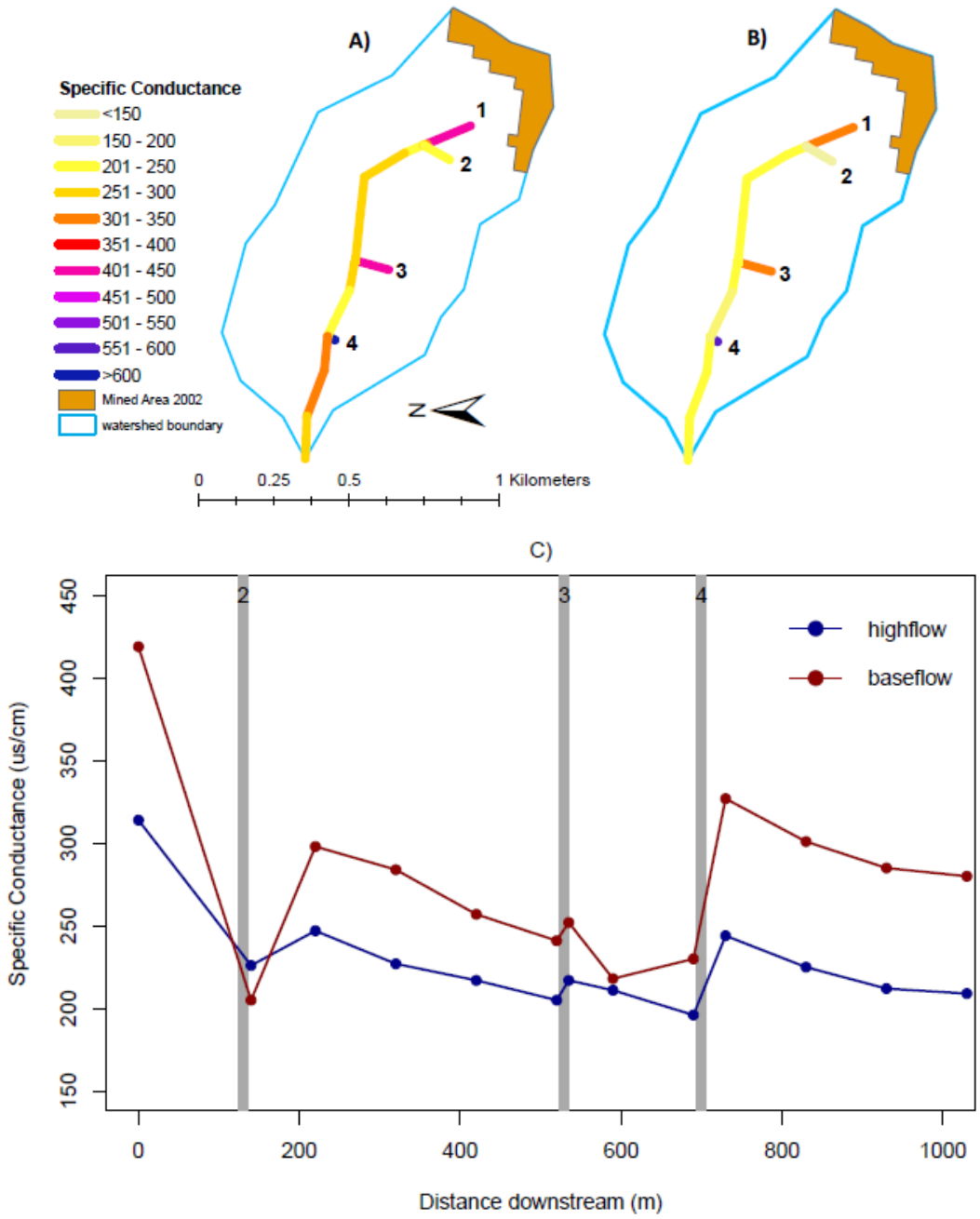

Figure 2-7: Spatial maps of specific conductance (SC) under **(A)** baseflow and **(B)** highflow conditions for Longlick Branch East Fork, WV. **(C)** Specific conductance with distance downstream under baseflow and highflow. Tributaries are marked with gray-shaded lines and labeled with numbers corresponding to location in figures **(A)** and **(B)**.

During highflow conditions, there was also a general dilution in SC with distance downstream (Figure 2-8b-c). However, the effects of tributaries were reduced compared to baseflow conditions. For example, tributary 1, which reduced SC by half under baseflow, resulted in only a 28% reduction under highflow. Similarly, tributary 5 contributed to a 24% increase in SC during highflow compared to 42% under baseflow. Sodium was the only major ion to be enriched at the most downstream sampled location compared to origin concentrations (Figure C-3). The other major ions followed the trend of SC dilution along the stream network. Highflow had a greater impact on relative concentrations of trace elements than the major ions (Figure C-4). Aluminum, while enriched under baseflow, was diluted under highflow. Manganese, B, and Sr were all enriched at the bottom of the stream network during highflow.

When directly comparing baseflow and highflow conditions, concentrations of all major ions excluding Na, were increased under highflow near the stream origin after the confluence of tributary 2 (Figure C-3). However, below this sample location, most major ion concentrations became more dilute. Conversely, K remained enriched relative to baseflow concentrations at every sample location. Trace element concentrations were more variable than major ions (Figure C-4). Strontium and Ba had patterns similar to the majority of major ions, with lower concentrations under highflow compared to baseflow conditions. Conversely, concentrations of B and Mn were higher during highflow than at baseflow at every sample location.

ROL

In contrast to the other two stream networks sampled, ROL had an expanded network length under highflow, including three tributaries that were dry under baseflow (Figure 2-8a-b). Specific conductance measured at the bottom of the watershed was 462 µs/cm under highflow and 662 µs/cm under baseflow. Tributary 1 was the only tributary present under baseflow (Figure 2-8a). For baseflow conditions, this tributary had lower SC than the mainstem (1003 vs. 1230 µs/cm) yet only contributed a 6% reduction in SC (Figure 2-8c). Specific conductance declined by 62% from stream origin to the most downstream location during baseflow conditions. Of the major ions sampled in this stream network, Ca, K, and Mg followed the same dilution pattern as SC (Figure C-5). Conversely, Na was enriched throughout the stream network downstream of tributary 1. Trace element concentrations were more variable than major ions (Figure C-6). Selenium showed dilution relative to initial concentrations, Ba was enriched throughout the stream network, and Mn, Fe, and Al were variable with spikes of enrichment in several sample locations.

Under highflow, the stream network length increased, and three tributaries that were dry under baseflow were sampled (Figure 2-8b). Tributaries 2, 3, and 4 had lower SC than the mainstem whereas tributary 1, which had lower SC than the mainstem under baseflow, had higher SC than the mainstem under highflow. Despite lower SC at each sample location, I observed a similar pattern of SC reduction by 58% from stream origin to the downstream sampling location under highflow. After initial enrichment of Mg and Na near the stream origin, I observed dilution of all major ions sampled compared to origin concentrations (Figure C-5).

Trace elements concentrations under highflow displayed similar patterns to baseflow, except for Ba, which was diluted relative to origin concentration (Figure C-6).

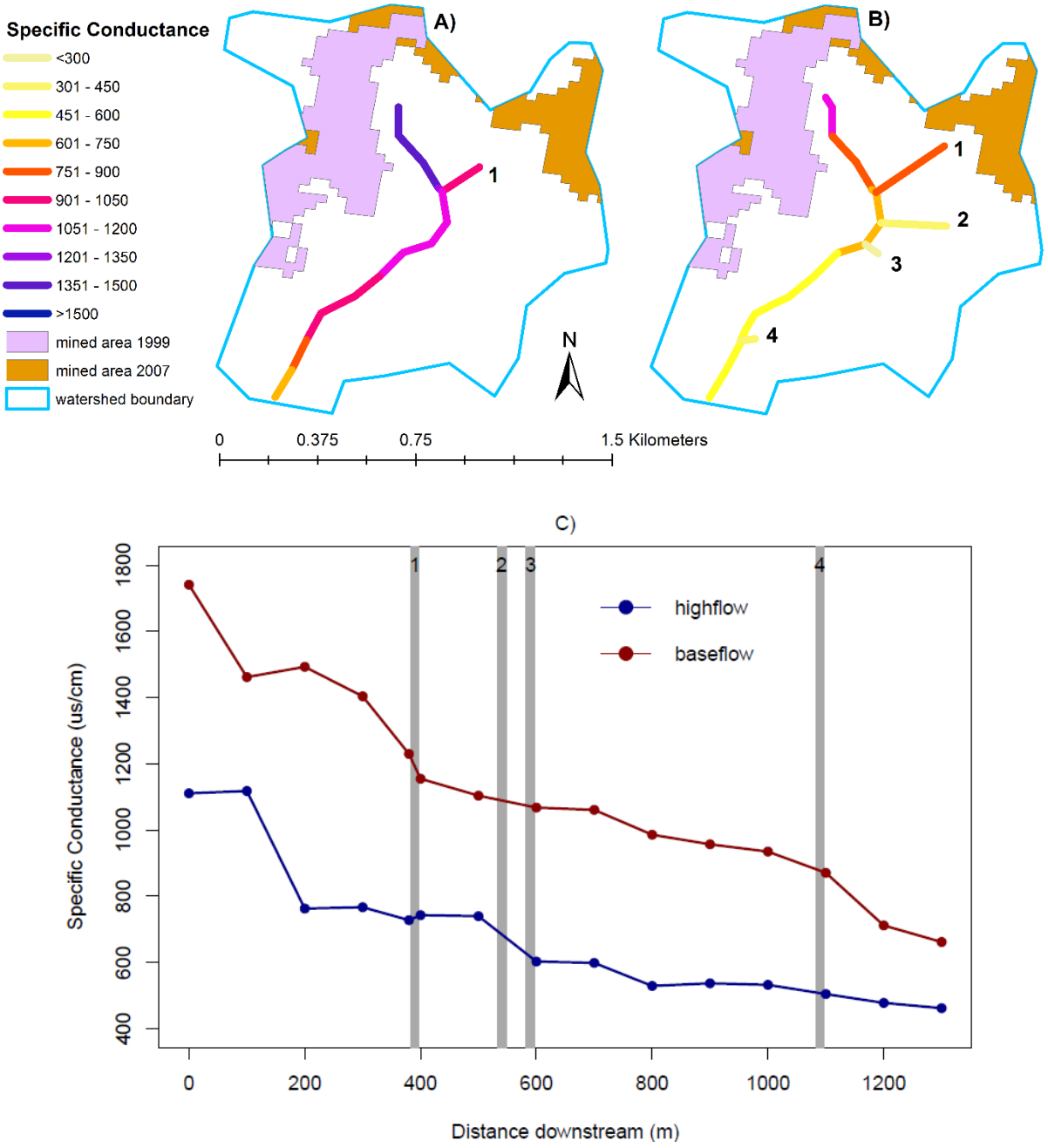

Figure 2-8: Spatial maps of specific conductance (SC) under **(A)** baseflow and **(B)** highflow at Roll Pone Branch, VA. **(C)** Specific conductance with distance downstream under baseflow and highflow. Tributaries are marked with gray-shaded lines and labeled with numbers corresponding to location in figures **(A)** and **(B)**.

A direct comparison between baseflow and highflow conditions demonstrated lower major ion concentrations at the bottom of the stream network during highflow; however, K had the least dilution under highflow compared to the other major ions (Figure C-5). Sodium, K, and Mg had initial enrichment near the stream origin with highflow, but concentrations became lower compared to baseflow concentrations moving downstream. Trace element concentrations were more variable than major ion concentrations (Figure C-6). All trace element concentrations at the stream origin, except for Mn, were elevated under high flows compared to baseflow. Differences between baseflow and highflow Se were variable throughout the stream network. Iron, Mn, Al, and Zn were enriched with highflow at the bottom of the watershed with Mn concentration being approximately nine times higher than baseflow concentrations at the furthest downstream sample location.

DISCUSSION

In this work, I assessed temporal trends in water chemistry and benthic macroinvertebrate communities across 24 headwater streams during a seven-year period in the central Appalachian coalfield. In addition, I evaluated spatial and flow-driven variation in water chemistry at a subset of three surface mining-influenced headwater streams. Results indicate that surface coal mining has long-term impacts on water chemistry and benthic macroinvertebrate communities in central Appalachian headwater streams. Some test streams in this study had gradual decreasing trends in SC measured between 2011 and 2018. However, benthic macroinvertebrates, particularly Ephemeroptera and scrapers, showed little response to these improvements. A limitation of this study is that measurements of water chemistry and benthic macroinvertebrate communities were made at one location within each stream. To that end, my results further demonstrate that water chemistry is variable within a stream reach and under different flow conditions, highlighting future research needs to better characterize impacts of surface mining across entire stream networks.

Temporal Trends in SC, Ion Matrix, and Benthic Macroinvertebrates

I evaluated long-term SC trends (2011-2018) in both test and reference streams to assess recovery following surface mining considering natural water chemistry variation. Undisturbed, central Appalachian headwater streams naturally vary in salinity over time in response to such factors as climatic conditions and thus flow variation (Timpano et al. 2018a). For the five reference sites, I observed two increasing and two decreasing significant trends, albeit with small magnitudes of imputed annual change -3.3 µs/cm yr^{-1} (-2.6% yr^{-1}) to 0.6 µs/cm yr^{-1} (1.7% yr^{-1}).

In contrast, eight test streams had decreasing long-term trends in SC, and at annual rates exceeding reference conditions, thus indicating possible recovery from mining conditions. However, the magnitude of SC decline in these streams suggests long recovery times (ca. decades) to return to “reference conditions”. The average annual mean SC of the eight streams with decreasing SC was 728 µs/cm with an average trend of -15 µs/cm yr^{-1}. Assuming that these temporal trends remain constant over time, it would take roughly 30 years for these streams to

have annual mean SC <300 µs/cm, which has been established as the regional stream SC benchmark (USEPA 2011b). Moreover, it would take ca. 45 years for these streams to reach the average annual mean SC of the reference streams in this study (67 µs/cm). The highest annual mean SC stream with a decreasing trend was KUT located in Wise County, VA. This stream has an annual mean SC of 1,080 µs/cm and a decreasing trend of -16 µs/cm yr^{-1}, suggesting ca. 50 years to reach an annual mean SC lower than the EPA benchmark and 63 years to reach observed reference conditions. Further, nine test streams had no change over the seven-year study, indicating long-term impacts from surface mining and highlighting the need for continued monitoring of these streams over longer time periods.

Two test streams (FRY and RFF) had increasing trends in SC. The increasing trend at FRY (1.1% yr^{-1}) was comparable to increases found in reference streams. However, observed increases at RFF (9.8% yr^{-1}) were well above increases observed for the reference streams. The FRY and RFF watersheds received additional mining (0.8% and 20.8% of watershed area, respectively) during the study period, likely explaining increasing SC trends, especially at RFF, which received the most new mining activity of any site. However, eight other test streams received additional mining in their watersheds (estimated at 0.5-7.7%), albeit lower than the 20.8% observed in RFF, and did not have increasing trends in SC (Table B-1). Therefore, the significance of recent mining to temporal trends in SC is inconsistent.

Along with gradual declines in SC, changes in ion matrix are expected to occur in streams following termination of mining activity and with continued weathering of waste material as documented in laboratory leaching studies (Orndorff et al. 2015, Daniels et al. 2016, Clark et al. 2018). Observed negative trends in SO_4:HCO_3 ratios at some of the test streams suggests weathering of overburden rock and thus further recovery, albeit slow, at a subset of my test sites. Out of the 19 test streams, 12 had decreasing trends in SO_4:HCO_3 ratio; of these 12 sites, seven also had significant decreasing SC trends. There were no decreasing trends in reference streams indicating stable ratios of these two anions. Decreasing trends in test streams were expected based on previous laboratory studies showing that sulfate is the dominant anion early in the leaching process of mine spoils and slowly decreases in concentration with repeated leaching events (Orndorff et al. 2015; Daniels et al. 2016). However, seven test streams showed no significant trends, concordant with their lack of SC trends. I expected that the Ca:Mg ratio would increase over time as a result of aging mine spoils and a gradual return to reference-like conditions. However, I found no increasing trends for Ca:Mg in test streams.

Despite some test sites showing slow recovery of water quality conditions, I found limited evidence of coincident recovery of benthic macroinvertebrate communities over the seven-year study period (2011-2018). Benthic macroinvertebrate community metrics, particularly metrics for Ephemeroptera groups, were negatively affected by SC across test streams during fall and spring seasonal sampling periods. However, these biological metrics showed little response in the sites with decreasing SC trends. Four Ephemeroptera metrics had no significant positive trends present in streams with decreasing SC and had few trends present in streams with no

change in SC. The four biological metrics that do not focus on Ephemeroptera taxa, also showed limited response to decreasing SC. For these metrics, no more than 25% of streams with decreasing SC had associated positive trends in metric scores. Further, scraper richness showed no positive trends in sites with decreasing SC.

Absence of positive trends (i.e. biological recovery) in Ephemeroptera metrics across all test streams is important to note because of the well-documented decline of sensitive Ephemeroptera taxa in headwater streams influenced by surface mining in the central Appalachian coalfield (Merricks et al. 2007, Pond et al. 2008, 2010, 2014, Timpano et al. 2015, 2018b). Similarly, the scraper functional feeding group has been shown to be reduced in surface mining-influenced streams, primarily as a result of the loss of several Ephemeroptera scraper taxa (Pond et al. 2014, Timpano et al. 2018b). These results suggest that sensitive benthic macroinvertebrates (i.e. scrapers and Ephemeroptera) may have limited recovery despite gradual recovery of water chemistry (i.e. decreases in SC and SO_4:HCO_3). However, I critically note the difference between measures of temporal trends in 30-minute, continuous SC data compared to estimated trends in biological metrics using only seasonal sampling. A more high-resolution sampling approach (e.g., monthly) of macroinvertebrate community metrics may be more effective at identifying temporal trends in biological metrics (Boehme et al. 2016) moving forward with this long-term dataset and in future studies.

Specific conductance may not be the only stressor to benthic macroinvertebrates in these headwater streams. Drover (2018) found significant, negative correlations of Ephemeroptera and scraper richness metrics with water column selenium (Se) concentrations in a subset of the same central Appalachian headwater streams used in this study. Selenium is a naturally occurring trace element but can be elevated to potentially harmful levels in streams influenced by surface mining (USEPA 2016) and has been shown to bioaccumulate to potentially toxic levels in benthic macroinvertebrates (DeBruyn and Chapman 2007, Conley et al. 2009, Whitmore et al. 2018, Chapter 3). In particular, Se can bioaccumulate into stream biofilm (Arnold et al. 2017, Whitmore et al. 2018, Chapter 3), which is consumed by scrapers and several sensitive Ephemeroptera taxa. Therefore, it is possible that Se is an additional stressor to these groups, potentially explaining some of the discrepancy between gradual recovery in water chemistry (i.e. decreasing SC) and absence of positive trends in biological metrics, particularly in Ephemeroptera and scrapers. Long-term assessment of Se temporal trends would help to further identify stressors and lags in macroinvertebrate recovery.

Spatial Patterns in Water Chemistry

Water chemistry in surface mining-influenced headwater streams varies spatially within stream networks. In the absence of tributaries, I observed a general dilution pattern in SC and dissolved major ion concentrations with distance downstream from mined areas under both highflow and baseflow conditions. I suspect this is a result of more dilute groundwater from less intensively mined areas, which increasingly contributes to flow with distance downstream from surface mining activities. For example, in the ROL site, SC after the confluence with Tributary 1

was reduced by 43% under baseflow conditions likely caused by groundwater dilution. Similar patterns, albeit less pronounced, were observed in the other two study streams evaluated for spatial patterns. In addition to groundwater input, tributaries also influenced dissolved ion concentrations, resulting in both enrichment and dilution in my study streams. At site LLE, three tributaries contributed SC-enriched streamwater under highflow and baseflow. Tributary 4 at this site had SC approximately three times higher than the mainstem under baseflow. Conversely, ROL had three dilute tributaries at highflow contributing to lower SC in the mainstem. At site HUR, tributary 5 originating below a valley fill increased the mainstem SC by 49% under baseflow. These results show that tributaries and groundwater can have substantial influence on the salinity of headwater streams by adding water enriched or diluted in dissolved ions.

Flow conditions can also contribute to water chemistry variation within surface mining-influenced stream networks. In the mainstems of the three sampled stream networks, major ion concentrations and SC were typically lower under highflow compared to baseflow conditions and were conservative, tracking with salinity (i.e. SC) at each sample location. Similarly, the majority of tributaries sampled in this study had lower SC and dissolved ion concentrations under highflow conditions. However, one tributary became more enriched with highflow, which likely extended groundwater and surface water networks into new sources of high concentrations of dissolved ions (e.g., recent valley fill material) (Paybins 2003).

My results highlight key drivers of downstream water chemistry in surface mining-influenced watersheds by demonstrating: i) general conservative behavior of major ions, ii) locations and times for elevated ion contribution from specific tributaries, and iii) groundwater dilution from relatively undisturbed areas. Potential downstream consequences for larger, mixed-land use watersheds have been explored by other studies in the central Appalachian coalfield. For example, Johnson et al. (2019) sampled 60 sites in one large eastern Kentucky watershed influenced by surface mining. The authors found high variability in major ions in small sub-watersheds <15 km^2, but then convergent patterns across larger sub-watersheds (>75 km^2) as streams merged into larger orders. Their research and complimentary modeling work (Johnson et al. 2010) suggest that downstream water chemistry represents a mix of land-use activities in headwater catchments and that undisturbed streams provide a vital source of water diluted in dissolved ions. However, this previous work does not directly address the local-scale influence of tributaries and groundwater on dissolved ion concentrations or SC within a watershed or even within a stream reach. My data indicate that these sources for enrichment or dilution can have an influence on dissolved ion concentrations within small headwater watersheds and point to future work to better understand emergent outcomes for downstream water quality.

Despite observations of increased major ion loading from surface mining in the central Appalachian coalfield (Johnson et al. 2010, 2019), less is known about delivery and downstream variation of trace elements, which can have important implications for the condition of aquatic communities. Spatial patterns of trace elements were different than patterns of major ions

throughout my three sampled streams and largely did not track with patterns in SC. Strontium was a notable exception showing conservative patterns in each stream more akin to major ions than the other trace elements. Several trace elements (i.e. Al, Zn, Al, and Fe) had variable concentrations throughout the stream network under both highflow and baseflow conditions. In contrast, downstream Mn concentrations were consistently enriched above stream-origin concentrations in all streams. Concentrations of Mn were also higher under highflow compared to baseflow at the bottom of the stream network in all streams. The lack of dilution of many trace elements and enrichment of others under highflow could have negative, downstream impacts for biological communities. For example, native mussels show decline in richness and abundance in the Clinch and Powell Rivers (Ahlstedt et al. 2005), which have headwaters originating in the central Appalachian coalfield. Elevated concentrations of major ions are likely not the major driver of mussel decline in these rivers (Ciparis et al. 2015). Instead, it has been suggested that chronically elevated concentrations of certain trace elements are a potential cause for regional native mussel decline (Naimo 1995, Zipper et al. 2016). My findings suggest that future work is needed to address delivery of potentially toxic trace elements from surface mining-influenced headwaters to downstream waters.

CONCLUSION

Results from 24 headwater streams in the central Appalachian coalfield suggest that surface coal mining impacts water chemistry and benthic macroinvertebrate communities for at least decades after mining activities cease. I found limited evidence of declining temporal trends in salinity across 19 surface mining-influenced headwater streams over a 7-year period. The magnitude of negative trends in salinity that were observed suggest recovery times on the order of decades for conditions to return to those observed in reference streams. Moreover, the study streams with negative trends in salinity often did not have associated recovery of benthic macroinvertebrate communities. Ephemeroptera and scrapers appear to be the most sensitive of the measured benthic macroinvertebrate metrics to elevated salinity over time. Continuation of this long-term dataset, which is unique in its scope and length, would be invaluable for expanding our understanding of the long-term impacts of surface mining.

The high-resolution spatial sampling of SC, major ions, and trace elements in a subset of three surface mining-influenced headwater streams demonstrated that water chemistry varies substantially within these small watersheds (<1.5 km^2). My results suggest that it is imperative to consider when (i.e. flow conditions) and where (i.e. location in the watershed) water and benthic macroinvertebrate samples are collected to assess stream condition. The marked spatial variability in water chemistry that I observed within surface mining-influenced streams suggests future work to address associated variability in benthic macroinvertebrate community structure. Trace elements did not show the same conservative, dilution patterns of major ions and can be enriched with potential implications for the condition of aquatic organisms in higher-order systems downstream of surface mining. Continuing research into the interaction between groundwater, surface water, and weathering overburden waste rock is needed to

expand knowledge of spatial and flow-variation in water chemistry and aquatic biota in surface mining-influenced headwater streams.

LITERATURE CITED

Ahlstedt, S. A., Fagg, M. T., Butler, R. S., & Connell, J. F. (2005). Long-term trend information for freshwater mussel populations at twelve fixed-station monitoring sites in the Clinch and Powell rivers of Eastern Tennessee and Southwestern Virginia 1979–2004. *Final Report, US Fish and Wildlife Service, Cookeville, TN*, *38501*.

American Public Health Association (APHA). 2005. Standard methods for the examination of water and wastewater. 21st ed. American Public Health Assoc., Washington, DC.

Arnold, M. C., Bier, R. L., Lindberg, T. T., Bernhardt, E. S., & Di Giulio, R. T. (2017). Biofilm mediated uptake of selenium in streams with mountaintop coal mine drainage. *Limnologica*, *65*, 10-13.

Barbour, M. T., Gerritsen, J., Snyder, B. D., & Stribling, J. B. (1999). *Rapid bioassessment protocols for use in streams and wadeable rivers: periphyton, benthic macroinvertebrates and fish* (2nd ed., p. 339). Washington, DC: US Environmental Protection Agency, Office of Water.

Beggel, S., & Geist, J. (2015). Acute effects of salinity exposure on glochidia viability and host infection of the freshwater mussel Anodonta anatina (Linnaeus, 1758). *Science of the Total Environment*, *502*, 659-665.

Blakeslee, C. J., Galbraith, H. S., Robertson, L. S., & St John White, B. (2013). The effects of salinity exposure on multiple life stages of a common freshwater mussel, Elliptio complanata. *Environmental Toxicology and Chemistry*, *32*(12), 2849-2854.

Boehme, E. A., Zipper, C. E., Schoenholtz, S. H., Soucek, D. J., & Timpano, A. J. (2016). Temporal dynamics of benthic macroinvertebrate communities and their response to elevated specific conductance in Appalachian coalfield headwater streams. *Ecological Indicators*, *64*, 171-180.

Burton, J., & Gerritsen, J. (2003). A stream condition index for Virginia non-coastal streams. *Virginia Department of Environmental Quality, Richmond, Virginia, USA*.

Cañedo-Argüelles, M., Hawkins, C. P., Kefford, B. J., Schäfer, R. B., Dyack, B. J., Brucet, S., ... & Coring, E. (2016). Saving freshwater from salts. *Science*, *351*(6276), 914-916.

Ciparis, S., Phipps, A., Soucek, D. J., Zipper, C. E., & Jones, J. W. (2015). Effects of environmentally relevant mixtures of major ions on a freshwater mussel. *Environmental Pollution*, *207*, 280-287.

Clark, E. V., Daniels, W. L., Zipper, C. E., & Eriksson, K. (2018a). Mineralogical influences on water quality from weathering of surface coal mine spoils. *Applied Geochemistry*, *91*, 97-106.

Clark, E. V., Zipper, C. E., Daniels, W. L., & Keefe, M. J. (2018). Appalachian coal mine spoil elemental release patterns and depletion. *Applied Geochemistry*, *98*, 109-120.

Conley, J. M., Funk, D. H., & Buchwalter, D. B. (2009). Selenium bioaccumulation and maternal transfer in the mayfly *Centroptilum triangulifer* in a life-cycle, periphyton-biofilm trophic assay. *Environmental Science & Technology*, *43*(20), 7952-7957.

Daniels, W. L., Zipper, C. E., Orndorff, Z. W., Skousen, J., Barton, C. D., McDonald, L. M., & Beck, M. A. (2016). Predicting total dissolved solids release from central Appalachian coal mine spoils. *Environmental Pollution*, *216*, 371-379

DeBruyn, A. M., & Chapman, P. M. (2007). Selenium toxicity to invertebrates: will proposed thresholds for toxicity to fish and birds also protect their prey?. *Environmental Science & Technology*, *41*(5), 1766-1770.

Drover, D. R. (2018). *Benthic macroinvertebrate community structure responses to multiple stressors in mining-influenced streams of central Appalachia USA* (Doctoral dissertation, Virginia Tech).

Evans, D. M., Zipper, C. E., Donovan, P. F., & Daniels, W. L. (2014). Long-term trends of specific conductance in waters discharged by coal-mine valley fills in central Appalachia, USA. *Journal of the American Water Resources Association*, *50*(6), 1449-1460.

Gerritsen, J., Burton, J., & Barbour, M. T. (2000). A stream condition index for West Virginia wadeable streams. *US EPA Region*, *3*.

Griffith, M. B., Norton, S. B., Alexander, L. C., Pollard, A. I., & LeDuc, S. D. (2012). The effects of mountaintop mines and valley fills on the physicochemical quality of stream ecosystems in the central Appalachians: a review. *Science of the Total Environment*, *417*, 1-12.

Helsel, D. R., & Hirsch, R. M. (2002). *Statistical methods in water resources* (Vol. 323). Reston, VA: US Geological Survey.

Hess, A., Iyer, H., & Malm, W. (2001). Linear trend analysis: a comparison of methods. *Atmospheric Environment*, *35*(30), 5211-5222.

Higgins, C. L., & Wilde, G. R. (2005). The role of salinity in structuring fish assemblages in a prairie stream system. *Hydrobiologia*, *549*(1), 197-203.

Johnson, B. R., Haas, A., & Fritz, K. M. (2010). Use of spatially explicit physicochemical data to measure downstream impacts of headwater stream disturbance. *Water Resources Research*, *46*(9).

Johnson, B., Smith, E., Ackerman, J. W., Dye, S., Polinsky, R., Somerville, E., ... & D'Amico, E. (2019). Spatial Convergence in Major Dissolved Ion Concentrations and Implications of Headwater Mining for Downstream Water Quality. *Journal of the American Water Resources Association*.

Li, J., Zipper, C. E., Donovan, P. F., Wynne, R. H., & Oliphant, A. J. (2015). Reconstructing disturbance history for an intensively mined region by time-series analysis of Landsat imagery. *Environmental Monitoring and Assessment*, *187*(9), 557.

Merricks, T. C., Cherry, D. S., Zipper, C. E., Currie, R. J., & Valenti, T. W. (2007). Coal-mine hollow fill and settling pond influences on headwater streams in southern West Virginia, USA. *Environmental Monitoring and Assessment*, *129*(1-3), 359-378.

Naimo, T. J. (1995). A review of the effects of heavy metals on freshwater mussels. *Ecotoxicology*, *4*(6), 341-362.

Orndorff, Z. W., Daniels, W. L., Zipper, C. E., Eick, M., & Beck, M. (2015). A column evaluation of Appalachian coal mine spoils' temporal leaching behavior. *Environmental Pollution*, *204*, 39-47.

Palmer, M. A., Bernhardt, E. S., Schlesinger, W. H., Eshleman, K. N., Foufoula-Georgiou, E., Hendryx, M. S., ... & White, P. S. (2010). Mountaintop mining consequences. *Science*, *327*(5962), 148-149.

Paybins, K. S. (2003). Flow origin, drainage area, and hydrologic characteristics for headwater streams in the mountaintop coal-mining region of southern West Virginia, 2000–01. *Water Resources Investigations Report*, 02-4300.

Pericak, A. A., Thomas, C. J., Kroodsma, D. A., Wasson, M. F., Ross, M. R., Clinton, N. E., ... & Amos, J. F. (2018). Mapping the yearly extent of surface coal mining in Central Appalachia using Landsat and Google Earth Engine. *PloS one*, *13*(7), e0197758.

Pond, G. J., Passmore, M. E., Borsuk, F. A., Reynolds, L., & Rose, C. J. (2008). Downstream effects of mountaintop coal mining: comparing biological conditions using family-and genus-level macroinvertebrate bioassessment tools. *Journal of the North American Benthological Society*, *27*(3), 717-737.

Pond, G. J. (2010). Patterns of Ephemeroptera taxa loss in Appalachian headwater streams (Kentucky, USA). *Hydrobiologia*, *641*(1), 185-201.

Pond, G. J., Passmore, M. E., Pointon, N. D., Felbinger, J. K., Walker, C. A., Krock, K. J., ... & Nash, W. L. (2014). Long-term impacts on macroinvertebrates downstream of reclaimed mountaintop mining valley fills in central Appalachia. *Environmental Management*, *54*(4), 919-933.

Szöcs, E., Coring, E., Bäthe, J., & Schäfer, R. B. (2014). Effects of anthropogenic salinization on biological traits and community composition of stream macroinvertebrates. *Science of the Total Environment*, *468*, 943-949.

Temnerud, J., & Bishop, K. 2005. Spatial variation of streamwater chemistry in two Swedish boreal catchments: Implications for environmental assessment. *Environmental Science & Technology*, *39*(6), 1463-1469.

Timpano, A. J., Schoenholtz, S. H., Soucek, D. J., & Zipper, C. E. (2015). Salinity as a limiting factor for biological condition in Mining-Influenced central Appalachian headwater streams. *Journal of the American Water Resources Association*, *51*(1), 240-250.

Timpano, A. J., Vander Vorste, R., Soucek, D. J., Whitmore, K., Zipper, C. E., & Schoenholtz, S. H. (2017). Stream ecosystem response to mining-induced salinization in central Appalachia. *Final report to the Office of Surface Mining Reclamation and Enforcement (OSMRE Cooperative Agreement S15AC20028). Virginia Water Resources Research Institute*.

Timpano, A. J., Zipper, C. E., Soucek, D. J., & Schoenholtz, S. H. (2018a). Seasonal pattern of anthropogenic salinization in temperate forested headwater streams. *Water Research*, *133*, 8-18.

Timpano, A. J., Schoenholtz, S. H., Soucek, D. J., & Zipper, C. E. (2018b). Benthic macroinvertebrate community response to salinization in headwater streams in Appalachia USA over multiple years. *Ecological Indicators*, *91*, 645-656.

Tiwari, T., Buffam, I., Sponseller, R. A., & Laudon, H. (2017). Inferring scale-dependent processes influencing stream water biogeochemistry from headwater to sea. *Limnology and Oceanography*, *62*(S1), S58-S70.

USEPA. (1971). Method 160.1: residue, filterable (gravimetric, dried at 180 °C). Methods for the chemical analysis of water and wastes (MCAWW) (EPA/600/4-79/020)

USEPA. (1996). U. S. *Method1669: Sampling Ambient Water for Trace Metals at EPA Water Quality Criteria Levels*. EPA-821-R-96-011.

USEPA. (2011a). The Effects of Mountaintop Mines and Valley Fills on Aquatic Ecosystems of the Central Appalachian Coalfields. Office of Research and Development, National Center for Environmental Assessment, Washington, DC. EPA/600/R-09/138F

USEPA. (2011b). A field-based aquatic life benchmark for conductivity in central Appalachian streams. Washington, DC: U.S. Environmental Protection Agency, NCEA; 2011. EPA/600/R-10/023A. Available from:http://cfpub.epa.gov/ncea/cfm/recordisplay.cfm?deid=233809.

USEPA. (2016). Aquatic Life Ambient Water Quality Criterion for Selenium – Freshwater. https://www.epa.gov/wqc/aquatic-life- criterion-selenium

Wallace, J. B., & Webster, J. R. (1996). The role of macroinvertebrates in stream ecosystem function. *Annual Review of Entomology*, *41*(1), 115-139.

Whitmore, K. M., Schoenholtz, S. H., Soucek, D. J., Hopkins, W. A., & Zipper, C. E. (2018). Selenium dynamics in headwater streams of the central Appalachian coalfield. *Environmental Toxicology and Chemistry*, *37*(10), 2714-2726.

Zimmer, M. A., Bailey, S. W., McGuire, K. J., & Bullen, T. D. (2013). Fine scale variations of surface water chemistry in an ephemeral to perennial drainage network. *Hydrological Processes*, *27*(24), 3438-3451.

Zipper, C. E., Donovan, P. F., Jones, J. W., Li, J., Price, J. E., & Stewart, R. E. (2016). Spatial and temporal relationships among watershed mining, water quality, and freshwater mussel status in an eastern USA river. *Science of the Total Environment*, *541*, 603-615.

CHAPTER 3 – SELENIUM BIOACCUMULATION ACROSS TROPHIC LEVELS AND ALONG A LONGITUDINAL GRADIENT IN HEADWATER STREAMS INFLUENCED BY SURFACE COAL MINING

INTRODUCTION

Contamination of aquatic systems by the trace element selenium (Se) is a global environmental concern because of its high toxicity and bioaccumulation potential (Lemly 2004). Selenium can be released to the environment from numerous sources, including agricultural irrigation, landfills, metal smelting, phosphate and coal mining, and coal fly-ash waste (Lemly 2004). Selenium is a unique aquatic contaminant because it is both an essential micronutrient and potential toxin. Selenium is utilized at the active site in many proteins, such as selenocysteine and selenomethionine (Young et al. 2010), which perform important roles in numerous biological processes, including immune response, DNA synthesis, and antioxidant defense (Zwolak and Zaporowska 2012). However, even marginal increases in Se concentrations and subsequent uptake can induce stress in aquatic organisms, particularly in egg-laying (oviparous) vertebrates (Fan et al. 2002; Unrine et al. 2006). For example, elevated Se uptake can result in teratogenesis from maternal transfer of Se to embryos (Young et al. 2010). Selenium can also substitute for sulfur in amino acids and produce reactive oxygen species, resulting in oxidative stress (Janz et al. 2010). Further, chronically elevated levels can result in Se ecotoxicity caused by dietary biomagnification through food webs (Lemly 2004), highlighting the importance of monitoring across trophic levels in aquatic systems vulnerable to Se contamination.

In the central Appalachian coalfield region, elevated amounts of Se can be delivered to headwater streams as a result of surface mining activities (USEPA 2011). Surface coal mining is the main driver of land use change in this region (Sayler 2008) with associated impacts to hydrology and chemistry of headwater streams (Bernhardt and Palmer 2011). Surface mining activities expose buried coal seams to the surface by removing overlaying layers of bedrock using explosives and earth-moving equipment (USEPA 2011). Selenium can be enriched in these coal seams and associated geologic materials (Young et al. 2010), where it commonly substitutes for organic sulfur (Coleman et al. 1993) and for sulfur in pyrite (Tuttle et al. 2009). In coal deposits, Se can be found at concentrations up to 80 times above background crustal levels (National Research Council 1980). The resulting waste rock, or overburden, is often deposited into adjacent valleys of headwater streams effectively burying stream channels (Palmer et al. 2010). Selenium is released to the water column from this deposited overburden because of accelerated natural weathering processes, thereby increasing loading of dissolved Se oxyanions (selenite and selenate) to headwater streams (Lussier 2003).

Selenium is of particular environmental concern because it can bioaccumulate in the aquatic food chain (USEPA 2016). Selenium is initially dissolved in the water column where it can be utilized by primary producers or stored in particulate matter, including biofilm, sediments, and

leaf detritus (Luoma and Presser 2009). Bioaccumulation of Se from the water column into particulate matter represents the highest magnification of Se in aquatic systems (USEPA 2016) Smaller, but still significant, increases in biomagnification occur in headwater streams through primary and secondary benthic macroinvertebrate consumers (Whitmore et al. 2018) and into top trophic levels, including fish (Presser 2013, Arnold et al. 2014). However, potential uptake of Se by fish and other aquatic life varies greatly and is driven by dietary preferences and bioavailability of Se at the base of the food web (Presser and Luoma 2010). Further, Se bioavailability differs among Se forms, where the reduced inorganic form, selenite, has higher uptake rates in primary producers (e.g. algae and bacteria) (Araie and Shiraiwa 2009; Franz et al. 2011; Lanctôt et al. 2017; Rosetta and Knight 1995). Despite oxygenated headwater streams being dominated by the less bioavailable and oxidized form, selenate, (Presser 2013), locations with low oxygen (e.g., pools and backwaters with longer water residence times) can increase amounts of selenite (Zhang and Moore 1996, Gao et al. 2000). As such, stream conditions and thus Se speciation can influence bioaccumulation dynamics.

Conceptual models have been used to characterize Se dynamics and trophic transfer in aquatic systems (Presser and Luoma 2010). Selenium bioaccumulation at the base of the food web can be quantified using Enrichment Factors (EF), which represent the ratios of particulate matter Se concentrations to total Se water column concentration. Rates of Se enrichment in particulate matter tend to decline as water Se levels increase, leading to lower EFs at higher Se water column concentrations; such results may indicate that algae and microbes are regulating uptake of Se as needed to meet their metabolic needs (DeForest et al. 2007, 2016). Trophic transfer factors (TFF) quantify Se biomagnification in higher trophic levels as the ratio of Se concentration of an organism to the concentration of its food source. Similar to EFs, TTFs also tend to decline as food-source Se concentrations increase (DeForest et al. 2007). Using this conceptual model, Se bioaccumulation dynamics can be compared across different sites, aquatic species, trophic levels, and stream conditions (Presser and Luoma 2010, Whitmore et al. 2018).

Selenium bioaccumulation in fish tissue is a particular concern because of its negative effects on reproductive success (USEPA 2016). Selenium concentration in fish tissue has been considered by USEPA (2016) as a preferred metric to analyze Se toxicity in water and may replace water column total Se concentrations in regulatory programs (USEPA 2016). Despite the focus on fish tissue in Se bioaccumulation research in many lentic and high-order lotic systems (Arnold et al. 2014; Brandt et al. 2017; Lemly 2002; Muscatello et al. 2008), there has been limited study of Se bioaccumulation in fish tissue in headwater streams of the central Appalachian region. Arnold et al. (2014) studied Se in filet, liver, and ovary tissue in green sunfish (*Lepomis cyanellus*) and creek chubs (*Semotilus atromaculatus*) from the Mud River, WV, which is influenced by surface mining. However, the Mud River is a third-order stream with a hydrologic regime and fish community structure that differs from first-order headwater streams. Research is needed to assess Se bioaccumulation in small-bodied fish in headwater streams influenced by surface mining and thus Se transfer to top aquatic trophic levels in these systems.

When fish are not present in headwater streams, salamanders can be used to analyze Se concentrations in top trophic levels (Patnode et al. 2005). Salamanders are ubiquitous in Appalachian forest ecosystems and consume aquatic macroinvertebrates, yet they have not been well-studied in central Appalachian coalfield streams for Se bioaccumulation. Patnode et al. (2005) found elevated Se levels in several species of Plethodontid salamanders below valley fills compared to reference conditions. However, this study did not link salamander Se concentrations to those in water column and lower trophic levels (e.g., benthic macroinvertebrates). Salamanders perform an important ecological role by transferring energy between aquatic and terrestrial systems in headwater streams (Davic and Welsh 2004). Therefore, it is possible that salamanders represent a critical, but largely unknown, link in the transfer of Se originating in headwater streams below surface mining to adjacent terrestrial systems (Patnode et al. 2005).

Similarly, little is known about how Se bioaccumulation dynamics may change with distance downstream in headwater streams influenced by surface mining. Selenium water column concentrations may decrease with distance from Se source because of upstream bioaccumulation and possible dilution by groundwater. However, bioaccumulated Se can be carried downstream through physical displacement (e.g., drift of particulates and macroinvertebrates) and organism movement. Further, stream conditions can influence Se speciation (Zhang and Moore 1996, Lemly 1999, Gao et al. 2000, Oram et al. 2010), highlighting an additional driver of Se bioaccumulation that may vary with stream length. Therefore, it is unclear if bioaccumulation levels in various ecosystem components will decline moving downstream from the surface mining impact and thus the Se source.

OBJECTIVES

In this study, I evaluated Se bioaccumulation in multiple trophic levels within and across six central Appalachian headwater stream reaches with variable water column Se concentrations to address three primary objectives:

1. Assess bioaccumulation into top trophic levels at each site by comparing Se concentrations across ecosystem media, including fish and salamanders.
2. Evaluate site differences by comparing Se concentrations in individual media types and Se dynamics (i.e. EFs and TTFs) across study streams.
3. Assess longitudinal trends in Se concentrations and bioaccumulation dynamics within each study stream.

METHODS

Site Selection

Reconnaissance trips were made during the winter of 2018 to identify six study streams from a larger set of 24 streams that have been monitored in other studies (Timpano et al. 2018, Chapter 2) for surface mining impacts to water quality and benthic macroinvertebrate community structure. The six study streams were selected to meet the following criteria: 1) at least 1 km of stream reach without tributaries, 2) forested riparian buffer throughout the stream reach, and 3) lack of features such as settling ponds that could influence Se bioavailability. The selected streams were divided into three categories (reference, low-Se, and high-Se) based on historic Se water column measurements (Timpano 2017) and Se bioaccumulation in *Gomphidae* larvae and *Cambaridae* (Whitmore et al. 2018) (Table 3-1). The six study streams spanned a gradient of salinity (i.e. dissolved ions measured as specific conductance) (Table 3-1) and geographic area within the central Appalachian coalfield from southwestern Virginia to southern West Virginia (Figure 3-1).

Table 3-1: Watershed characteristics of six central Appalachian headwater streams selected for selenium bioaccumulation study.

Site ID	sub category	study reach length (m)	annual mean SC[1] (µs/cm)	water column Se µg/L (2013-2018)[2]	watershed area (km^2)	Tissue Samples (µg/g dry wt)[5] *Gomphidae*	*Cambaridae*
EAS	Reference	1200	26	<MDL[3]	2.42	-	0.97
HCN	Reference	1600	67	<MDL	5.96	2.11	0.58
FRY	Low Se	1200	382	<MRL[4]	5.66	5.17	-
CRA	Low Se	1600	425	<MRL	9.77	-	-
LLC	High Se	1600	1218	8.5	4.34	11.82	6.86
ROC	High Se	1600	719	11.8	7.13	-	9.07

[1]Annual mean specific conductance (SC) calculated using 30-minute continuous data from Chapter 1. [2]Median Se water column concentration from historic, biannual monitoring of 24 headwater streams in the central Appalachian coalfield (Timpano 2017) [3]<MDL – less than the method detection limit of 0.5 µg/L Se. [4]<MRL – less than the method reporting limit of 2.5 µg/L Se. [5]Selenium tissue concentrations of *Gomphidae* larvae and *Cambaridae* adults from Whitmore et al. (2018).

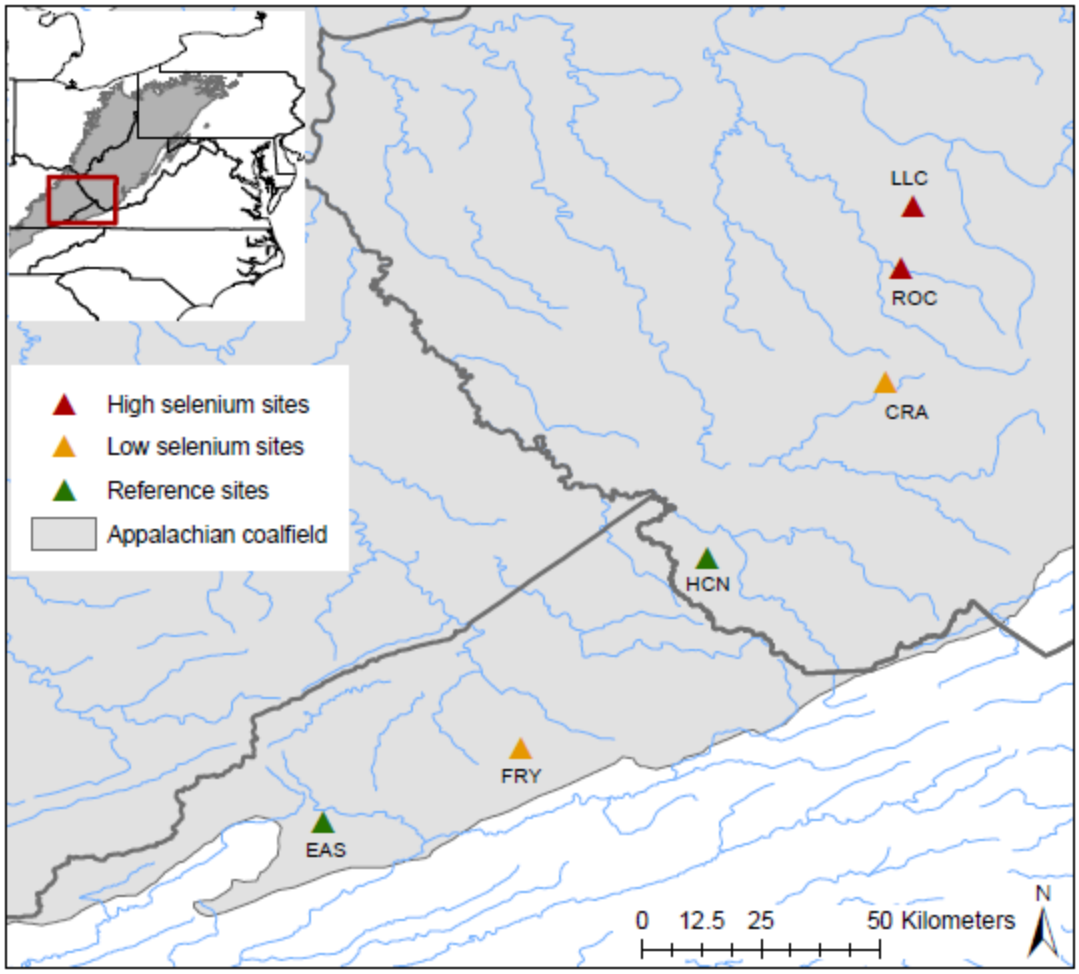

Figure 3-1: Location of the six central Appalachian headwater streams for selenium bioaccumulation study. Stream Se categories are based on water column Se concentrations measured from fall 2013-spring 2018 (Timpano 2017) and Se concentrations in *Gomphidae* and *Cambaridae* measured in summer 2015 (Whitmore et al. 2018).

Study Stream Sampling Design

During the summer of 2018 (June-August), I collected a full suite of Se bioaccumulation media, including streamwater, leaf detritus, biofilm, sediment, benthic macroinvertebrates, salamanders, and fish (when present) from each study stream. Water column Se concentrations were sampled every 400 m (Figure 3-2). All other ecosystem media (leaf detritus, sediment, biofilm, benthic macroinvertebrates, salamanders, and fish) were collected within a 50-m reach upstream of each water sample location. The 50-m reach was further divided into 10-m sections for representative collection of streambed sediment. Four streams had five collection points for a total of 1,600 m of stream length and two streams had four collections points for a total of 1,200 m of stream length.

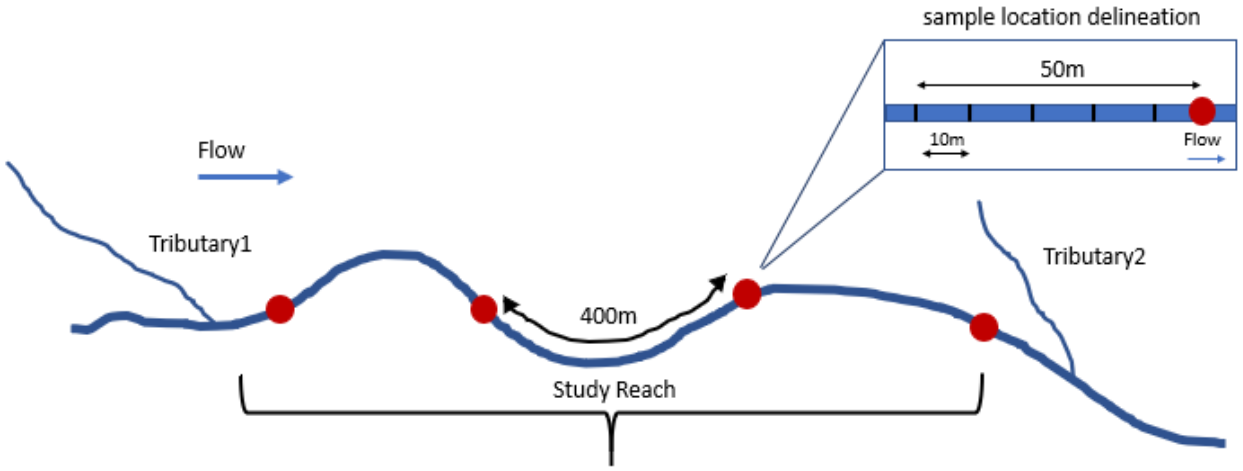

Figure 3-2: Schematic of experimental design (flow is from left to right). The study stream reach begins below Tributary1 and ends above Tributary2 to isolate a single Se source. Water column Se concentrations were sampled every 400m (represented by the red circle). All other ecosystem media (leaf detritus, sediment, biofilm, benthic macroinvertebrates, salamanders, and fish) were collected within a 50 m reach upstream of each water sample location. The 50 m reach was further divided into 10 m sections for representative collection of streambed sediment.

Field and Laboratory Methods

Water Column Sampling and Analysis

At each sample location (Figure 3-2), water for analysis of Se was collected at a point location in a clean, plastic bucket below a riffle where streamwater was vertically mixed. Collected water was drawn into a sterile 60-ml syringe and pushed through a 0.45 µm pore filter into pre-labeled, sterile Fisherbrand® whirl-pak bags. Approximately six drops of 1+1 concentrated ultrapure nitric acid was added to lower the pH below 2 (USEPA 1996a). Samples were kept in a cooler on ice and transported to the lab where they were stored in a cold room at 4°C until analysis on an ICP-MS for total Se (Thermo iCAP-RQ) (USEPA 1996a) (Table 3-7).

Water for analysis of Se speciation was collected at in a clean, plastic bucket below a riffle where streamwater was vertically mixed. Unfiltered streamwater was stored in pre-labeled, sterile Fisherbrand® whirl-pak bags and kept on ice until storage at 4°C. A custom method was developed for selenium speciation analysis of selenomethionine (SeMet), selenite (SeIV), and selenate (SeVI) in streamwater. Samples were filtered through 0.45 µm PTFE membranes before being injected for analysis. After filtration, the Se species were analyzed by first separating the species using an Agilent 1100 series HPLC system equipped with two Agilent Poroshell 120 EC-C18 columns (4.6 mm x 50 mm x 2.7 µm). These columns were chosen because of their effective retention of analytes combined with low pressure builds. The isocratic separation utilized a flow rate of 0.5 mL/min of an aqueous buffer that was compatible

with both the columns and the ICP-MS. The buffer was comprised of 25 mM ammonium citrate, 5 mM tetrabutylammonium chloride, and 2% (v/v) methanol. The separated Se species were then detected at 78 m/z using an Agilent 7900 ICP-MS operating in helium collision cell mode to reduce or remove potential polyatomic interferences.

Media Sampling and Processing

Streambed Sediment: A composite sample of stream bed sediment was made within each 50-m sample location using an acid-washed plastic scoop. Collection was limited to a depth of 1-3 cm to isolate biologically active sediments (USEPA 2001). Samples were taken from representative hydrologic features (i.e. pool, run, and riffle) inside each 10-m sub-section (Figure 3-2) and composited to obtain a representative sample for the sample location. Sediment was placed in a light-excluding Fisherbrand® whirl-pak bag and kept on dry ice during transport. Sediment was stored at -20 ^{0}C until sample processing. In the laboratory, sediment was thawed and hand-pressed through a stainless-steel 1-mm sieve and collected into a stainless-steel bowl (USEPA 2001). The sieved sample was homogenized and stored in Corning® brand 15-ml sterile vials and re-frozen. Samples were lyophilized for at least four days to ensure complete drying before digestion.

Biofilm: When present within the 50-m sample reach, epilithic biofilm was collected into light-excluding Fisherbrand® whirl-pak bags by scraping rocks with an acid-washed plastic knife. However, epilithic biofilm was not present at numerous sample locations likely because of dense shade present at these forested, headwater streams in summer. When epilithic biofilm was not present, sandy substrate visibly covered with biofilm was collected using an acid-washed plastic scoop and stored in light-excluding Fisherbrand® whirl-pak bags. Biofilm samples were kept on dry ice until storage in the freezer at -20 ^{0}C. In the laboratory, epilithic biofilm was thawed and gently rinsed of sediment and other extraneous materials using deionized (DI) water. Sandy biofilm samples were thawed and placed in an acid-washed glass beaker. To remove excess sediment from these samples, I followed methods in Whitmore et al. (2018). Specifically, DI water was added to the glass beaker containing the biofilm mixture and shaken to thoroughly mix the sample. Contents of the beaker were allowed to settle and then decanted into another acid-washed glass beaker. This process was repeated to arrive at a composite biofilm sample effectively reduced of mineral sediments. Biofilms were stored in Corning® brand 15-ml sterile vials and re-frozen. Samples were lyophilized for at least four days to ensure complete drying before digestion.

Leaf Detritus: All brown, submerged leaves found within each 50-m sample reach were collected into light-excluding Fisherbrand® whirl-pak bags. Green leaves were not collected because of their short residence time in the stream environment. Leaves were found in logjams, caught between rocks, and in leaf-packs. Composite leaf samples were kept on dry ice until storage in the freezer at -20^{0}C. Leaves were thawed in the laboratory and identified to species if possible (Appendix B). However, most of the collected leaf material was unidentifiable. Thawed leaf material was gently washed with DI water to remove sediment and

other debris and was dried in the oven at 65^{0}C for >5 days to ensure complete drying. After drying, leaf mid-stems were removed, and the remaining leaf material was prepared for digestion by grinding the sample in a ball mill for 1 min at a vibration frequency of 25 sec^{-1} (Whitmore et al. 2018).

Benthic Macroinvertebrates: Benthic macroinvertebrates were sampled within the 50m sample locations in each study stream using a D-frame kicknet and multi-habitat procedures (Barbour et al. 1999). Collected specimens were gently placed into plastic tubs filled with streamwater and separated into glass beakers based on whether they were prey or predator. Approximately 10 cm^3 of both prey and predator benthic macroinvertebrates were collected for the purpose of ensuring adequate biomass ($\geq$0.25 g dry wt) for Se analysis. Prey and predator benthic macroinvertebrates were placed with streamwater in Fisherbrand® whirl-pak bags and kept on dry ice until storage at -20 ^{0}C. In the laboratory, the benthic macroinvertebrates were quickly thawed and identified to family (Appendix D). In cases where a family taxon had both predacious and non-predacious functional feeding groups based on Merritt and Cummins (1996), individuals were further identified to genus. Individuals from the *Tipula* and *Pteronarcys* families were separated from the other prey taxa because of their disproportionately large body sizes. Separated benthic macroinvertebrates were stored in Corning® brand 15-ml sterile vials and re-frozen. Samples were lyophilized for at least four days to ensure complete drying. To prepare samples for digestion, the composite samples for prey and predator macroinvertebrates, *Tipula*, and *Pteronarcys* were then ground to a coarse powder with a mortar and pestle.

Salamanders: Two species of salamanders, the northern dusky salamander (*Desmognathus fuscus*) and seal salamander (*Desmognathus monticola*) were collected within the 50-m sample locations in each study stream. These salamanders are common in headwater streams in forests of Virginia and West Virginia and are the top predator in such stream ecosystems; they generally feed at night and consume both terrestrial and aquatic macroinvertebrates (Felix and Pauley 2006; Shipman et al. 1999). Salamanders were collected with an aquatic dipnet by overturning logs and rocks at the streambank interface where they are commonly found. Captured salamanders where euthanized in a solution of ethyl 3-aminobenzoate methane-sulphate (MS-222) buffered with sodium bicarbonate. Euthanized salamanders were kept in Fisherbrand® whirl-pak bags, transported back to the lab on dry ice, and stored at -20 ^{o}C. In the laboratory, salamanders were quickly thawed and then identified to species, measured for length, and stored in Corning® brand 15-ml sterile vials and re-frozen (Appendix D). Salamanders were lyophilized for at least four days to ensure complete drying. Prior to digestion, individual salamanders were homogenized and ground to a coarse powder with a mortar and pestle.

Fish: Predominately two species of fish, blacknose dace (*Rhinichthys atratulus*) and creek chub (*Semotilus atromaculatus*) were collected within the 50-m sample locations in each study stream. These fishes are largely insectivores and are top predators in headwater streams of

central Appalachia when present (McMahon 1982; Trial et al. 1983). Other collected species included the mottled sculpin (*Cottus bairdi*), bluegill (*Lepomis macrochirus*), and white shiner (*Luxilus albeolus*). Fish were collected using barrel minnow traps baited with oyster crackers. Collected fish were euthanized in a solution of ethyl 3-aminobenzoate methane-sulphate (MS-222) buffered with sodium bicarbonate. Euthanized fish were kept in Fisherbrand® whirl-pak bags, transported back to the lab on dry ice, and stored at -20 ^{o}C. In the laboratory, fish were quickly thawed, identified to species, and measured for length (Appendix B). Stomach contents of fish were removed to avoid any possible contamination from recent ingestion. Individual fish were homogenized in a blender and lyophilized for at least four days to ensure complete drying before digestion.

Acid Digestion and Se Analysis

Dry-weight Se concentrations of freeze-dried media were analyzed using microwave acid digestion (USEPA 1996b). For sediment, <2.0 g of freeze-dried sample material was used, whereas <0.6 g was used for all other media. Samples were weighed and placed in Teflon vessels along with 10ml of trace metal grade nitric acid (70% HNO_3). Vessels were sealed and placed in a microwave digestion unit (Mars6Express, CEM Corp., Matthews, NC). Vessels were brought up to a temperature of 200 ^{o}C within a ramp time of 15 minutes and held at 200 ^{o}C for 20 minutes. Vessels were allowed to cool overnight. Then, the content of each vessel was quantitatively poured into a 50-ml volumetric flask, brought up to volume with DI water, and shaken vigorously to ensure complete mixing. Samples were allowed to settle for >4 hours and were poured into sterile scintillation vials. This solution underwent a further 1:10 dilution before analysis for Se on an ICP-MS (Thermo iCAP-RQ).

Samples were analyzed in batches of 20 with two replicates of certified reference material (Tort-3, National Research Council Canada) and one blank exposed to the same laboratory procedures. 93% of reference material digestions were within the certified range of 9.9-11.9 mg Se/kg and 100% of blanks were <MDL for Se (0.07 µg/L). Lab duplicates were made for every ten samples and averaged 9.4% difference.

DATA ANALYSIS

R-studio software (RStudio, Boston, MA) was used for all statistical analyses. Enrichment factors (EF) and trophic transfer factors (TTF) of Se were calculated from equations provided in Presser and Luoma (2010) (Table 3-2). Enrichment factors were calculated as the ratio of Se concentrations in living and non-living particulates at the bottom of the food chain (i.e. leaf detritus, sediment, and biofilm) to water column Se concentration. Dissolved Se concentrations in the water column that produced <MDL results were statistically analyzed as half the MDL, a value of 0.035 µg/L Se. Trophic transfer factors were calculated as the ratio of Se concentration in an individual taxon to the Se concentration in its food source. Three TFFs were calculated for primary consumers: $TTF_{1^{0}\,consumer\text{-}sediment}$, $TTF_{1^{0}\,consumer\text{-}leaf\,detritus}$, and $TTF_{1^{0}\,consumer\text{-}biofilm}$ (Table 3-2). A final TFF was calculated between Se concentrations in primary-consumer macroinvertebrates and predator macroinvertebrates ($TTF_{predator\text{-}1^{0}\,consumer}$). *Tipula* and

Pteronarcys were not included in calculations of primary-consumer Se concentrations. Trophic transfer factors for fish and salamanders were not calculated because of their variable dietary preferences, which include media other than predator macroinvertebrates, including terrestrial inputs as well as particulate material and primary consumers.

Table 3-2: Equations for Enrichment Factors (EF) and Trophic Transfer Factors (TTF) used to assess selenium dynamics in headwater streams of the central Appalachian coalfield.

Enrichment Factors[1]	**Trophic Transfer Factors**[1]	
EF	**TTF_1**	**TTF_2**
$EF_{sediment} = \frac{\text{sediment}}{\text{water column}}$	$TTF_{1^oconsumer\text{-}sediment} = \frac{\text{Invertebrate prey}}{\text{sediment}}$	$TTF_{predator\text{-}1^oconsumer} = \frac{\text{Invertebrate predator}}{\text{Invertebrate prey}}$
$EF_{biofilm} = \frac{\text{biofilm}}{\text{water column}}$	$TTF_{1^oconsumer\text{-}biofilm} = \frac{\text{Invertebrate prey}}{\text{biofilm}}$	
$EF_{leaf\ detritus} = \frac{\text{leaf detritus}}{\text{water column}}$	$TTF_{1^oconsumer\text{-}leaf\ detritus} = \frac{\text{Invertebrate prey}}{\text{leaf detritus}}$	

[1]EFs and TTFs calculated as ratios of Se concentrations in media.

Site-level Comparisons of Media Se Concentrations

To assess bioaccumulation at each site, I used Se media concentrations from all sampling locations in a one-way ANOVA to test for differences among media types. If the result of the ANOVA was statistically significant, a TukeyHSD was used to test all pairwise comparisons. An alpha value of 0.05 was used for all tests.

Across-Site Comparison of Media Se Concentrations, EFs, and TTFs

To evaluate site differences, I compared site-level results (via 4-5 sampling locations per stream) for individual media Se concentrations, EFs, and TTFs across all study streams. I used a one-way ANOVA to test differences among sites, followed by a TukeyHSD when statistically significant to test all pairwise comparisons. An alpha value of 0.05 was used for all tests.

Within-Site Variation Along a Longitudinal Gradient

I also assessed within-site variation and possible longitudinal trends in Se concentrations and dynamics using simple linear regressions of Se dry-weight concentrations, EFs, and TTFs from each sampling location versus distance downstream. I also conducted a simple linear regression between %selenate and %selenite and distance downstream in one high-Se stream (ROC) to explore possible influences of Se speciation on bioaccumulation rates. A Shapiro-Wilk test was used to test the normality of the data and a Breusch-Godfrey test was used to test for autocorrelation.

RESULTS

Site-level Comparisons of Media Se Concentrations

Results demonstrated Se biomagnification (from water column to particulates to macroinvertebrates) across all study streams (Figure 3-3). Biofilm had the highest mean particulate Se concentration in five streams, with Se concentrations statistically higher than sediment in five streams and higher than leaf detritus in three streams. In all streams except HCN, primary-consumer macroinvertebrates and predator macroinvertebrates had the highest mean Se concentrations compared to all other media. Four study streams did not show a significant difference between primary-concern and predator macroinvertebrate Se concentrations. The reference stream EAS had significantly higher Se concentrations in predator macroinvertebrates, whereas the high-Se stream ROC had statistically higher Se concentrations in primary-consumer macroinvertebrates.

Salamanders had significantly lower Se concentrations than both primary-consumer and predator macroinvertebrates in all but one study stream (Figure 3-3). In the reference stream EAS, salamander Se concentrations were statistically lower than predator macroinvertebrates but not statistically different from primary-consumer macroinvertebrates. I observed no significant difference between Se concentrations in salamander species (seal and northern dusky) across all study streams.

Similar to salamanders, fish Se concentrations were consistently lower compared to macroinvertebrate concentrations. Three species of fish (blacknose dace, creek chub, mottled sculpin) were collected at the reference stream, HCN. In this stream, there was not a significant difference in Se concentrations among macroinvertebrates and blacknose dace and mottled sculpin (Figure 3-3). However, creek chub had significantly lower Se concentrations than macroinvertebrates and the other fish species. Only the blacknose dace had higher Se concentrations than the salamanders. No fish were collected from the reference stream, EAS. In both low-Se streams (FRY, CRA), blacknose dace was the only fish species collected, with significantly higher Se concentrations compared to both salamander species. Blacknose dace Se concentrations were not different from macroinvertebrate Se concentrations at CRA but were significantly lower than primary-consumer macroinvertebrate concentrations at FRY (Figure 3-3).

Three species of fish (bluegill, white shiner, and creek chub) were collected at the high-Se stream ROC. Selenium concentrations in these three species of fish were not statistically different from one another (Figure 3-3). Although mean Se concentrations were numerically greater in these fish than salamanders, I did not detect any significant differences between them. However, Se concentrations in all fish species were significantly lower compared to macroinvertebrates. At the other high-Se stream, LLC, mottled sculpin had significantly greater Se concentrations than blacknose dace and creek chub, which themselves did not differ statistically (Figure 3-3). Selenium concentrations in blacknose dace and mottled sculpin were statistically greater than in salamanders, but creek chub Se did not differ statistically from

salamander Se in LLC. Selenium concentrations in creek chub and blacknose dace were statistically lower than macroinvertebrate concentrations. I did not detect a difference between mean Se concentrations in mottled sculpin and macroinvertebrates.

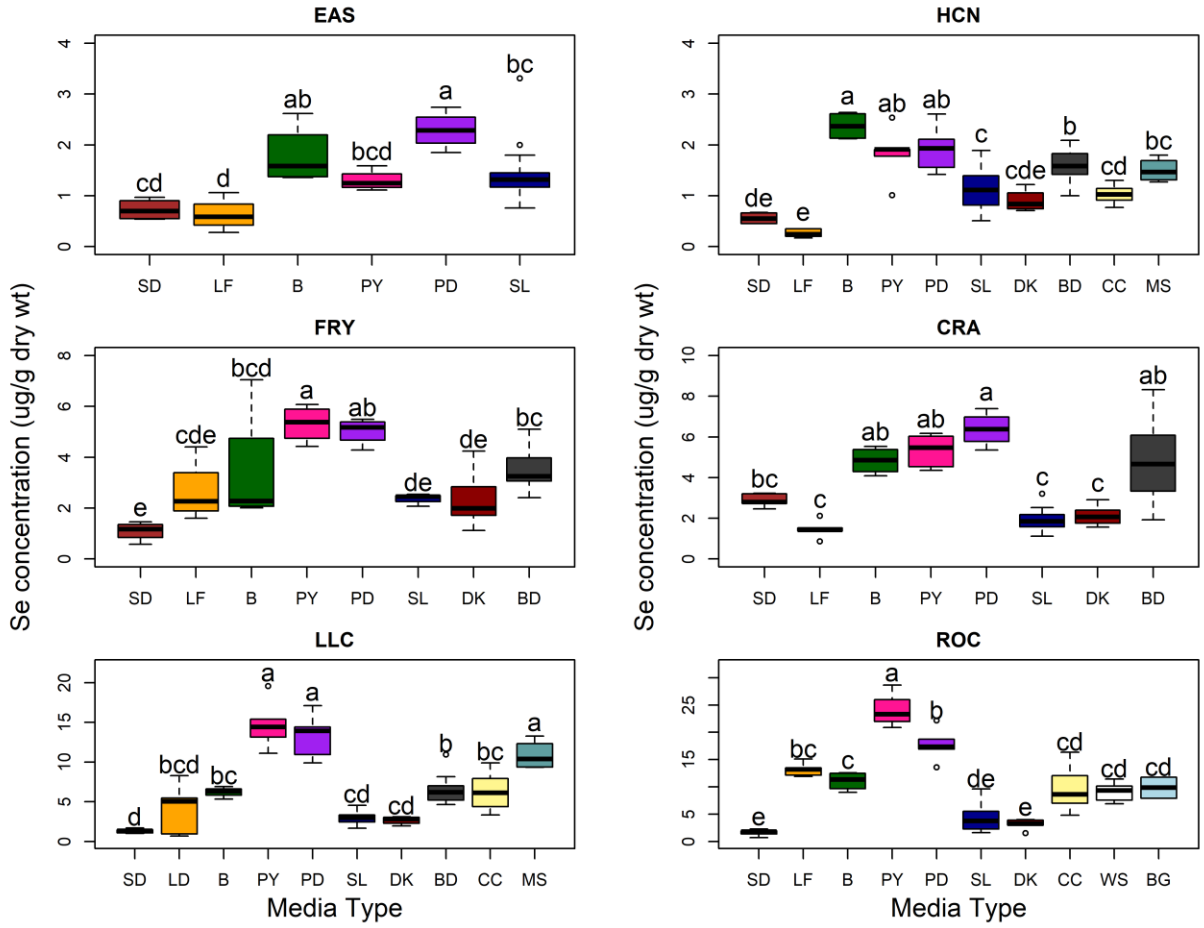

Figure 3-3: Boxplots of selenium (Se) concentrations in ecosystem media within each stream collected at 4-5 sampling locations per stream (Top-ref, Middle-low-Se, Bottom-high-Se) in the central Appalachian coalfield. Letters represent statistically significant differences in media Se concentration within each stream based on TukeyHSD, alpha=0.05. SD-sediment, LF-leaf detritus, B-biofilm, PY-primary consumer benthic macroinvertebrates, PD-predator benthic macroinvertebrates, SL-seal salamander, DK, northern dusky salamander, BD-blacknose dace, CC-creek chub, MS-mottled sculpin, WS-white shiner, BG-bluegill.

Across-Site Comparison of Media Se Concentrations, EFs, and TTFs

I compared mean Se concentrations in individual media types across sites to assess the influence of water column Se on media Se concentrations. Water column Se concentrations were <MDL (0.07 µg/L) for all nine sample locations at the two reference streams (EAS, HCN)

(Figure 3-4). Although this precluded pairwise comparisons with the reference streams, Se concentrations at the two low-Se streams were approximately six times greater than the MDL. Water column Se concentrations in the high-Se streams were significantly greater than in the low-Se streams (Figure 3-4), with values approximately 20 times greater than low-Se streams and 110 times greater than the MDL. Only the high-Se streams (ROC, LLC) had Se concentrations of sufficient magnitude to analyze for Se speciation. For these two streams, selenate was the dominate form, accounting for 97% of measured Se at ROC and 100% at LLC. Selenomethionine (SeMet) was below detection for both sites. Selenite was detected at only ROC, accounting for approximately 3% of measured Se.

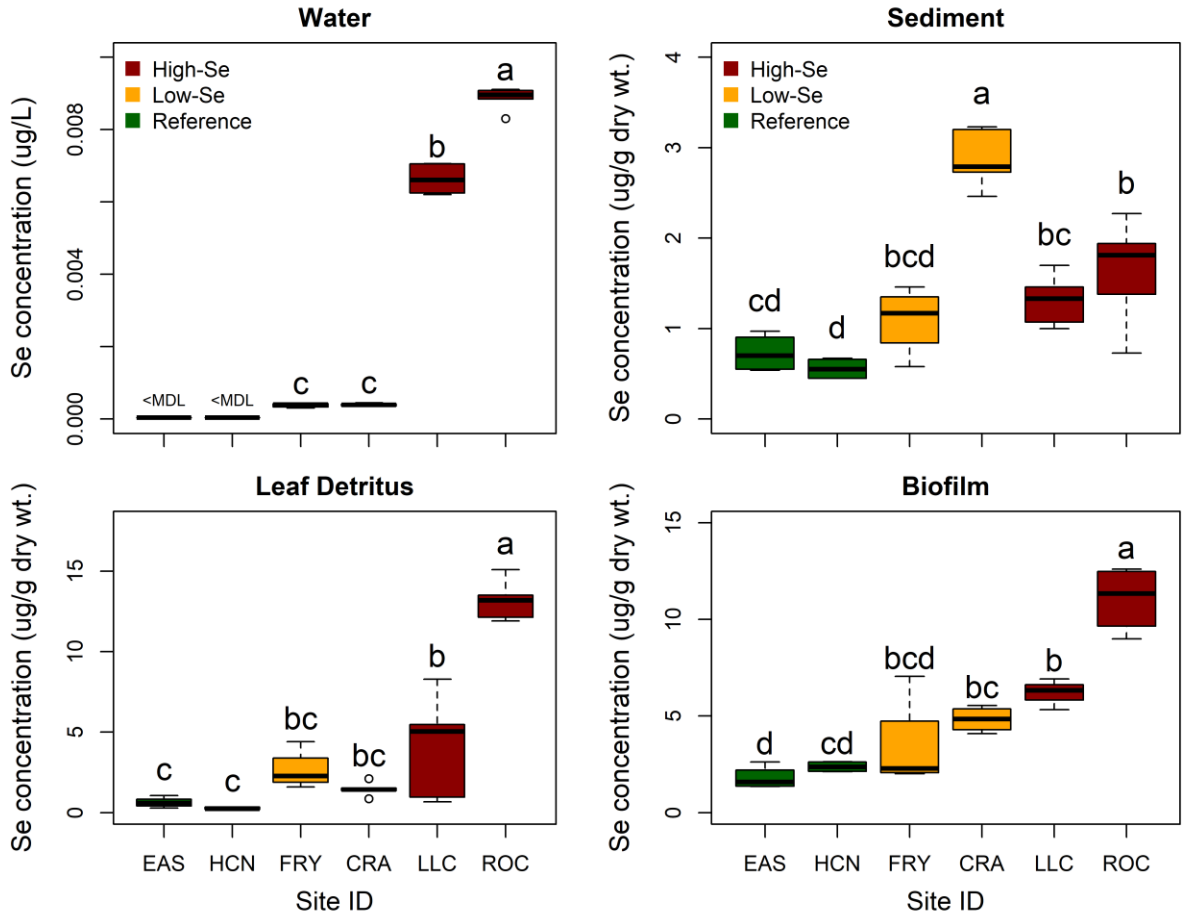

Figure 3-4: Boxplots of Se concentrations in water column and particulate matter across sites collected at 4-5 sampling locations per site in the central Appalachian coalfield. Letters represent statistically significant differences in particulate matter Se concentrations among sites according to TukeyHSD, alpha=0.05.

Despite clear site differences in water-column Se concentrations, sediment concentrations were more similar across study sites (0.54 – 3.23 µg Se g^{-1} dw) (Figure 3-4). The low-Se stream CRA had significantly higher concentrations compared to the other five study streams (Figure 3-4). Significant differences in sediment Se concentration were also detected between the two high-Se streams (ROC, LLC) and the reference stream (HCN). Selenium concentration in leaf detritus was more variable across sites (0.28 – 8.29 µg Se g^{-1} dw), with significantly higher Se concentrations in high-Se streams than in reference streams. The high-Se stream ROC had the highest mean Se concentration in leaf-detritus. For biofilm, Se concentrations were also highest in the high-Se stream ROC. The other high-Se stream, LLC, had significantly higher biofilm concentrations, along with ROC, compared to both reference streams (HCN, EAS).

For primary-consumer macroinvertebrates, high-Se streams had elevated Se concentrations compared to the other study streams for all media sampled (Figure 3-5). Primary-consumer macroinvertebrate Se concentrations were approximately 12 times higher at high-Se streams than at reference streams and four times higher than low-Se streams. However, primary-consumer macroinvertebrate Se concentrations from low-Se and reference streams did not differ statistically. Selenium concentrations in predator macroinvertebrates showed the same trend, with high-Se streams concentrations being approximately seven times higher than reference stream concentrations and three times higher than low-Se stream concentrations. However, salamander Se concentrations were more similar across streams with statistical differences only being observed in the northern dusky salamander between ROC (high-Se) and HCN (low-Se) and in the seal salamander between both high-Se streams and both reference streams (Figure 3-5). Fish (blacknose dace and creek chub) showed clear differences across streams (Figure 3-5). Selenium concentrations in both species were significantly different among all streams where these fish were sampled, with lowest Se concentrations in reference streams and highest Se concentrations in high-Se streams. Blacknose dace Se concentrations in the high-Se stream LLC were approximately four times higher than in the reference stream HCN. Creek chub Se concentrations were approximately nine times higher in the high-Se stream ROC than at the reference stream HCN.

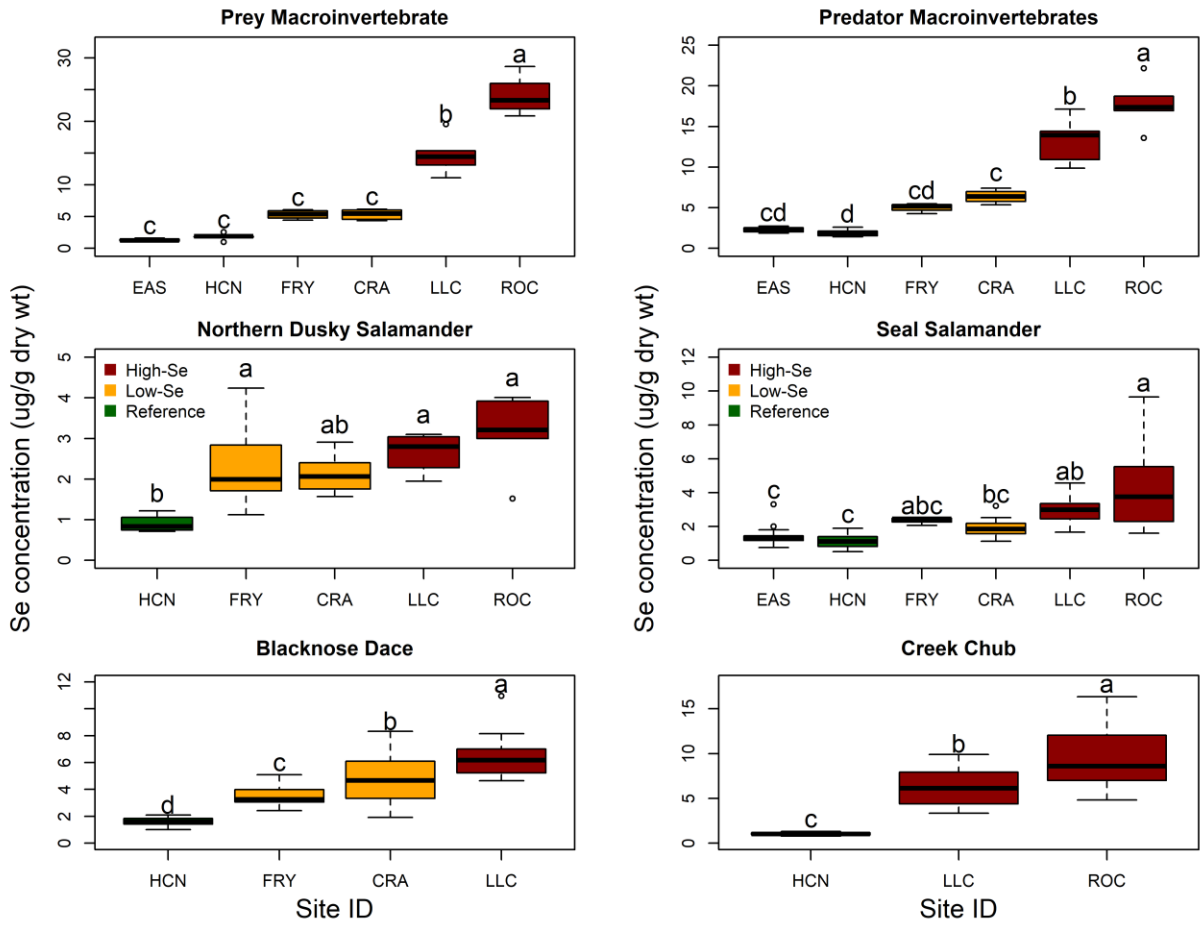

Figure 3-5: Boxplots of Se concentrations in consumers across study streams collected at 4-5 sampling locations per stream in the central Appalachian coalfield. Letters represent statistically significant differences in particulate matter Se concentrations among sites according to TukeyHSD, alpha=0.05.

Enrichment of Se from the water column to sediment, leaf detritus, and biofilm was significantly higher in the reference streams than in low-Se and high-Se streams (Figure 3-6). Enrichment of water column Se to sediment ($EF_{sediment}$) in the reference streams was significantly higher than at the other streams and approximately 95 times higher than high-Se streams (Figure 3-6). Enrichment of water column Se to leaf detritus ($EF_{leaf\text{-}detritus}$) was highest in the reference stream EAS, and approximately four times higher than low-Se sites and 30 times higher than high-Se sites. However, there was no statistical difference between low-Se and high-Se streams for $EF_{leaf\text{-}detritus}$ (Figure 3-6). Enrichment of water column Se to biofilm ($EF_{biofilm}$) was also higher in reference streams than at low-Se and high-Se streams, with $EF_{biofilm}$ approximately five times and 53 times higher at reference streams than low-Se and high-Se streams, respectively. Similar to $EF_{leaf\text{-}detritus}$, there was no significant difference in $EF_{biofilm}$ between low-Se and high-Se sites.

Trophic transfer from sediment to primary-consumer macroinvertebrates ($TTF_{1^0\ consumer\text{-}sediment}$) showed the opposite pattern than EFs, where these TTFs were approximately five times higher in the high-Se streams than at reference streams (Figure 3-6). There was no statistically significant difference between $TTF_{1^0\ consumer\text{-}\ sediment}$ in reference and low-Se streams. Trophic transfer from leaf detritus to primary-consumers ($TTF_{1^0\ consumer\text{-}leaf\ detritus}$) was variable, and no significant differences were observed. Trophic transfer of biofilm to primary-consumers ($TTF_{1^0\ consumer\text{-}biofilm}$) also varied across sites, with higher values in high-Se streams. Both high-Se streams and one low-Se stream (FRY) were significantly higher than reference streams, with $TTF_{1^0\ consumer\text{-}biofilm}$ approximately three times higher in high-Se streams than reference streams. Trophic transfer from primary-consumers to predator benthic macroinvertebrates ($TTF_{predator\text{-}1^0\ consumer}$) showed a similar pattern to EFs with higher values in reference streams than in low-Se and high-Se streams. However, the only statistically significant difference detected was between EAS (higher) and all the other streams.

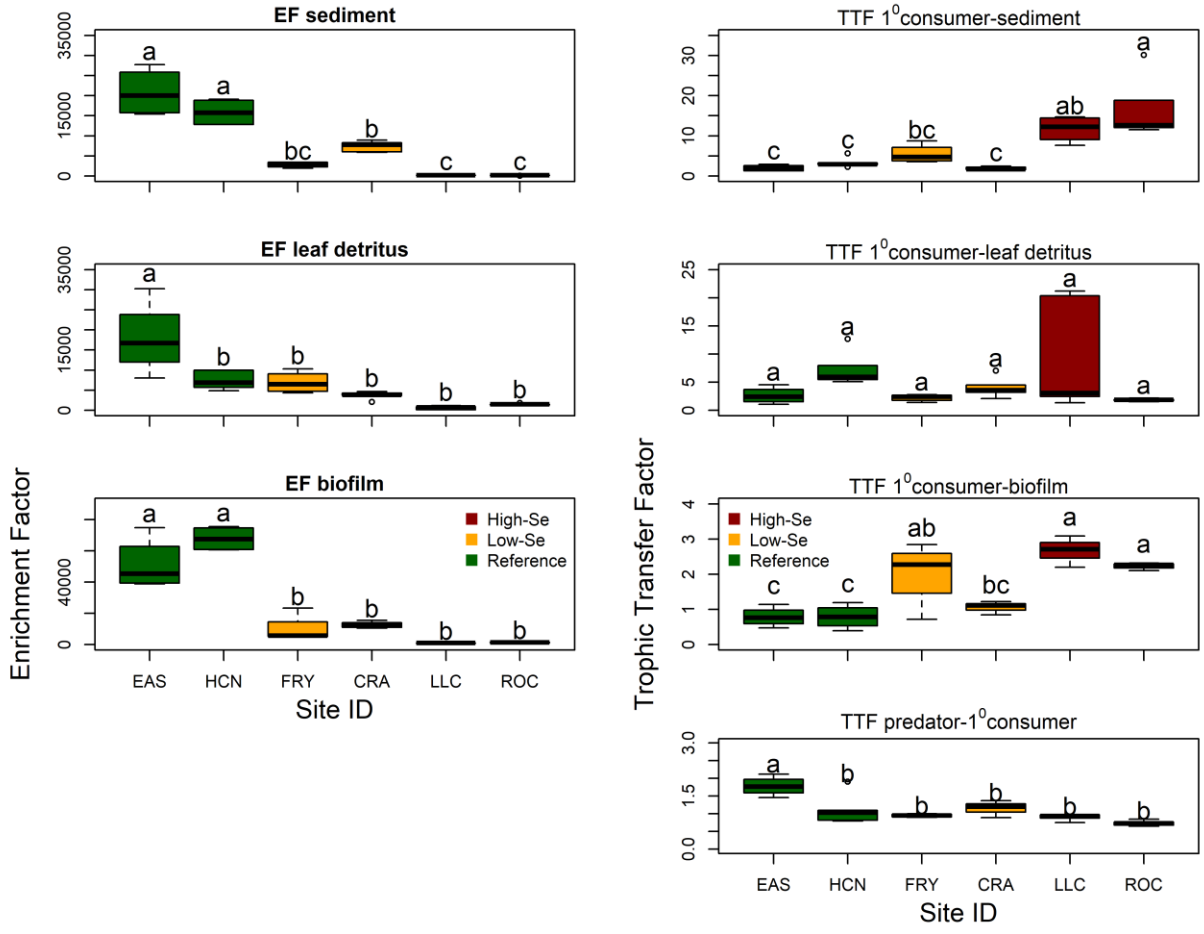

Figure 3-6: Boxplots of selenium enrichment factors (EFs) and selenium trophic transfer factors (TTFs) across study streams using 4-5 sampling locations per stream I the central Appalachian coalfield. Letters represent statistically significant differences in EFs or TTFs across sites according to TukeyHSD, alpha=0.05

Within-Site Variation Along a Longitudinal Gradient

In addition to site-level differences in media concentrations and associated EFs and TTFs, I also observed some within-site variation (i.e. boxplot distributions for each stream in Figures 3-4 – 3-6). However, I found few statistically significant trends in Se concentrations or dynamics along longitudinal downstream gradients within my study streams (Table 3-3) (Appendix D). Reference streams had no significant longitudinal trends. One low-Se stream (CRA) had three significant trends with distance downstream: 1) decreasing leaf detritus Se concentrations (p-value=0.016), 2) decreasing EF leaf detritus-water (p-value = 0.037), and 3) increasing $TTF_{1^0 \text{ consumer-leaf detritus}}$ (p-value=0.028). Both high-Se streams had decreasing longitudinal trends in water column Se (LLC p-value=0.091, ROC p-value=0.045). Despite these decreases in water column Se concentrations, there were few downstream trends in Se media concentrations or Se dynamics in these two high-Se streams. At ROC, I observed an increasing trend in enrichment of biofilm from the water column ($EF_{biofilm}$, p-value=0.023). At LLC, Se concentration in leaf detritus (p-value=0.023) and $EF_{leaf\text{-}detritus}$ (p-value=0.037) decreased with distance downstream, whereas $TTF_{1^0 \text{ consumer- sediment}}$ increased (p-value=0.006).

Table 3-3: Summary table of downstream trends in Se bioaccumulation in headwater streams of the central Appalachian coalfield.

		Se tissue concentrations										EFs[2]			TTFs[3]			
Site ID	**Type**	**water column**	**leaf detritus**	**sediment**	**biofilm**	**1^0consumer BMI**	**predator BMI**	***Pteronarcys***	***Tipula***	**salamanders**	**fish**	**sediment**	**leaf detritus**	**biofilm**	**1^0consumer-sediment**	**1^0consumer-biofilm**	**1^0consumer-leaf detritus**	**predator-1^0consumer**
HCN	ref	-	-	-	-	-	-	-	ND	-	-	-	-	-	-	-	-	-
EAS	ref	-	-	-	-	-	-	-	ND	-	ND	-	-	-	-	-	-	-
FRY	low-Se	-	-	-	-	-	-	-	-	-	-	-	-	-	-	-	-	-
CRA	low-Se	-	▼[1]	-	-	-	-	ND	-	-	-	-	▼	-	-	-	▲	-
ROC	high-Se	▼	-	-	-	-	-	ND	-	-	ND	-	-	▲	-	-	-	-
LLC	high-Se	▼*	▼	-	-	-	-	-	ND	-	-	-	▼	-	▲	-	-	-

[1]Arrows indicate directionality of significant longitudinal trends (e.g. ▼ means decrease with distance downstream) at an alpha value of 0.05. (-) represents non-significant trends (P value >0.05). ND represents no data. [2]Enrichment Factors (EFs) calculated by dividing the Se concentration in particulate matter (i.e. sediment, leaf detritus, and biofilm) by the Se concentration in stream water. [3]Trophic Transfer Factors (TTFs) calculated by dividing the Se concentration in benthic macroinvertebrates by the Se concentration in various food sources.

As a preliminarily assessment of a potential driver of downstream differences in Se bioaccumulation, I analyzed a high-Se stream, ROC, for Se speciation at each of five sample locations. I observed longitudinal trends (albeit non-significant) for the three major forms, where total Se decreased (p-value = 0.065), %selenate increased (p-value = 0.053), and %selenite decreased (p-value = 0.053) (Table 3-4). Selenomethionine was below detection for all sample locations within the stream. Selenate ranged from 95.10-96.48%. Selenite ranged from 3.52-4.90%.

Table 3-4: Water-column selenium speciation at sample locations within the high-Se stream ROC in the central Appalachian coalfield.

Distance downstream	[Se as Sum of Species]	%selenate	%selenite	%SeMet
0	7.77	95.10	4.90	ND
400	7.82	95.54	4.46	ND
800	7.66	95.73	4.27	ND
1200	7.53	95.56	4.44	ND
1600	6.85	96.48	3.52	ND

[1]Selenite concentrations were below the limit of quantification (1.00 µg/L), but above the assigned limit of detection (0.3 µg/L) and should be considered estimated values. [2]ND- values below the limit of detection (0.3 µg/L).

DISCUSSION

In this work, I assessed Se bioaccumulation and dynamics across six headwater streams in the central Appalachian coalfield. In addition, I evaluated longitudinal trends in Se bioaccumulation and dynamics within each study stream. I also conducted preliminary analysis of Se speciation at two high-Se streams and along a longitudinal gradient in one high-Se stream. Findings clearly demonstrated Se biomagnification, from water column to particulate matter and higher trophic levels in these headwater streams. Further, there was little evidence of longitudinal trends in Se concentrations and dynamics within individual stream reaches over limited stream lengths (1-2 km) with no tributaries. Few other published studies have analyzed Se bioaccumulation and speciation in central Appalachian headwater streams (Whitmore et al. 2018), highlighting the importance of this and future research to further understand the consequences and drivers of Se bioaccumulation and toxicity in headwaters, which account for 70-80% of the total stream network length in central Appalachia (USEPA 2011).

Site-level Comparisons in Media Se concentrations

Surface coal mining can increase concentrations of dissolved Se in headwater streams in central Appalachia (USEPA 2011), with subsequent bioaccumulation into ecosystem media (Presser 2013, Arnold et al. 2014, 2017, Whitmore et al. 2018). At three of the four surface mining-

influenced streams in this study, both biofilm and leaf detritus had greater mean Se concentrations than streambed sediment. Whitmore et al. (2018) found similar results from six surface mining-influenced headwater streams in central Appalachia across seasons (i.e. spring and fall). Primary-consumer and predator benthic macroinvertebrates had the highest mean Se concentrations in all study streams. However, I did not find greater Se concentrations in predator benthic macroinvertebrates than primary-consumer macroinvertebrates in any low-Se or high-Se streams. In one high-Se stream, primary-consumer benthic macroinvertebrates had significantly higher Se concentrations than predator macroinvertebrates. In contrast, Whitmore et al. (2018) and Presser (2013) found elevated Se concentrations in composite predator macroinvertebrates compared to primary-consumer macroinvertebrates as predicted by trophic transfer models (Presser and Luoma 2010). I suspect that differences in seasonal community composition of composite primary-consumer and predator samples may be a cause of this discrepancy.

Notably, across all streams, Se concentrations were lower in salamanders and fish compared to benthic macroinvertebrates. I suspect that lower concentrations in these higher trophic levels are primarily a result of their varied feeding habits. Benthic macroinvertebrates feed exclusively on aquatic media (e.g. leaf detritus and biofilm) that are exposed to Se in the water column, whereas fish and salamanders can consume a variety of food (i.e. not exclusively benthic macroinvertebrates), including terrestrial media not exposed to Se (Jenkins and Burkhead 1993, Felix and Pauley 1996). In addition, salamanders and fish are more mobile than macroinvertebrates. Consequently, salamanders and fish may be feeding in downstream reaches with lower concentrations of Se as a result of diluted tributary inputs. Similar to the results of my study, Presser (2013) also found lower Se concentrations in creek chub compared to composite invertebrate samples in surface mining-influenced streams in southern WV. However, comparisons to other fish species were not made by Presser (2013).

In contrast, I observed some variability in Se concentrations among fish species. At the high-Se stream LLC, whole-body Se concentrations were highest in mottled sculpin and lower in blacknose dace and creek chub. At the reference stream HCN, blacknose dace had higher Se whole-body concentrations than creek chub. Differences in Se concentrations among fish species is likely a result of different feeding habits (Besser et al. 1996, USEPA 2016). Mottled sculpin are predominately benthic insectivores feeding on aquatic insect larvae, whereas blacknose dace and creek chubs are opportunistic omnivores feeding on a variety of food, including aquatic invertebrates, algae, zooplankton, terrestrial insects, and other fish (Jenkins and Burkhead 1993). These results suggest that in surface mining-influenced headwater streams, elevated Se concentrations in benthic macroinvertebrates are major contributors to Se concentrations in fish tissue, particularly the insectivorous mottled sculpin, and that considering feeding habits is important when selecting fish species for sampling in headwater streams.

In summary, these results demonstrate that in these headwater ecosystems: 1) enrichment of particulate material, especially biofilms and leaf detritus, is an important step in the trophic pathway of Se, 2) benthic macroinvertebrates have the highest Se concentrations among sampled media, and 3) Se concentrations differ among fish species, with important implications for monitoring and regulation of Se influenced by surface mining.

Across-Site Comparison of Media Se Concentrations, EFs, and TTFs

Despite clear differences in water column Se concentrations, Se sediment concentrations were relatively similar across all six study streams. Previous work has shown that as much as 90% of the total amount of Se in aquatic systems can be stored in the top few centimeters of sediment and organic detritus (Lemly and Smith 1987). Selenium becomes immobilized in sediments when the oxygenated form, selenate, is reduced to selenite by chemical and biological processes. Reduced Se can undergo adsorption onto clay particles, coprecipitation, and complexation (Lemly 1999). However, this process is slow and is more pronounced in lentic systems (Presser 2013). It is likely that in the fast-moving headwater streams studied here, immobilization of Se into sediment is limited by water residence time. Whitmore et al. (2018) found elevated Se concentrations in streambed sediment from surface mining-influenced streams compared to reference conditions. However, similar to results in this study, the difference between Se sediment concentrations among their surface mining-influenced and reference streams was small.

Site differences for Se concentrations in biofilm, leaf detritus, and benthic macroinvertebrates followed water column Se concentrations more closely than sediment. Biofilm Se concentrations in this study were approximately two times higher at high-Se streams than at low-Se streams and two times higher in low-Se streams than in reference streams. Similarly, Arnold et al. (2017) observed increased Se concentrations in multiple types of biofilm (2.7 ± 0.2 µg Se g^{-1} dw) from one surface mining-influenced reach of the Mud River, WV compared to reference conditions (1.3 ± 0.1 µg Se g^{-1} dw). Whitmore et al. (2018) also documented elevated Se concentrations in biofilms from six surface mining-influenced headwater streams (0.49 – 5.15 µg Se g^{-1} dw) compared to reference conditions (0.26 – 0.86 µg Se g^{-1} dw). Selenium concentrations in leaf detritus followed a similar patter to biofilm being approximately four times higher in high-Se streams than in low-Se streams and five times higher in low-Se streams than in reference streams, comparable to results found in Whitmore et al. (2018). Primary-consumer benthic macroinvertebrates Se concentrations were also elevated at surface mining-influenced streams, being approximately four times higher in high-Se streams than low-Se and three times higher in low-Se than reference. Similarly, predator Se concentrations were approximately three times higher in high-Se streams than low-Se and three times higher in low-Se than reference. Whitmore et al. (2018) reported similar concentrations in primary-consumer and predator benthic macroinvertebrates in central Appalachian headwater streams.

Salamanders in high-Se streams had higher whole-body Se concentrations compared to other study streams. Whole-body salamander Se concentrations from low-Se and high-Se streams in this study (0.51 – 9.65 µg Se g^{-1} dw) are within the range of concentrations found in other *Desmognathus* salamanders (1.06 – 14.32 µg Se g^{-1} dw) living in streams and seeps below surface mining in the central Appalachian coalfield (Patnode et al. 2005). Although there is an absence of empirical studies addressing the toxicity of Se to these salamanders, Patnode et al. (2005) used literature-based toxicity data to estimate risk potential. They estimated a Se toxicity reference value (TRV) of 4.0 µg Se g^{-1} dry weight and found reduced species diversity and abundance in salamander species assemblages in headwater streams that exceeded this value. Approximately 26% of salamanders collected from my high-Se streams and 6% of salamanders collected from my low-Se streams exceeded this TRV. These results indicate that Se may be negatively impacting salamanders in high-Se streams as well as highlight the need for future research that addresses Se toxicity to salamanders in the central Appalachian coalfield.

Similar to salamanders, fish sampled from streams with elevated water column Se also had higher whole-body Se concentrations than fish in reference streams. Blacknose dace (*Rhinichthys atratulus*) was the most commonly collected fish species being present in four of the six study streams. Blacknose dace whole-body Se concentrations were approximately two times higher at high-Se streams compared to low-Se streams and three times higher at low-Se streams compared to reference streams. Creek chub whole-body Se concentrations followed a similar pattern being approximately seven times higher at high-Se streams compared to reference streams.

A major consequence of elevated water column Se in aquatic systems is bioaccumulation into fish tissues and subsequent impacts on reproductive success (USEPA 2016). To address this problem, USEPA (2016) established an aquatic life criterion for Se concentration in whole-body fish of 8.5 µg Se g^{-1} dw. Fish tissue Se concentrations are preferred to water column measurements of Se and will likely take precedent in regulatory matters (USESPA 2016). The whole-body criterion was established as the fifth percentile of 15 genus mean critical values (GMCVs) calculated using literature studies of Se reproductive effects. In my study, fish species sampled did not exceed the aquatic life criterion at reference or low-Se streams. However, several fish at the two high-Se streams exceeded this criterion. Five mottled sculpin individuals (100%), four creek chub (27%), one blacknose dace (8%), and one bluegill (50%) exceeded whole-body Se concentration of 8.5 µg Se g^{-1} dw in high-Se streams. A full analysis of fish deformities associated with high whole-body Se concentrations was outside of the scope of this study; however, a general visual inspection revealed no obvious abnormalities in fish collected at high-Se sites. Nevertheless, my results indicate that Se is bioaccumulating to levels exceeding established criteria (USEPA 2016) in some of the species collected, particularly the mottled sculpin. Other species, such as the creek chub and blacknose dace, may not be as affected despite high water column Se concentrations. More detailed toxicological studies addressing the reproductive impacts of Se in these headwater fish species is needed as they are absent from the USEPA (2016) analysis of GMCVs. These GMCVs include bigger gamefish species such

as brown trout (*Salmo trutta*), northern pike (*Esox lucius*), and largemouth bass (*Micropterus salmoides*) while largely ignoring smaller-sized fish species that are more common in headwater streams of the region.

Enrichment of Se from water to particulate matter is the largest increase in Se bioaccumulation, with rates highly dependent on water column Se concentrations (Presser and Luoma 2010). Enrichment factors for the three particulate materials in my study were higher in reference streams (8,000 – 30,826) than low-Se streams (1,912 – 23,456) and high-Se streams (80 – 1,489). DeForest et al. (2007) and Whitmore et al. (2018) observed similar patterns where water column Se increases were associated with relative decreases in enrichment of Se into particulate matter. Enrichment factors from high-Se streams (80 – 1,489) are within range of others presented in the literature. For example, Kuchapski and Rasmussen (2015) reported enrichment of Se concentrations from water column to biofilm in two rivers in the Canadian Rockies (1,400 and 2,230 respectively). Presser and Luoma (2010) presented EFs ranging from 107 to >2,000 in lentic and lotic systems in a review of Se bioaccumulation field studies. In the central Appalachian coalfield, Presser (2013) observed EFs of water column Se to suspended particulate material ranging from 180 to 1,365.

Across the six study streams, I observed first-level trophic enrichment of Se from particulate material to primary-consumer benthic macroinvertebrates with $TTF_{1^0\ consumer\text{-}sediment}$ and $TTF_{1^0\ consumer\text{-}biofilm}$ highest in high-Se streams, whereas $TTF_{1^0\ consumer\text{-}leaf\ detritus}$ had no significant differences across sites. Mean first-level TTFs calculated in this study (1.8 – 8.8) were elevated compared to some other values in the literature. Presser and Luoma (2010) found first-level TTFs ranging from 2.3 to 3.2 in multiple groups of benthic macroinvertebrates including stoneflies, caddisflies, Chironomid, and composite samples. Similarly, Kuchapski and Rasmussen (2015) found mean first-level TTFs (1.82– 3.20) from Se concentrations in biofilm to composite invertebrates. However, Whitmore et al. (2018) presented higher first-level TTFs than this study (2.4 – 24.5) in similar central Appalachian headwater streams.

Second-level trophic transfer of Se between primary-consumer and predator macroinvertebrates varied across the study streams. Reference stream, EAS, was the only study stream that showed trophic transfer of Se from primary-consumer macroinvertebrates to predator macroinvertebrates with $TTF_{predator\text{-}1^0consumer}$ ranging from 1.46 – 2.12. Consequently, EAS was the only stream with statistically higher Se concentrations in predator macroinvertebrates than primary-consumer macroinvertebrates. Conversely, the high-Se stream, ROC, was the only stream to have statistically higher Se concentrations in primary-consumer macroinvertebrates than predator macroinvertebrates. As a result, trophic transfer from primary-consumer macroinvertebrates to predator macroinvertebrates was less than one in this stream (0.65 – 0.85). The remaining four study streams did not have statistically different Se concentrations between primary-consumer and predator macroinvertebrates. Trophic transfer factors in these streams ranged from 0.75 – 1.37. Mean second-level TTFs in this study

(0.7 – 1.8) were lower than those found in other central Appalachian headwater streams (1.3 – 2.6) by Whitmore et al. (2018).

Within-Site Variation and Longitudinal Trends in Se Bioaccumulation

Selenium concentrations in ecosystem media as well as enrichment into particulate material and subsequent transfer to higher trophic levels were not constant across sample locations within a stream. However, I found no significant longitudinal trends in Se media concentrations or dynamics in reference streams and only a few trends in the low-Se study streams. Four significant longitudinal trends were found in the high-Se streams despite moderate decreasing trends in water column Se. These data suggest that, within headwater stream reaches of similar size (1-2km) and hydrology, Se concentrations in ecosystem media are influenced by chronic, temporally dynamic water column Se concentrations (Appendix F) and possible physical and organismal movement of bioaccumulated material. However, more research is needed over larger spatial scales, where dilution may be more pronounced.

Longitudinal trends in Se speciation do not appear to be a factor in bioaccumulation dynamics within these headwater streams at the spatial scale of this study. Headwater streams sampled in this study are dominated by selenate (>95%), which is the least bioavailable form of selenium to algal autotrophs (Araie and Shiraiwa 2009; Franz et al. 2011; Lanctôt et al. 2017; Rosetta and Knight 1995). Presser (2013) found similar results from rivers in southern WV influenced by surface mining with five streams containing 86-96% selenate. However, I did observe moderately significant (p-value = 0.053) longitudinal trends in Se speciation in one high-Se stream, where the proportion of total Se as selenate increased by 1.38% with concordant decreases in selenite. Loss of the more reduced selenite may be attributable to oxidation or preferential biological uptake (Simmons and Wallschläger 2005). These results from one headwater stream are preliminary, but highlight a need for future study of Se speciation to better understand its role in local and downstream bioaccumulation dynamics in the central Appalachian coalfield.

CONCLUSION

This study demonstrated bioaccumulation of Se to potentially toxic levels in headwater streams influenced by surface mining in the central Appalachian coalfield. Particulate matter, benthic macroinvertebrates, salamanders, and fish had consistently elevated Se concentrations in surface mining-influenced streams compared to reference conditions. Biofilm and leaf detritus had higher mean Se concentrations than sediment, highlighting important pathways for Se uptake in these systems. High levels of Se enrichment in biofilm may be an important confounding factor in the sharp declines in scraper richness in headwater streams influenced by surface mining (see Chapter 2). A more detailed analysis of Se concentrations in primary-consumer macroinvertebrates separated by functional feeding group would inform our understanding of macroinvertebrate taxa most at risk to elevated water column Se. This is important future research because benthic macroinvertebrates, not top trophic levels (i.e. fish and salamanders), had the highest Se concentrations of ecosystem media evaluated in these

streams. Nonetheless, my results demonstrated that salamanders and fish can bioaccumulate Se to potentially harmful levels in surface mining-influenced headwater stream systems, highlighting the need for research that addresses toxicity of Se to salamanders and fish species found in headwater streams within the study region. Moreover, Se concentrations varied among fish species, likely related to dietary preference and movement patterns, further underscoring the need to further assess species-specific Se toxicity. Lastly, my research found little evidence of longitudinal trends in Se concentrations or dynamics, but these observations were limited to relatively short stream lengths of <2 km. Future work would advance our understanding of Se dynamics in these headwater stream systems by including tributaries and expanding to larger stream lengths with particular focus on drivers of bioaccumulation (e.g., Se speciation) that may vary over longer distances with downstream implications.

LITERATURE CITED

Araie, H., & Shiraiwa, Y. (2009). Selenium utilization strategy by microalgae. *Molecules*, *14*(12), 4880-4891.

Arnold, M. C., Lindberg, T. T., Liu, Y. T., Porter, K. A., Hsu-Kim, H., Hinton, D. E., & Di Giulio, R. T. (2014). Bioaccumulation and speciation of selenium in fish and insects collected from a mountaintop removal coal mining-impacted stream in West Virginia. *Ecotoxicology*, *23*(5), 929-938.

Arnold, M. C., Bier, R. L., Lindberg, T. T., Bernhardt, E. S., & Di Giulio, R. T. (2017). Biofilm mediated uptake of selenium in streams with mountaintop coal mine drainage. *Limnologica*, *65*, 10-13.

Barbour, M. T., Gerritsen, J., Snyder, B. D., & Stribling, J. B. (1999). *Rapid bioassessment protocols for use in streams and wadeable rivers: periphyton, benthic macroinvertebrates and fish* (2nd ed., p. 339). Washington, DC: US Environmental Protection Agency, Office of Water.

Bernhardt, E. S., & Palmer, M. A. (2011). The environmental costs of mountaintop mining valley fill operations for aquatic ecosystems of the Central Appalachians. *Annals of the New York Academy of Sciences*, *1223*(1), 39-57.

Besser, J. M., Giesy, J. P., Brown, R. W., Buell, J. M., & Dawson, G. A. (1996). Selenium bioaccumulation and hazards in a fish community affected by coal fly ash effluent. *Ecotoxicology and Environmental Safety*, *35*(1), 7-15.

Brandt, J. E., Bernhardt, E. S., Dwyer, G. S., & Di Giulio, R. T. (2017). Selenium ecotoxicology in freshwater lakes receiving coal combustion residual effluents: A North Carolina example. *Environmental Science & Technology*, *51*(4), 2418-2426.

Coleman, L., Bragg, L. J., & Finkelman, R. B. (1993). Distribution and mode of occurrence of selenium in US coals. *Environmental Geochemistry and Health*, *15*(4), 215-227.

Davic, R. D., & Welsh Jr, H. H. (2004). On the ecological roles of salamanders. *Annual Review of Ecology, Evolution, and Systematics*, *35*, 405-434.

DeForest, D. K., Brix, K. V., & Adams, W. J. (2007). Assessing metal bioaccumulation in aquatic environments: the inverse relationship between bioaccumulation factors, trophic transfer factors and exposure concentration. *Aquatic Toxicology*, *84*(2), 236-246.

DeForest, D. K., Pargee, S., Claytor, C., Canton, S. P., & Brix, K. V. (2016). Biokinetic food chain modeling of waterborne selenium pulses into aquatic food chains: Implications for water quality criteria. *Integrated Environmental Assessment and Management*, *12*(2), 230-246.

Fan, T. W. M., Teh, S. J., Hinton, D. E., & Higashi, R. M. (2002). Selenium biotransformations into proteinaceous forms by foodweb organisms of selenium-laden drainage waters in California. *Aquatic Toxicology*, *57*(1-2), 65-84.

Felix, Z. I., & Pauley, T. K. (2006). Diets of sympatric Black Mountain and seal salamanders. *Northeastern Naturalist*, *13*(4), 469-476.

Franz, E. D., Wiramanaden, C. I., Janz, D. M., Pickering, I. J., & Liber, K. (2011). Selenium bioaccumulation and speciation in Chironomus dilutus exposed to water-borne selenate, selenite, or seleno-DL-methionine. *Environmental Toxicology and Chemistry*, *30*(10), 2292-2299.

Gao, S., Tanji, K. K., Peters, D. W., & Herbel, M. J. (2000). Water selenium speciation and sediment fractionation in a California flow-through wetland system. *Journal of Environmental Quality*, *29*(4), 1275-1283.

Janz, D. M., DeForest, D. K., Brooks, M. L., Chapman, P. M., Gilron, G., Hoff, D., ... & Skorupa, J. P. (2010). Selenium toxicity to aquatic organisms. *Ecological Assessment of Selenium in the Aquatic Environment*, 141-231.

Jenkins, R. E., & Burkhead, N. M. (1993). *Freshwater fishes of Virginia* (p. 1079). American Fisheries Soc.

Kuchapski, K. A., & Rasmussen, J. B. (2015). Food chain transfer and exposure effects of selenium in salmonid fish communities in two watersheds in the Canadian Rocky Mountains. *Canadian Journal of Fisheries and Aquatic Sciences*, *72*(7), 955-967.

Lanctôt, C. M., Melvin, S. D., & Cresswell, T. (2017). Selenium speciation influences bioaccumulation in Limnodynastes peronii tadpoles. *Aquatic Toxicology*, *187*, 1-8.

Lemly, A. D. (1999). Selenium transport and bioaccumulation in aquatic ecosystems: a proposal for water quality criteria based on hydrological units. *Ecotoxicology and Environmental Safety*, *42*(2), 150-156.

Lemly, A. D. (2002). Symptoms and implications of selenium toxicity in fish: the Belews Lake case example. *Aquatic Toxicology*, *57*(1-2), 39-49.

Lemly, A. D. (2004). Aquatic selenium pollution is a global environmental safety issue. *Ecotoxicology and Environmental Safety*, *59*(1), 44-56.

Lemly, A. D., and G. J. Smith. (1987). *Aquatic Cycling of Selenium: Implications for Fish and Wildlife*, Fish and Wildlife Leaflet 12. U.S. Fish and Wildlife Service, Washington, DC.

Luoma, S. N., & Presser, T. S. (2009). Emerging Opportunities in Management of Selenium Contamination. *Environmental Science & Technology*, 43(22), 8483-8487.

Lussier, C., Veiga, V., & Baldwin, S. (2003). The geochemistry of selenium associated with coal waste in the Elk River Valley, Canada. *Environmental Geology*, *44*(8), 905-913.

McMahon, T. E. (1982). *Habitat suitability index models: creek chub* (No. 82/10.4). US Fish and Wildlife Service.

Merritt, R. W., & Cummins, K. W. (Eds.). (1996). *An introduction to the aquatic insects of North America*. Kendall Hunt.

Muscatello, J. R., Belknap, A. M., & Janz, D. M. (2008). Accumulation of selenium in aquatic systems downstream of a uranium mining operation in northern Saskatchewan, Canada. *Environmental Pollution*, *156*(2), 387-393.

National Research Council. (1980). Panel on the Trace Element Geochemistry of Coal Resource Development Related to Health. *Trace-element Geochemistry of Coal Resource Development Related to Environmental Quality and Health*. National Academy Press.

Oram, L. L., Strawn, D. G., Morra, M. J., & Möller, G. (2010). Selenium biogeochemical cycling and fluxes in the hyporheic zone of a mining-impacted stream. *Environmental Science & Technology*, *44*(11), 4176-4183.

Palmer, M. A., Bernhardt, E. S., Schlesinger, W. H., Eshleman, K. N., Foufoula-Georgiou, E., Hendryx, M. S., ... & White, P. S. (2010). Mountaintop mining consequences. *Science*, *327*(5962), 148-149.

Patnode, K., Kane, C., Ramsey, D., Rhodes, J., and Evans, B., 2005, Salamander assemblage survey of mercury and selenium contaminated headwater sites in the Appalachian mountains of Pennsylvania, Virginia, and West Virginia: United States Fish and Wildlife Service, Region 5, Wheeling West Virginia, 49 p., accessed August 21, 2013, at http:// www.fws.gov/northeast/ecologicalservices/es_test2/pdf/FWSReport_SalamanderAssemblageSurvey_01Aug05.pdf.

Presser, T. S. (2013). *Selenium in Ecosystems Within the Mountaintop Coal Mining and Valley-fill Region of Southern West Virginia: Assessment and Ecosystem-scale Modeling*. US Department of the Interior, US Geological Survey.

Presser, T. S., & Luoma, S. N. (2010). A methodology for ecosystem-scale modeling of selenium. *Integrated Environmental Assessment and Management*, *6*(4), 685-710.

Rosetta, T. N., & Knight, A. W. (1995). Bioaccumulation of selenate, selenite, and seleno-DL-methionine by the brine fly larvae Ephydra cinerea Jones. *Archives of Environmental Contamination and Toxicology*, *29*(3), 351-357.

Sayler, K. L. (2008). Land cover trends: central Appalachians. US Department of the Interior. *US Geological Survey, Washington*.

Shipman, P., Crosswhite, D. L., & Fox, S. F. (1999). Diet of the Ouachita dusky salamander (Desmognathus brimleyorum) in southeastern Oklahoma. *The American Midland Naturalist*, *141*(2), 398-401.

Simmons, D. B., & Wallschläger, D. (2005). A critical review of the biogeochemistry and ecotoxicology of selenium in lotic and lentic environments. *Environmental Toxicology and Chemistry*, *24*(6), 1331-1343.

Timpano, A. J. (2017). *Toward improved assessment of freshwater salinization as a benthic macroinvertebrate stressor* (Doctoral dissertation, Virginia Tech).

Trial, J. G., Stanley, J. G., Batcheller, M., Gebhart, G., Maughan, O. E., & Nelson, P. C. (1983). *Habitat suitability information: blacknose dace* (No. 82/10.41). US Fish and Wildlife Service.

Tuttle, M. L., Breit, G. N., & Goldhaber, M. B. (2009). Weathering of the New Albany Shale, Kentucky: II. Redistribution of minor and trace elements. *Applied Geochemistry*, *24*(8), 1565-1578.

Unrine, J. M., Jackson, B. P., Hopkins, W. A., & Romanek, C. (2006). Isolation and partial characterization of proteins involved in maternal transfer of selenium in the western fence lizard (Sceloporus occidentalis). *Environmental Toxicology and Chemistry*, *25*(7), 1864-1867.

USEPA. (1996a). U. S. *Method1669: Sampling Ambient Water for Trace Metals at EPA Water Quality Criteria Levels*. EPA-821-R-96-011.

USEPA. (1996b). Microwave assisted acid digestion of siliceous and organically based matrices. *OHW, Method*, *3052*.

USEPA. (2001). Methods for Collection, Storage and Manipulation of Sediments for Chemical and Toxicological Analyses: Technical Manual EPA 823-B-01-002.

USEPA. (2011). The Effects of Mountaintop Mines and Valley Fills on Aquatic Ecosystems of the Central Appalachian Coalfields. Office of Research and Development, National Center for Environmental Assessment, Washington, DC. EPA/600/R-09/138F.

USEPA. (2016). Aquatic Life Ambient Water Quality Criterion for Selenium – Freshwater. https://www.epa.gov/wqc/aquatic-life- criterion-selenium

Whitmore, K. M., Schoenholtz, S. H., Soucek, D. J., Hopkins, W. A., & Zipper, C. E. (2018). Selenium dynamics in headwater streams of the central Appalachian coalfield. *Environmental Toxicology and Chemistry*, *37*(10), 2714-2726.

Young T. F., K. Finley, W. J. Adams, J. Besser, W. D. Hopkins, D. Jolley, E. McNaughton, T. S. Presser, D. P. Shaw, J. Unrine. 2010. What You Need to Know about Selenium. In: Chapman PM, Adams JB, Brooks ML et al (eds) Ecological assessment of selenium in the aquatic Environment. CRC Press, Boca Raton, pp 7-46.

Zhang, Y., & Moore, J. N. (1996). Selenium fractionation and speciation in a wetland system. *Environmental Science & Technology*, *30*(8), 2613-2619.

Zwolak, I., & Zaporowska, H. (2012). Selenium interactions and toxicity: a review. *Cell Biology and Toxicology*, *28*(1), 31-46.

CHAPTER 4 - SUMMARY

RESEARCH CONTEXT

Surface coal mining activities are a major driver of land-use change in the central Appalachian coalfield region of the U.S. (Sayler 2008), with observed effects to water quality and biological communities in streams draining impacted areas (USEPA 2011). Previous work has documented that elevated concentrations of dissolved ions impact benthic macroinvertebrates communities in surface mining-influenced headwater streams (Boehme et al. 2016; Merricks et al. 2007; Pond et al. 2008, 2014 Timpano et al. 2015, 2018). Moreover, dissolved ion concentrations can remain elevated in these headwater streams long after mining activities cease (Evans et al. 2014, Pond et al. 2014, Timpano et al. 2018). However, there is limited knowledge regarding possible recovery times of both water quality conditions and benthic macroinvertebrate communities.

In addition to long-term temporal trends in water chemistry, concentrations of dissolved ions can vary spatially within stream networks and with different flow conditions (Timpano et al. 2015). For example, increased flow from storm events can lead to source activation of mined areas resulting in increased concentrations of dissolved ions (Paybins 2000). Further, such spatiotemporal variation may differ among specific water chemistry constituents. Major ions are generally considered conservative and thus exhibit dilution with increased flow downstream (Johnson et al. 2019), whereas trace elements may have more variable behavior across the stream network.

Selenium is a trace element of particular interest in the central Appalachian coalfield because of its toxicity and bioaccumulation potential (USEPA 2011). Selenium is a micronutrient but can result in reproductive deformities and oxidative stress in oviparous vertebrates if bioaccumulated to elevated levels (Fan et al. 2002; Unrine et al. 2006). However, diet and site-specific factors such as water residence time and Se speciation can strongly influence Se bioaccumulation potential. For example, lentic habitats are considered to have increased bioaccumulation potential compared to lotic habitats (USEPA 2016). However, studies have shown that Se can bioaccumulate to potentially toxic levels in headwater streams and rivers draining surface coal mining in central Appalachia (Presser 2013, Arnold et al. 2014, Whitmore et al. 2018).

Research conducted in our group has furthered understanding about surface mining impacts on water quality (Timpano et al. 2017, Timpano et al. 2018a), leaf decomposition (Vander Vorste et al. 2019), and aquatic life (Timpano et al. 2015, Boehme et al. 2016, Timpano et al. 2018b, Whitmore et al. 2018, Pence 2019) in central Appalachian headwater streams. In my study, I continued to build upon this previous work using a long-term dataset of 30-minute, continuous SC data and biannual sampling of benthic macroinvertebrates and water chemistry across 24 headwater streams. My objective was to assess long-term temporal trends in SC, ion matrix, and benthic macroinvertebrate community metrics. Additionally, I used high-spatial resolution sampling across three of these headwater streams to assess spatial and flow-driven variability

of water chemistry constituents. Lastly, I evaluated Se bioaccumulation in multiple trophic levels within and across stream reaches with variable water column Se concentrations.

RESEARCH FINDINGS

Results in Chapter 2 demonstrated very limited recovery of water quality conditions and benthic macroinvertebrate communities, suggesting that surfacing mining-influenced streams will remain altered for long periods of time (ca. decades). Moreover, certain types of benthic macroinvertebrates (i.e. Ephemeroptera and the scraper functional feeding group) appear to be particularly sensitive to surface mining impacts over time. Previous work has shown declines in these macroinvertebrate groups in association with elevated salinity (Pond et al. 2008, 2014, Timpano et al. 2018b). However, Se may be a significant confounding factor in this observed response (Drover 2018, Whitmore et al. 2018). A more detailed analysis of Se concentrations of primary-consumer macroinvertebrates separated by family or functional feeding group would help address this question of direct effects of salinity vs. Se. In addition, continuation of this already rich long-term dataset, which is unique in its scope and length, would be invaluable for expanding our understanding of the long-term impacts of surface mining to the condition of headwater streams.

Chapter 2 also presents results from spatial sampling of SC, major ions, and trace elements in a subset of three surface mining-influenced headwater streams. Other studies have analyzed convergent patterns of dissolved major ions (Johnson et al. 2019), but my work in small headwater catchments and inclusion of trace elements is unique in this region and highlights spatial and flow-driven variation of water chemistry in surface-mining influenced streams. Observed water quality patterns suggest that it is imperative to consider when (i.e. flow conditions) and where (i.e. location in the watershed) water and benthic macroinvertebrate samples are collected to assess stream condition. For example, at the HUR stream, the stream network would be considered unimpaired for SC (<300 µs/cm) above tributary 5 under both highflow and baseflow. However, elevated SC originating from tributary 5 resulted in mainstem SC that exceeds the US EPA 300 µs/cm benchmark level. It is also likely that benthic macroinvertebrates will vary along with SC within a stream network, with important implications for bioassessments. I suggest that future research uses co-located spatial sampling of both water chemistry and benthic macroinvertebrate communities to explore within-site spatial covariation and if across-site associations between water quality and biota are similar to those observed in other research (Timpano et al. 2018b). In addition, spatial and flow-driven concentrations of trace elements have not been well-studied in headwater streams below surface coal mines. My results show that some trace elements increase in concentration under highflow compared to baseflow. This may have important implications for downstream biota (e.g., endemic mussels) and suggests further research to monitor concentrations of trace elements under varying flow conditions in contrast to previous work exclusively focused on baseflow conditions (Timpano et al. 2015, Boehme et al. 2016, Timpano et al. 2018b, Pence 2019).

Results in Chapter 3 demonstrated Se bioaccumulation to potentially toxic levels in headwater streams influenced by surface mining in the central Appalachian coalfield. I found elevated levels of Se in all media types in surface mining-influenced streams compared to reference conditions. Notably, top trophic levels (i.e. fish and salamanders) had lower Se concentrations than benthic macroinvertebrates. However, multiple collected fish had whole-body Se concentrations above the EPA aquatic life criterion (USEPA 2016). Selenium concentrations also varied among fish species, with mottled sculpin having the highest Se concentrations in surface mining-influenced streams. I suspect that this is a result of their diet of aquatic benthic macroinvertebrates compared to the other fish in this study, which have a more varied diet including particulate matter and terrestrial inputs. This has important implications for Se monitoring because some states, including WV in central Appalachia, use Se fish tissue concentrations to assess Se impairment. Similar to fish, I found that salamanders can also bioaccumulate Se to potentially toxic levels (Patnode et al. 2005). However, to my knowledge, there has not been previous study of direct toxicity effects of Se to salamanders found in the central Appalachia coalfield. My results also suggest that salamanders could be used for monitoring of Se in locations where fish are absent (e.g., upstream reaches closest to mining activities).

Chapter 3 also presents preliminary findings for water column Se speciation to explore possible drivers of Se bioaccumulation. These results demonstrated that study headwater streams were dominated by selenate and that there was a slight increase in the proportional amount of selenate with distance downstream in one high-Se stream. Additional research is needed to determine if this decrease in selenate is ecologically important, as well as if this trend holds for longer distances and in other streams. In addition, my study streams did not have fill ponds upstream of sampling locations. These ponds, which are common in headwater streams draining surface mining, may have an effect on Se speciation as a result of lower oxygen conditions and longer water residence times, possibly contributing to higher selenite concentrations downstream.

Lastly, I did not find evidence of longitudinal trends in Se bioaccumulation or dynamics within small stream reaches (<2 km). My research suggests that tributaries may have a substantial effect on Se water column concentrations (Chapter 2) and thus media concentrations (Chapter 3). Building upon results presented in this thesis, future work should expand my sampling techniques to better understand Se transport and bioaccumulation dynamics across larger stream networks.

LITERATURE CITED

Boehme, E. A., Zipper, C. E., Schoenholtz, S. H., Soucek, D. J., & Timpano, A. J. (2016). Temporal dynamics of benthic macroinvertebrate communities and their response to elevated specific conductance in Appalachian coalfield headwater streams. *Ecological Indicators*, *64*, 171-180.

Drover, D. R. (2018). *Benthic macroinvertebrate community structure responses to multiple stressors in mining-influenced streams of central Appalachia USA* (Doctoral dissertation, Virginia Tech).

Evans, D. M., Zipper, C. E., Donovan, P. F., & Daniels, W. L. (2014). Long-term trends of specific conductance in waters discharged by coal-mine valley fills in central Appalachia, USA. *Journal of the American Water Resources Association*, *50*(6), 1449-1460.

Fan, T. W. M., Teh, S. J., Hinton, D. E., & Higashi, R. M. (2002). Selenium biotransformations into proteinaceous forms by foodweb organisms of selenium-laden drainage waters in California. *Aquatic Toxicology*, *57*(1-2), 65-84.

Johnson, B., Smith, E., Ackerman, J. W., Dye, S., Polinsky, R., Somerville, E., ... & D'Amico, E. (2019). Spatial Convergence in Major Dissolved Ion Concentrations and Implications of Headwater Mining for Downstream Water Quality. *Journal of the American Water Resources Association*.

Merricks, T. C., Cherry, D. S., Zipper, C. E., Currie, R. J., & Valenti, T. W. (2007). Coal-mine hollow fill and settling pond influences on headwater streams in southern West Virginia, USA. *Environmental Monitoring and Assessment*, *129*(1-3), 359-378.

Patnode, K., Kane, C., Ramsey, D., Rhodes, J., and Evans, B., 2005, Salamander assemblage survey of mercury and selenium contaminated headwater sites in the Appalachian mountains of Pennsylvania, Virginia, and West Virginia: United States Fish and Wildlife Service, Region 5, Wheeling West Virginia, 49 p., accessed August 21, 2013, at http://www.fws.gov/northeast/ecologicalservices/es_test2/pdf/FWSReport_SalamanderAssemblageSurvey_01Aug05.pdf.

Pence, R. A. (2019). *Comparison of Quantitative and Semi-Quantitative Assessments of Benthic Macroinvertebrate Community Response to Elevated Salinity in central Appalachian Coalfield Streams* (Doctoral dissertation, Virginia Tech).

Pond, G. J., Passmore, M. E., Borsuk, F. A., Reynolds, L., & Rose, C. J. (2008). Downstream effects of mountaintop coal mining: comparing biological conditions using family-and genus-level macroinvertebrate bioassessment tools. *Journal of the North American Benthological Society*, *27*(3), 717-737.

Pond, G. J., Passmore, M. E., Pointon, N. D., Felbinger, J. K., Walker, C. A., Krock, K. J., ... & Nash, W. L. (2014). Long-term impacts on macroinvertebrates downstream of reclaimed mountaintop mining valley fills in central Appalachia. *Environmental Management*, *54*(4), 919-933.

Sayler, K. L. (2008). Land cover trends: central Appalachians. US Department of the Interior. *US Geological Survey, Washington*.

Timpano, A. J., Schoenholtz, S. H., Soucek, D. J., & Zipper, C. E. (2015). Salinity as a limiting factor for biological condition in Mining-Influenced central Appalachian headwater streams. *Journal of the American Water Resources Association*, *51*(1), 240-250.

Timpano, A. J., Vander Vorste, R., Soucek, D. J., Whitmore, K., Zipper, C. E., & Schoenholtz, S. H. (2017). Stream ecosystem response to mining-induced salinization in central Appalachia. *Final report to the Office of Surface Mining Reclamation and Enforcement (OSMRE Cooperative Agreement S15AC20028). Virginia Water Resources Research Institute*.

Timpano, A. J., Zipper, C. E., Soucek, D. J., & Schoenholtz, S. H. (2018a). Seasonal pattern of anthropogenic salinization in temperate forested headwater streams. *Water Research*, *133*, 8-18.

Timpano, A. J., Schoenholtz, S. H., Soucek, D. J., & Zipper, C. E. (2018b). Benthic macroinvertebrate community response to salinization in headwater streams in Appalachia USA over multiple years. *Ecological Indicators*, *91*, 645-656.

Unrine, J. M., Jackson, B. P., Hopkins, W. A., & Romanek, C. (2006). Isolation and partial characterization of proteins involved in maternal transfer of selenium in the western fence lizard (Sceloporus occidentalis). *Environmental Toxicology and Chemistry*, *25*(7), 1864-1867.

USEPA (United States Environmental Protection Agency). 2011. The Effects of Mountaintop Mines and Valley Fills on Aquatic Ecosystems of the Central Appalachian Coalfields. Office of Research and Development, National Center for Environmental Assessment, Washington, DC. EPA/600/R-09/138F.

USEPA. (2016). Aquatic Life Ambient Water Quality Criterion for Selenium – Freshwater. https://www.epa.gov/wqc/aquatic-life- criterion-selenium

Vander Vorste, R., Timpano, A. J., Cappellin, C., Badgley, B. D., Zipper, C. E., & Schoenholtz, S. H. (2019). Microbial and macroinvertebrate communities, but not leaf decomposition, change along a mining-induced salinity gradient. *Freshwater Biology*, *64*(4), 671-684.

Whitmore, K. M., Schoenholtz, S. H., Soucek, D. J., Hopkins, W. A., & Zipper, C. E. (2018). Selenium dynamics in headwater streams of the central Appalachian coalfield. *Environmental Toxicology and Chemistry*, *37*(10), 2714-2726.

APPENDIX A - GRAPHS OF CONTINUOUS SC DURING THE STUDY PERIOD (2011-2019)

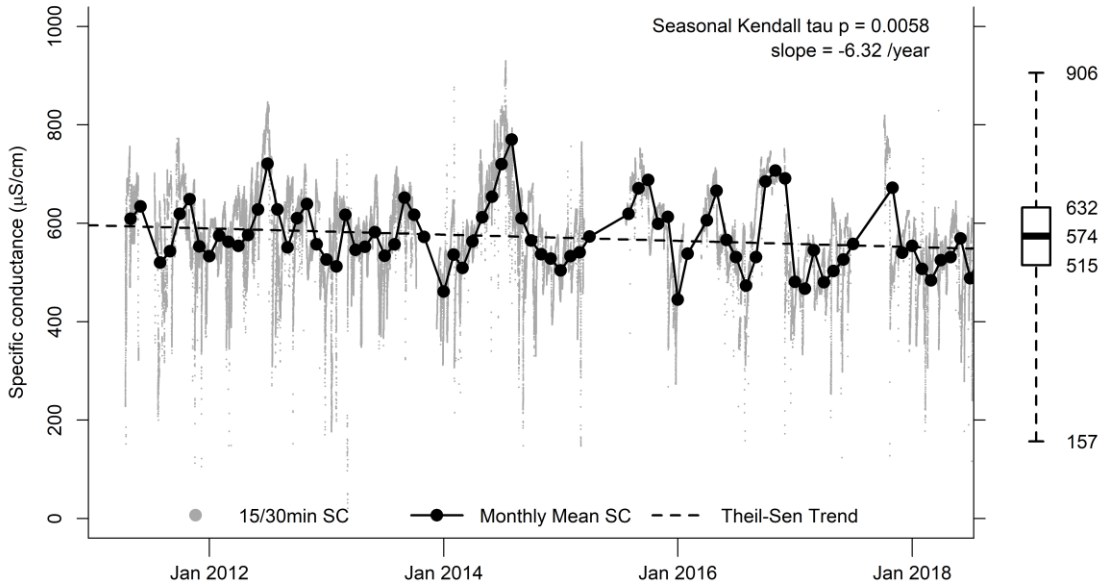

Figure A-1: Continuous (15/30-min interval) and monthly mean specific conductance (SC) for Birchfield creek (BIR, test stream). Seasonal Kendall tau P-value and Theil-Sen trend (dashed line) if statistically significant (P <0.05). Boxplot of 15/30 minute continuously SC showing interquartile range, extreme values, and median

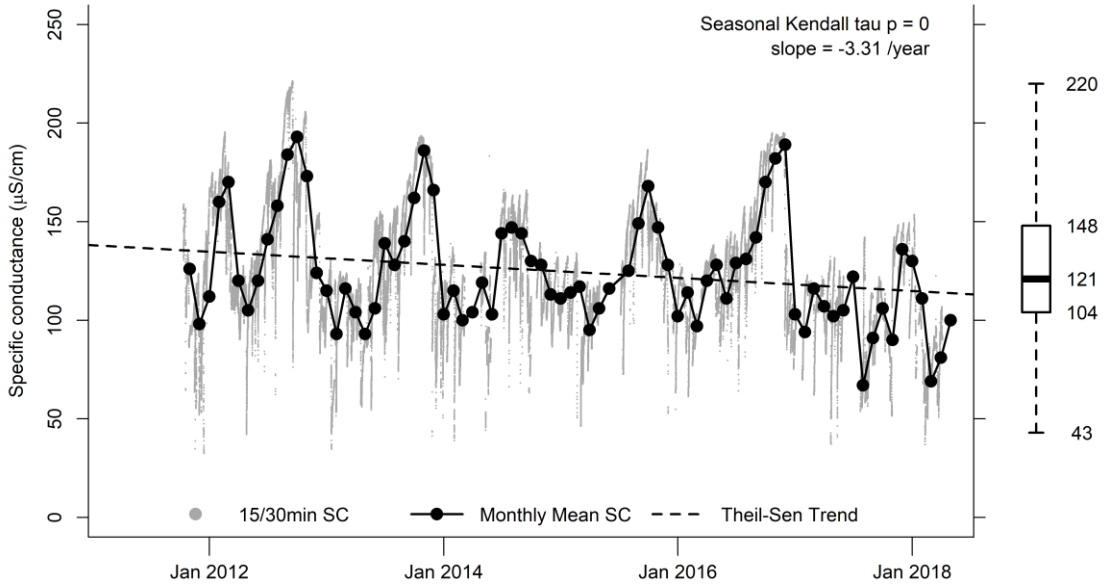

Figure A-2: Continuous (15/30-min interval) and monthly mean specific conductance (SC) for Copperhead Branch (COP, reference stream). Seasonal Kendall tau P-value and Theil-Sen trend (dashed line) if statistically significant (P <0.05). Boxplot of 15/30 minute continuously SC showing interquartile range, extreme values, and median.

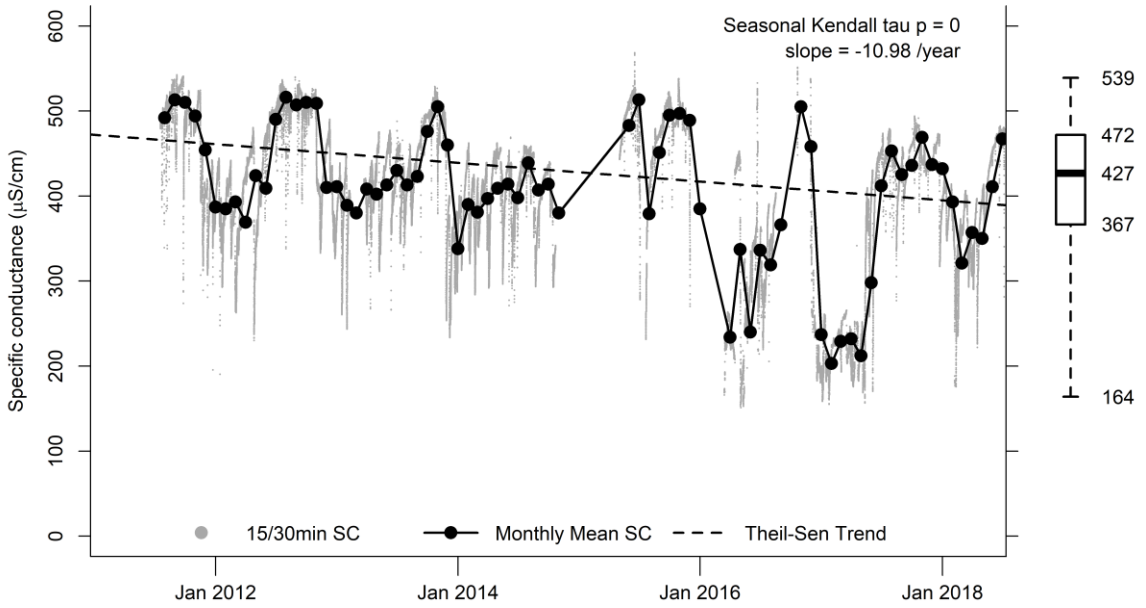

Figure A-3: Continuous (15/30-min interval) and monthly mean specific conductance (SC) for Crane Fork (CRA, test stream). Seasonal Kendall tau P-value and Theil-Sen trend (dashed line) if statistically significant (P <0.05). Boxplot of 15/30 minute continuously SC showing interquartile range, extreme values, and median.

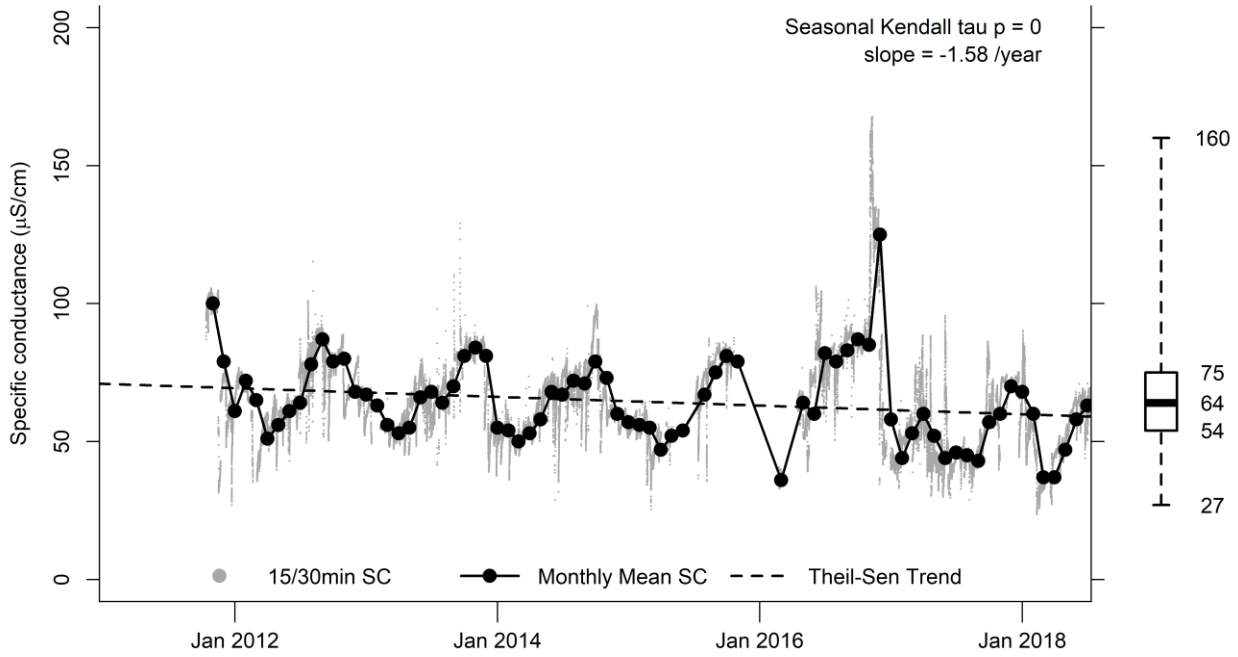

Figure A-4: Continuous (15/30-min interval) and monthly mean specific conductance (SC) for Crooked Branch (CRO, reference stream). Seasonal Kendall tau P-value and Theil-Sen trend (dashed line) if statistically significant (P <0.05). Boxplot of 15/30 minute continuously SC showing interquartile range, extreme values, and median.

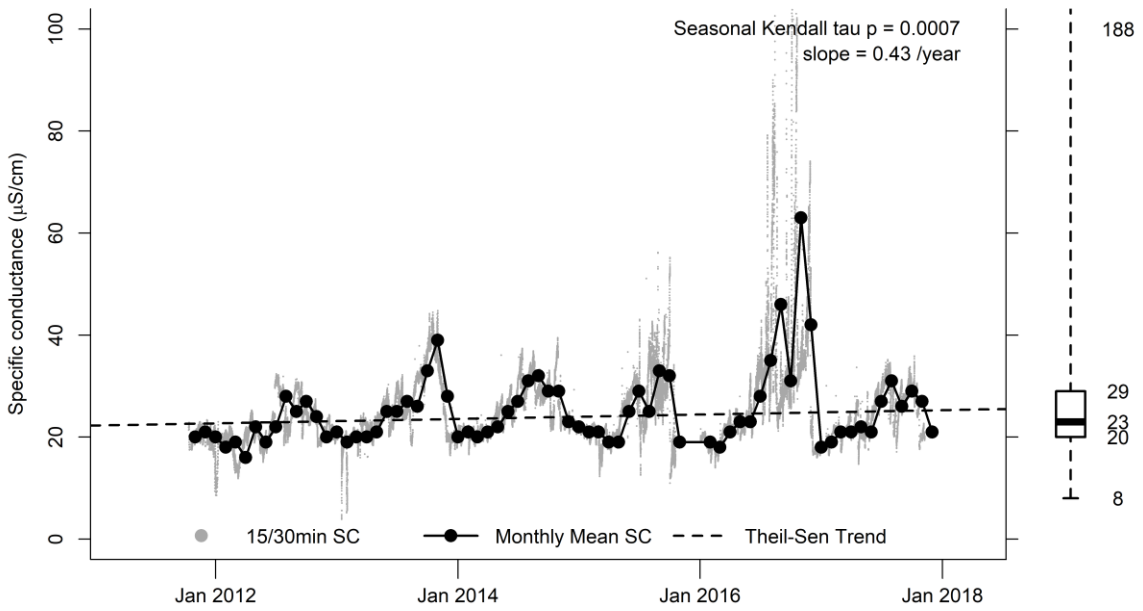

Figure A-5: Continuous (15/30-min interval) and monthly mean specific conductance (SC) for Eastland creek (EAS, reference stream). Seasonal Kendall tau P-value and Theil-Sen trend (dashed line) if statistically significant (P <0.05). Boxplot of 15/30 minute continuously SC showing interquartile range, extreme values, and median.

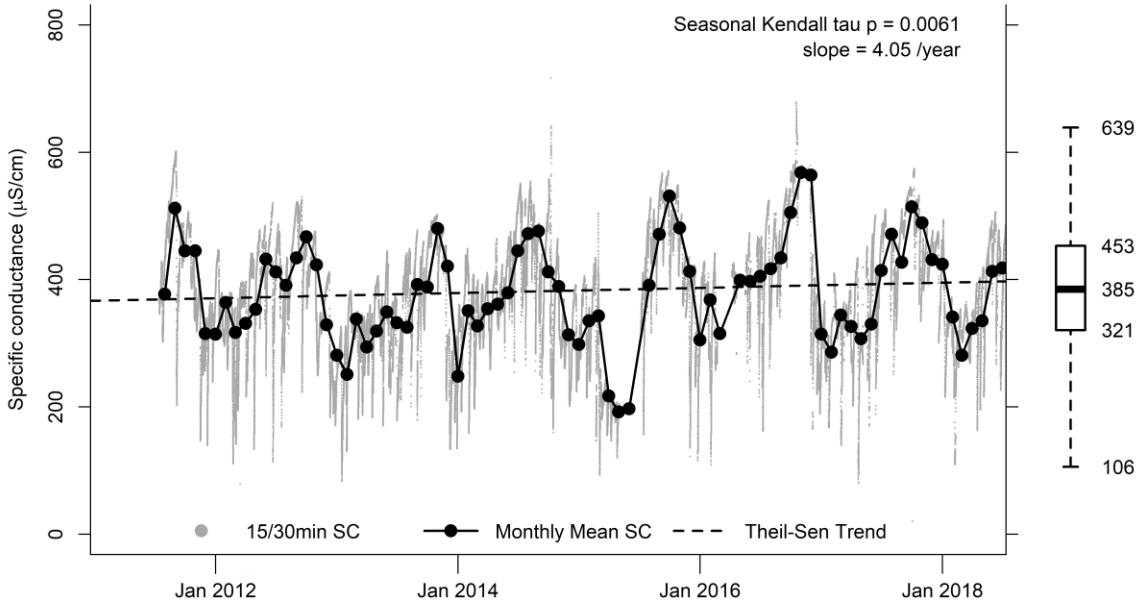

Figure A-6: Continuous (15/30-min interval) and monthly mean specific conductance (SC) for Fryingpan creek (FRY, test stream). Seasonal Kendall tau P-value and Theil-Sen trend (dashed line) if statistically significant (P <0.05). Boxplot of 15/30 minute continuously SC showing interquartile range, extreme values, and median.

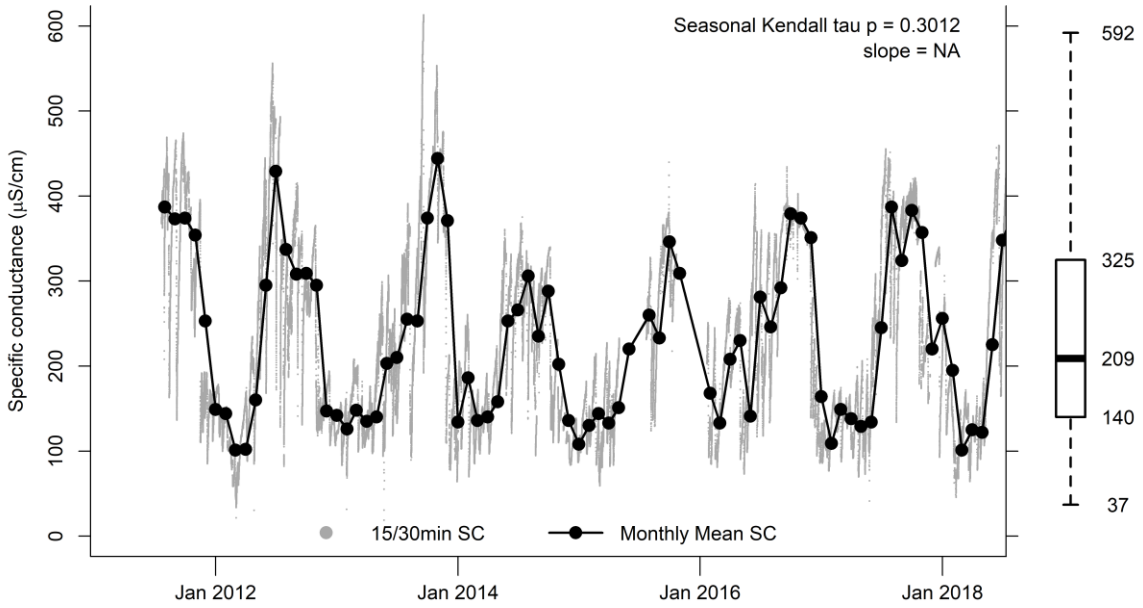

Figure A-7: Continuous (15/30-min interval) and monthly mean specific conductance (SC) for Grape Branch (GRA, test stream). Boxplot of 15/30 minute continuously SC showing interquartile range, extreme values, and median.

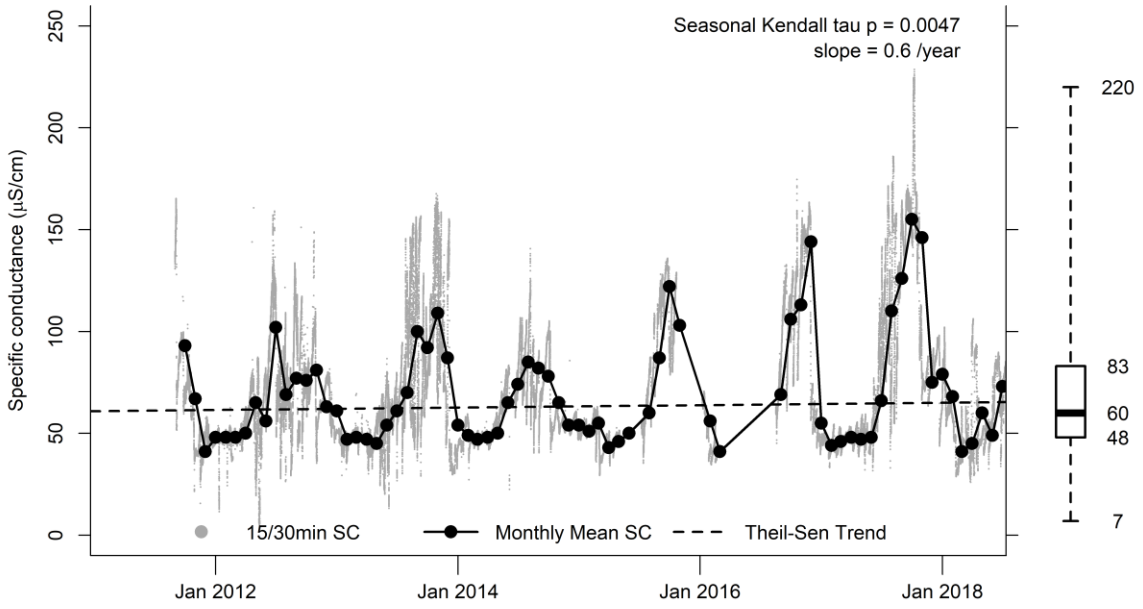

Figure A-8: Continuous (15/30-min interval) and monthly mean specific conductance (SC) for Hurricane Branch (HCN, reference stream). Seasonal Kendall tau P-value and Theil-Sen trend (dashed line) if statistically significant (P <0.05). Boxplot of 15/30 minute continuously SC showing interquartile range, extreme values, and median.

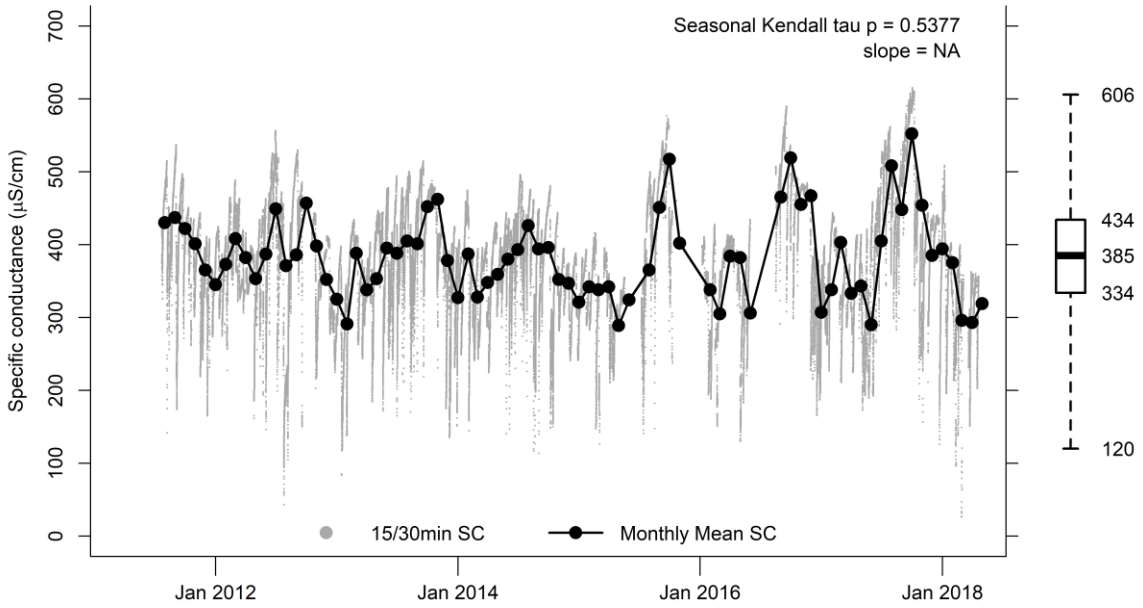

Figure A-9: Continuous (15/30-min interval) and monthly mean specific conductance (SC) for Hurricane Fork (HUR, test stream). Boxplot of 15/30 minute continuously SC showing interquartile range, extreme values, and median.

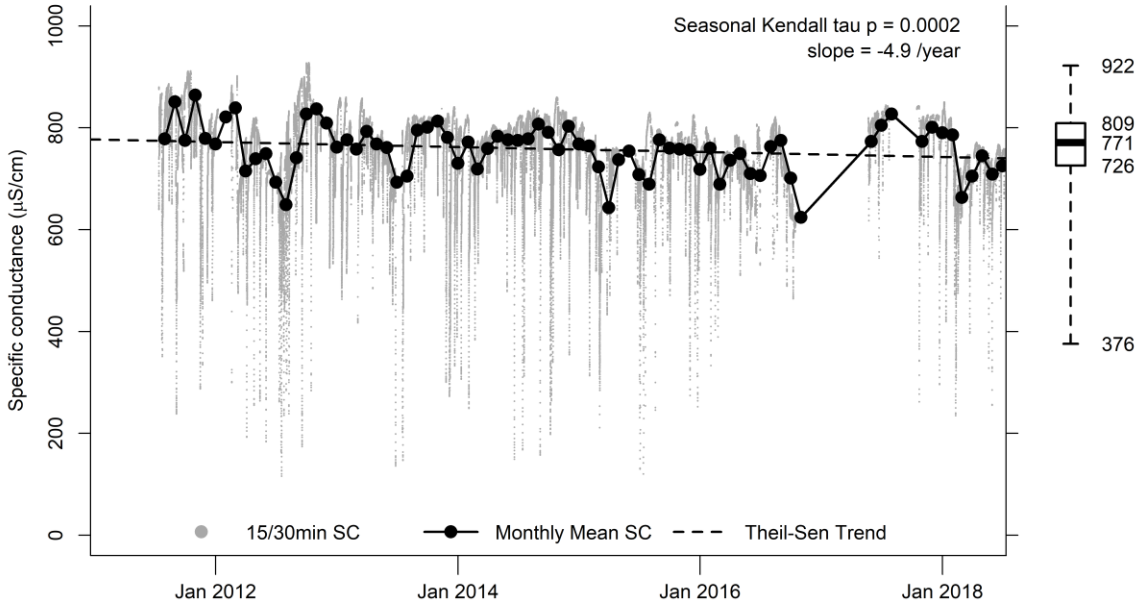

Figure A-10: Continuous (15/30-min interval) and monthly mean specific conductance (SC) for Kelly Branch (BIR, test stream). Seasonal Kendall tau P-value and Theil-Sen trend (dashed line) if statistically significant (P <0.05). Boxplot of 15/30 minute continuously SC showing interquartile range, extreme values, and median.

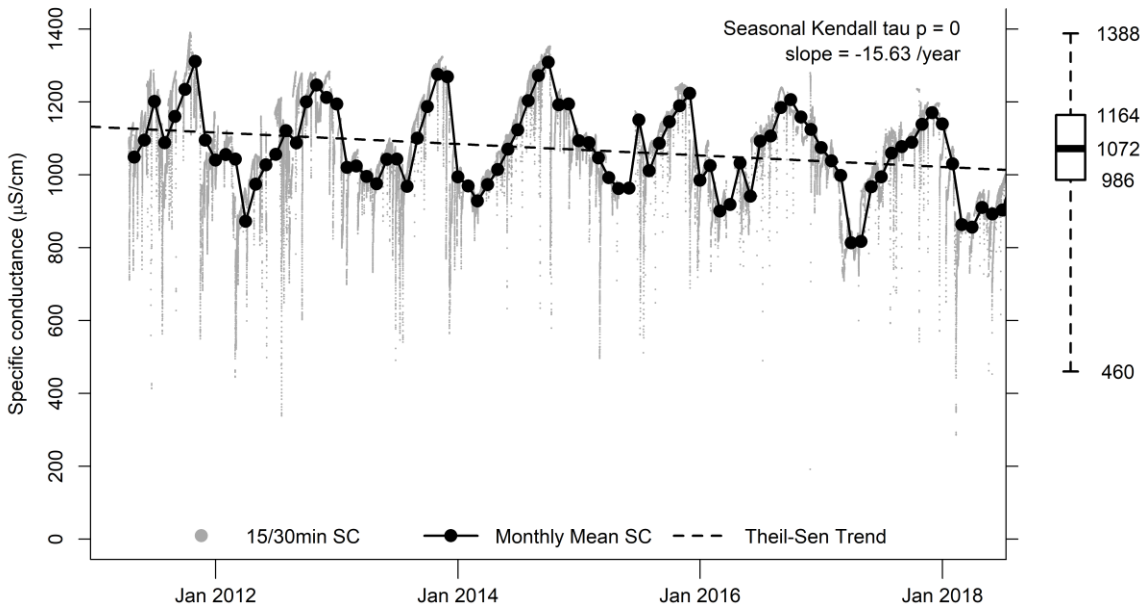

Figure A-11: Continuous (15/30-min interval) and monthly mean specific conductance (SC) for Kelly Branch Unnamed Tributary (KUT, test stream). Seasonal Kendall tau P-value and Theil-Sen trend (dashed line) if statistically significant (P <0.05). Boxplot of 15/30 minute continuously SC showing interquartile range, extreme values, and median

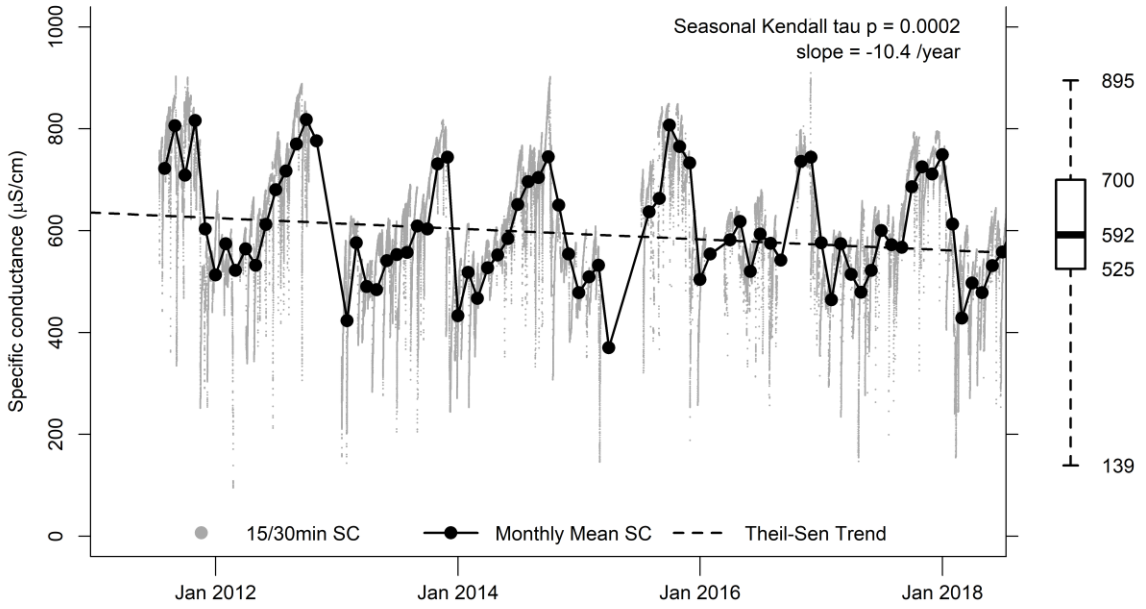

Figure A-12: Continuous (15/30-min interval) and monthly mean specific conductance (SC) for Laurel Branch (LAB, test stream). Seasonal Kendall tau P-value and Theil-Sen trend (dashed line) if statistically significant (P <0.05). Boxplot of 15/30 minute continuously SC showing interquartile range, extreme values, and median.

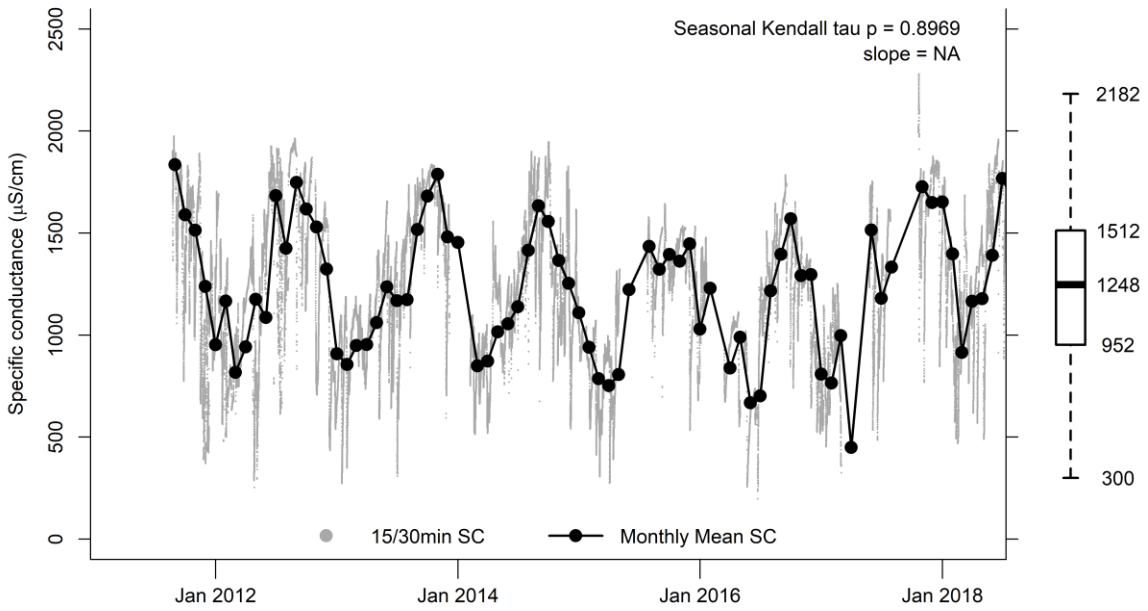

Figure A-13: Continuous (15/30-min interval) and monthly mean specific conductance (SC) for Left Fork of Long Fork of Coal Fork (LLC, test stream). Boxplot of 15/30 minute continuously SC showing interquartile range, extreme values, and median

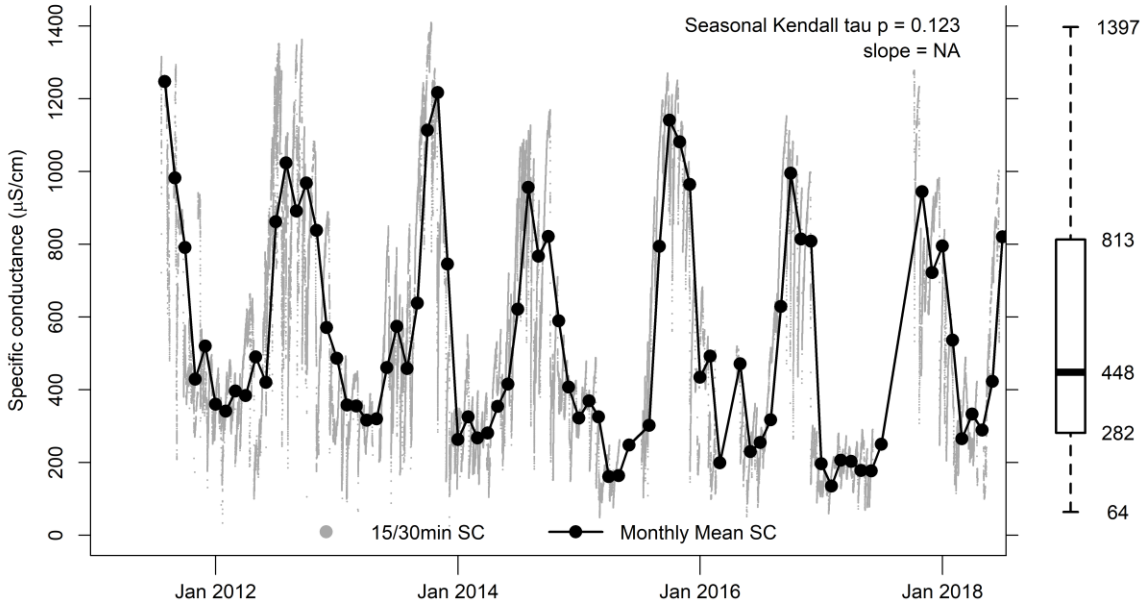

Figure A-14: Continuous (15/30-min interval) and monthly mean specific conductance (SC) for Longlick Branch East Fork (LLE, test stream). Boxplot of 15/30 minute continuously SC showing interquartile range, extreme values, and median

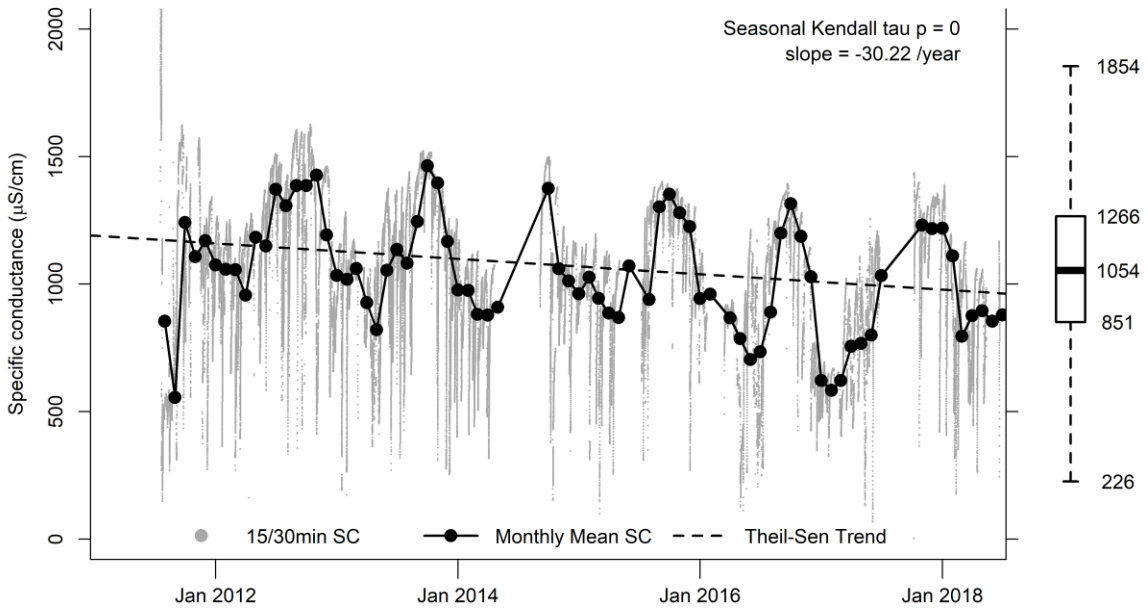

Figure A-15: Continuous (15/30-min interval) and monthly mean specific conductance (SC) for Longlick Branch West Fork (LLW, test stream). Seasonal Kendall tau P-value and Theil-Sen trend (dashed line) if statistically significant (P <0.05). Boxplot of 15/30 minute continuously SC showing interquartile range, extreme values, and median.

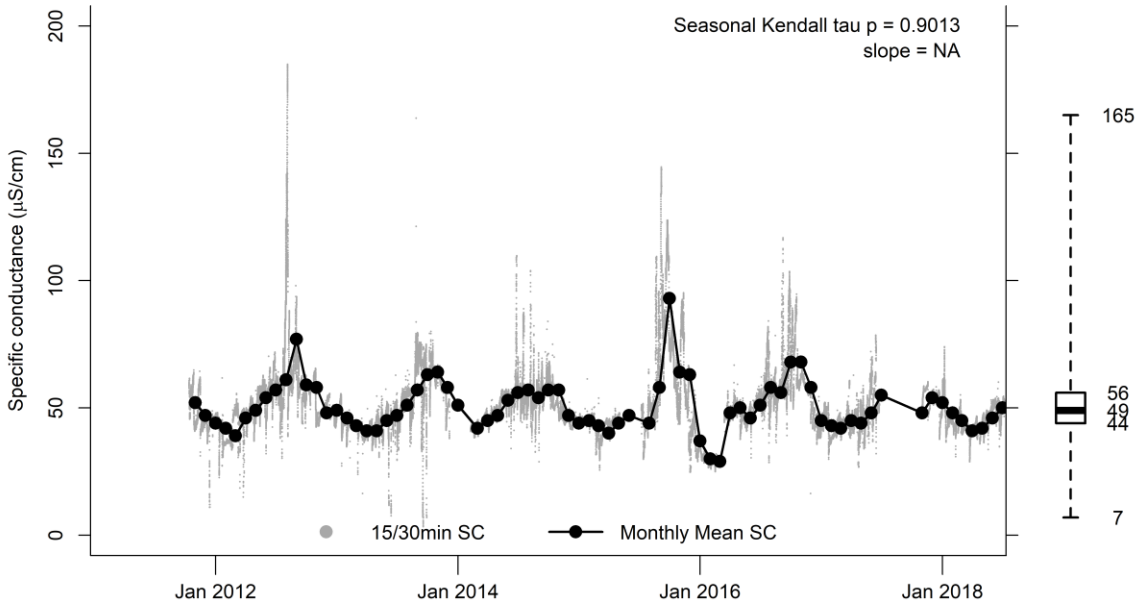

Figure A-16: Continuous (15/30-min interval) and monthly mean specific conductance (SC) for Middle Camp Branch (MCB, reference stream). Boxplot of 15/30 minute continuously SC showing interquartile range, extreme values, and median.

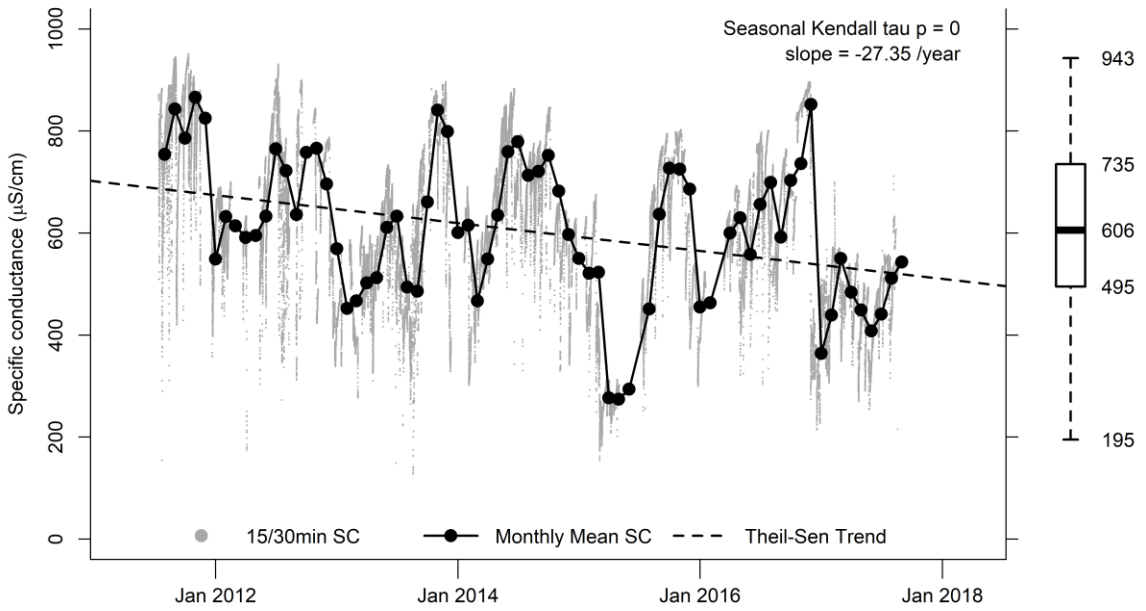

Figure A-17: Continuous (15/30-min interval) and monthly mean specific conductance (SC) for Mill Branch West Fork (MIL, test stream). Seasonal Kendall tau P-value and Theil-Sen trend (dashed line) if statistically significant (P <0.05). Boxplot of 15/30 minute continuously SC showing interquartile range, extreme values, and median.

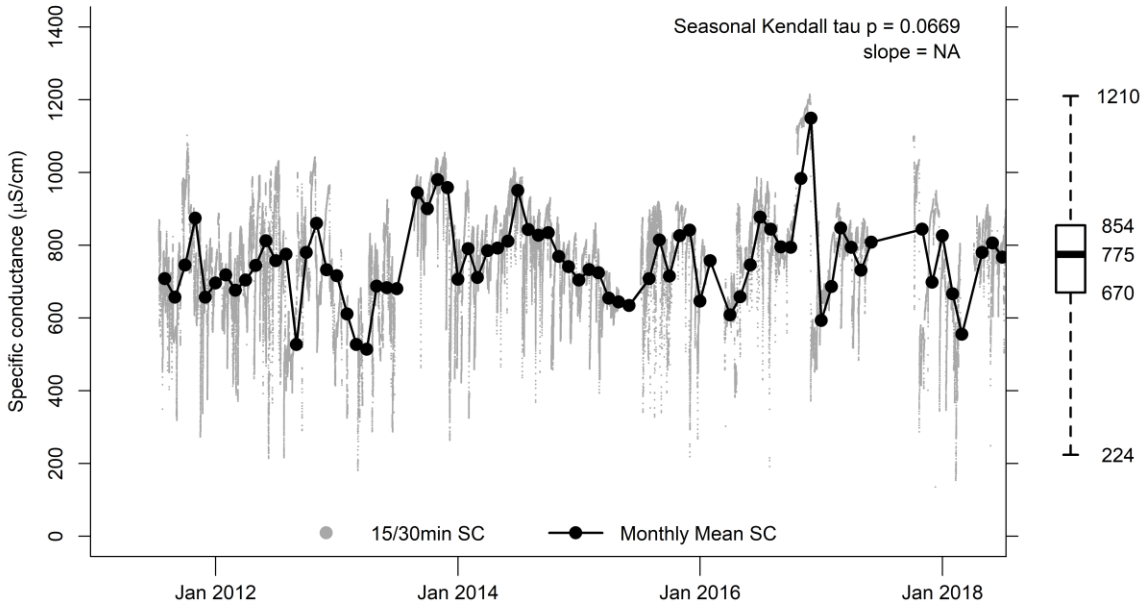

Figure A-18: Continuous (15/30-min interval) and monthly mean specific conductance (SC) for Powell River (POW, test stream). Boxplot of 15/30 minute continuously SC showing interquartile range, extreme values, and median.

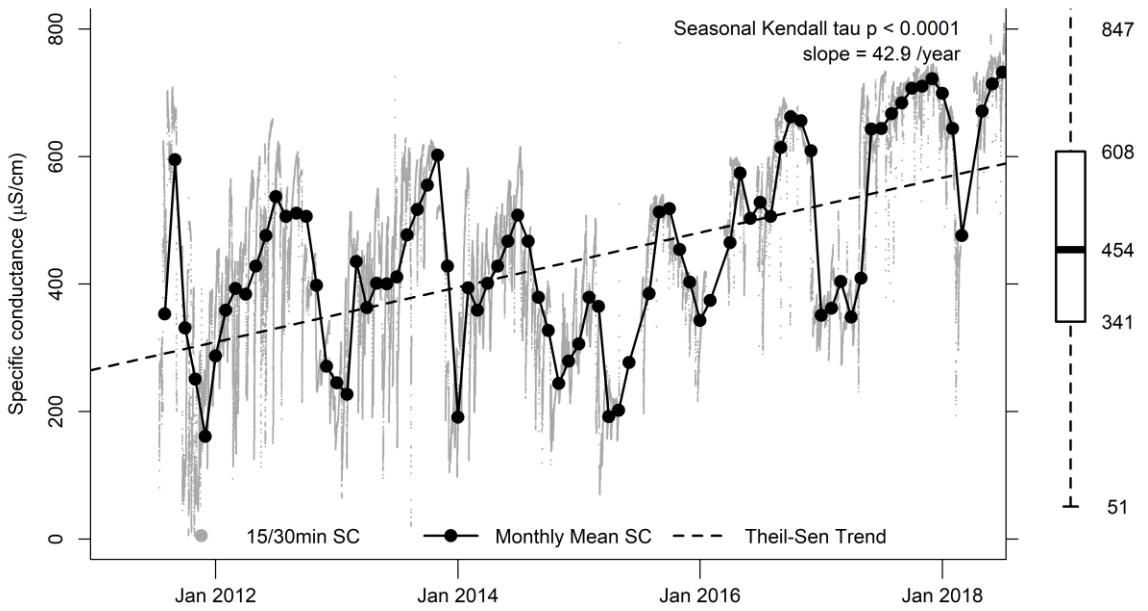

Figure A-19: Continuous (15/30-min interval) and monthly mean specific conductance (SC) for Right Fork Fryingpan Creek (RFF, test stream). Seasonal Kendall tau P-value and Theil-Sen trend (dashed line) if statistically significant (P <0.05). Boxplot of 15/30 minute continuously SC showing interquartile range, extreme values, and median.

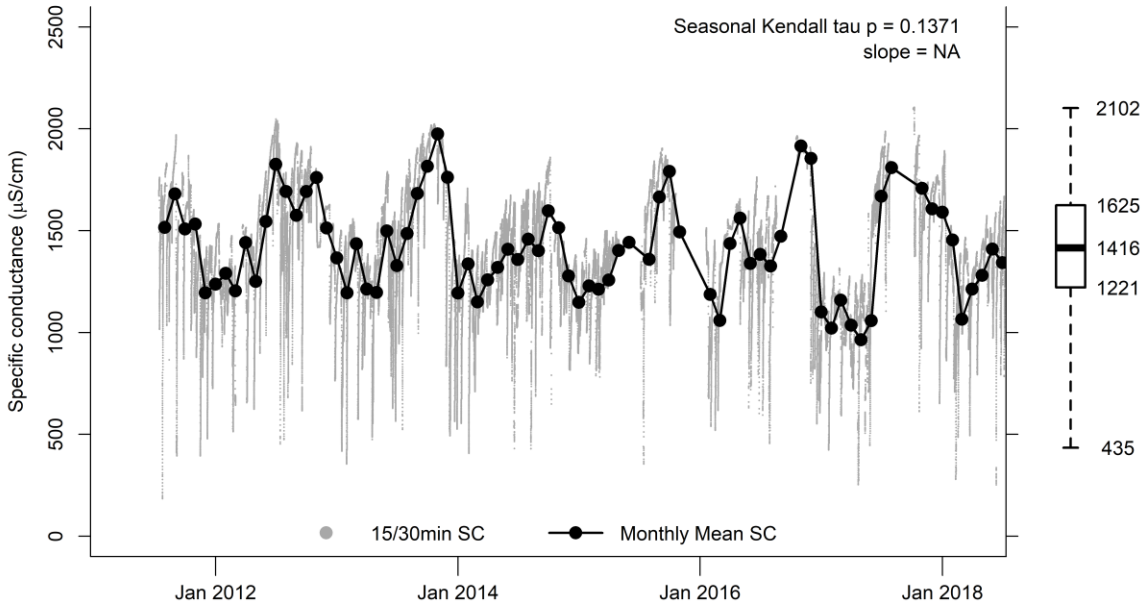

Figure A-20: Continuous (15/30-min interval) and monthly mean specific conductance (SC) for Rickey Branch (RIC, test stream). Boxplot of 15/30 minute continuously SC showing interquartile range, extreme values, and median.

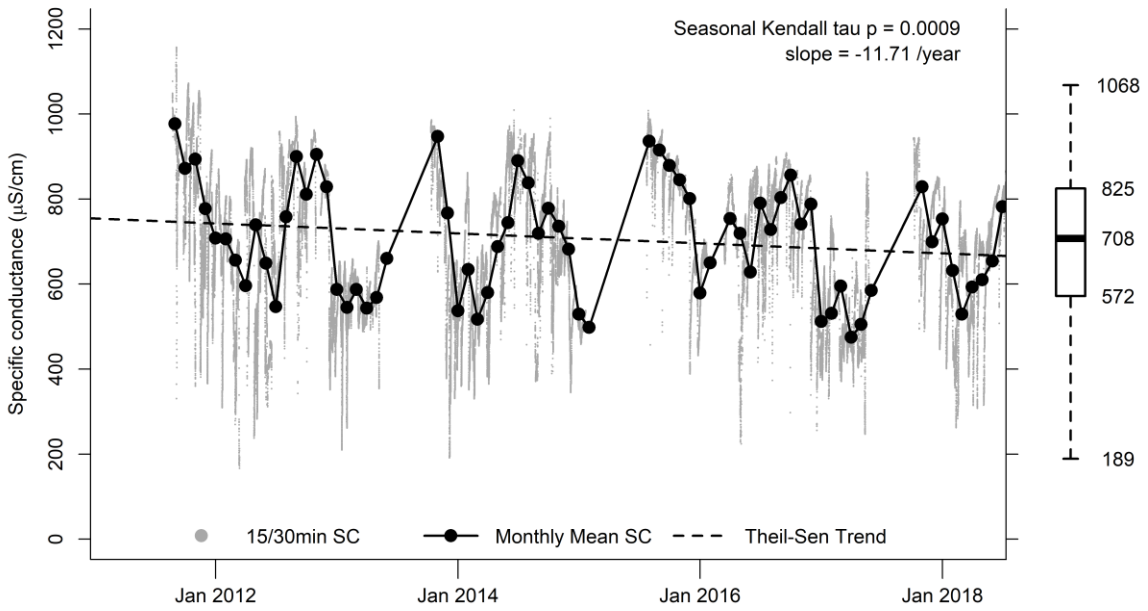

Figure A-21: Continuous (15/30-min interval) and monthly mean specific conductance (SC) for Rockhouse Fork (ROC, test stream). Seasonal Kendall tau P-value and Theil-Sen trend (dashed line) if statistically significant (P <0.05). Boxplot of 15/30 minute continuously SC showing interquartile range, extreme values, and median.

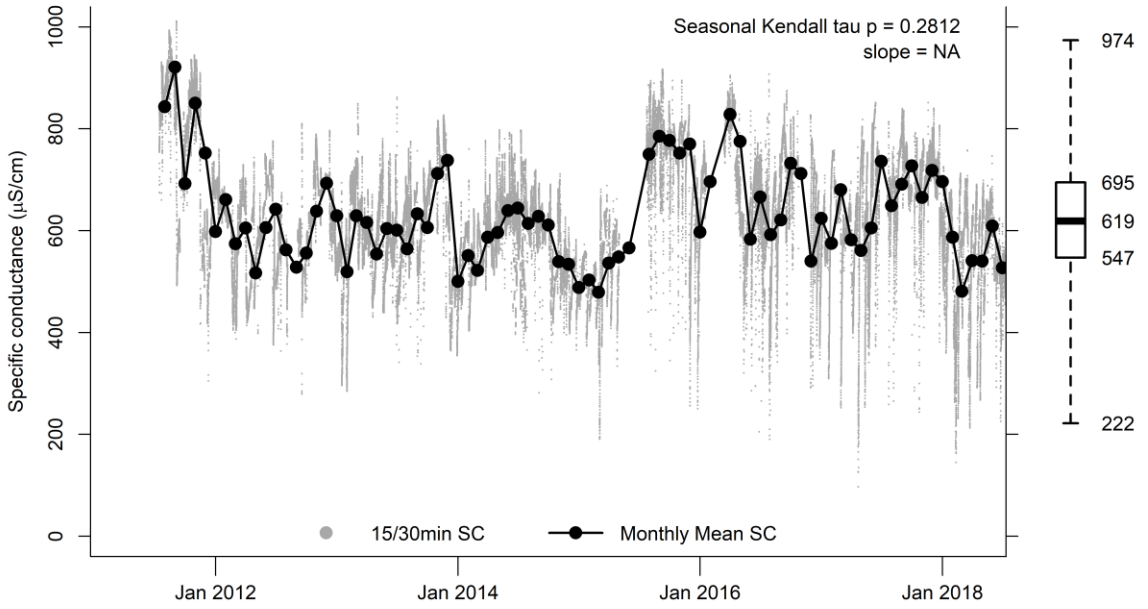

Figure A-22: Continuous (15/30-min interval) and monthly mean specific conductance (SC) for Roll Pone Branch (ROL, test stream). Boxplot of 15/30 minute continuously SC showing interquartile range, extreme values, and median.

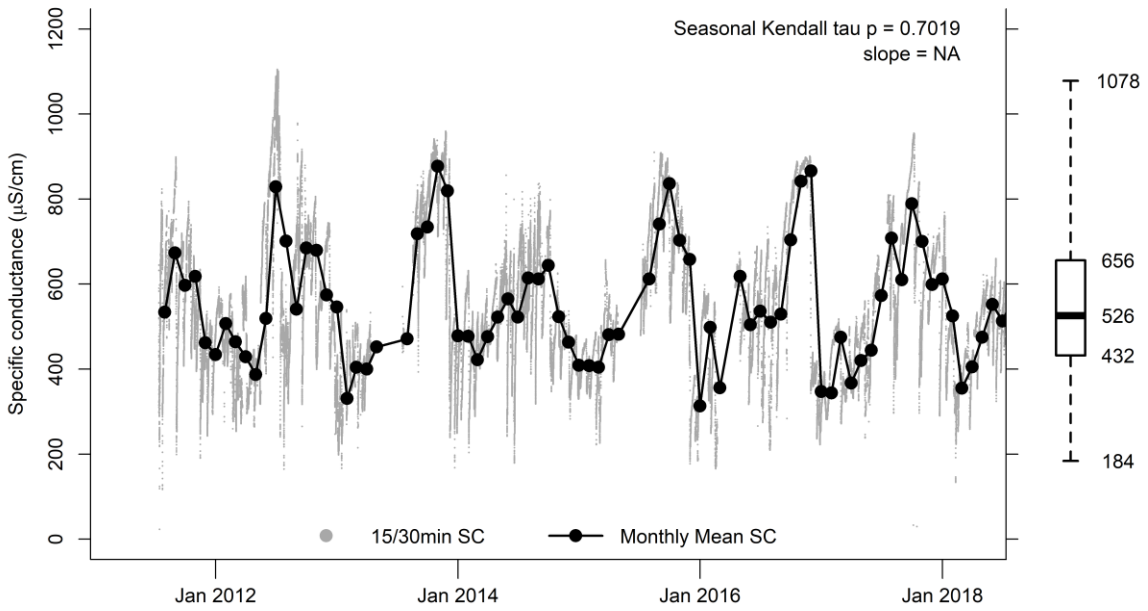

Figure A-23: Continuous (15/30-min interval) and monthly mean specific conductance (SC) for Rickey Branch Unnamed Tributary (RUT, test stream). Boxplot of 15/30 minute continuously SC showing interquartile range, extreme values, and median.

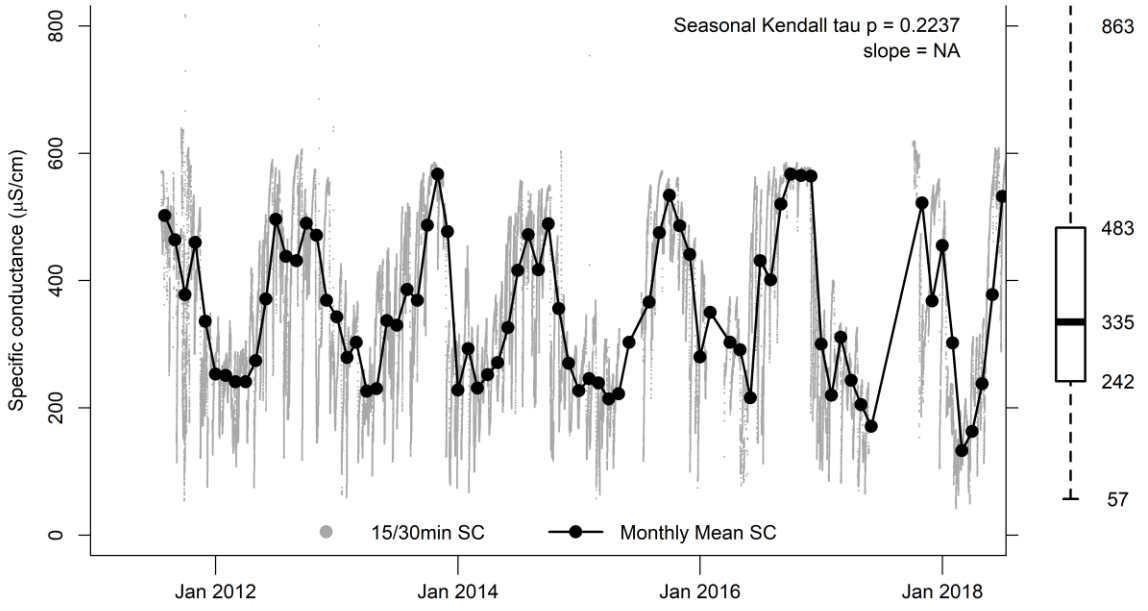

Figure A-24: Continuous (15/30-min interval) and monthly mean specific conductance (SC) for Spruce Pine Creek (SPC, test stream). Boxplot of 15/30 minute continuously SC showing interquartile range, extreme values, and median.

APPENDIX B - SUMMARY OF TEMPORAL TRENDS IN SPECIFIC CONDUCTANCE, ION MATRIX, AND BENTHIC MACROINVERTEBRATES COMMUNITY METRICS

Table B-1: Summary table of temporal trends in specific conductance (SC), ion matrix, and biological community metrics

Site	Site type	Mean SC	SC trend	SC slope	Tau	Richness	EPT richness	E richness	% Ephemeroptera	scraper richness	shannon diversity	ephemeroptera richness less Beatidae	%ephemeroptera less Beatidae	SO4 : HCO3	Ca : Mg	%mined 1980-2011	additional %mined 2011-2016
EAS	Ref	25	Pos	0.43	0.17											0	0
MCB	Ref	51			0.01					Neg					Neg	0	0
CRO	Ref	65	Neg	-1.58	-0.23	Pos									Neg	0	0
HCN	Ref	68	Pos	0.6	0.14											0	0
COP	Ref	127	Neg	-3.31	-0.22											0	0
GRA	Test	231			0.05											2.1	0
SPC	Test	353			0.06		Pos									3.8	0
FRY	Test	376	Pos	4.05	0.12											4.5	0.8
HUR	Test	383			0.03						Pos			Neg		20.7	0
CRA	Test	417	Neg	-10.98	-0.26									Neg		0	0
RFF	Test	438	Pos	42.9	0.49							Neg				0.2	20.8
RUT	Test	557			0.02				Neg					Neg	Neg	10.2	0
LLE	Test	562			-0.07			Pos	Pos		Pos		Pos	Neg		10.9	0
BIR	Test	578	Neg	-6.32	-0.13											5.4	0
LAB	Test	609	Neg	-10.4	-0.18	Pos					Pos			Neg		7.6	0
MIL	Test	618	Neg	-27.35	-0.27									Neg	Neg	51.6	0.8
ROL	Test	625			-0.05											29.9	0
ROC	Test	695	Neg	-11.71	-0.17					Neg				Neg	Neg	30.4	0.5
KEL	Test	762	Neg	-4.9	-0.18						Pos			Neg	Neg	56.3	2.4
POW	Test	763			0.09			Pos				Pos	Pos	Neg		60.7	7.7
LLW	Test	1068	Neg	-30.22	-0.21	Pos	Pos							Neg	Neg	26.4	0
KUT	Test	1080	Neg	-15.63	-0.33									Neg	Neg	39.3	0.5
LLC	Test	1225			0.01			Neg	Neg							19.2	5.7
RIC	Test	1423			-0.07									Neg	Neg	34.7	0

APPENDIX C - SPATIAL AND FLOW-DRIVEN DYNAMICS OF MAJOR IONS AND TRACE ELEMENTS

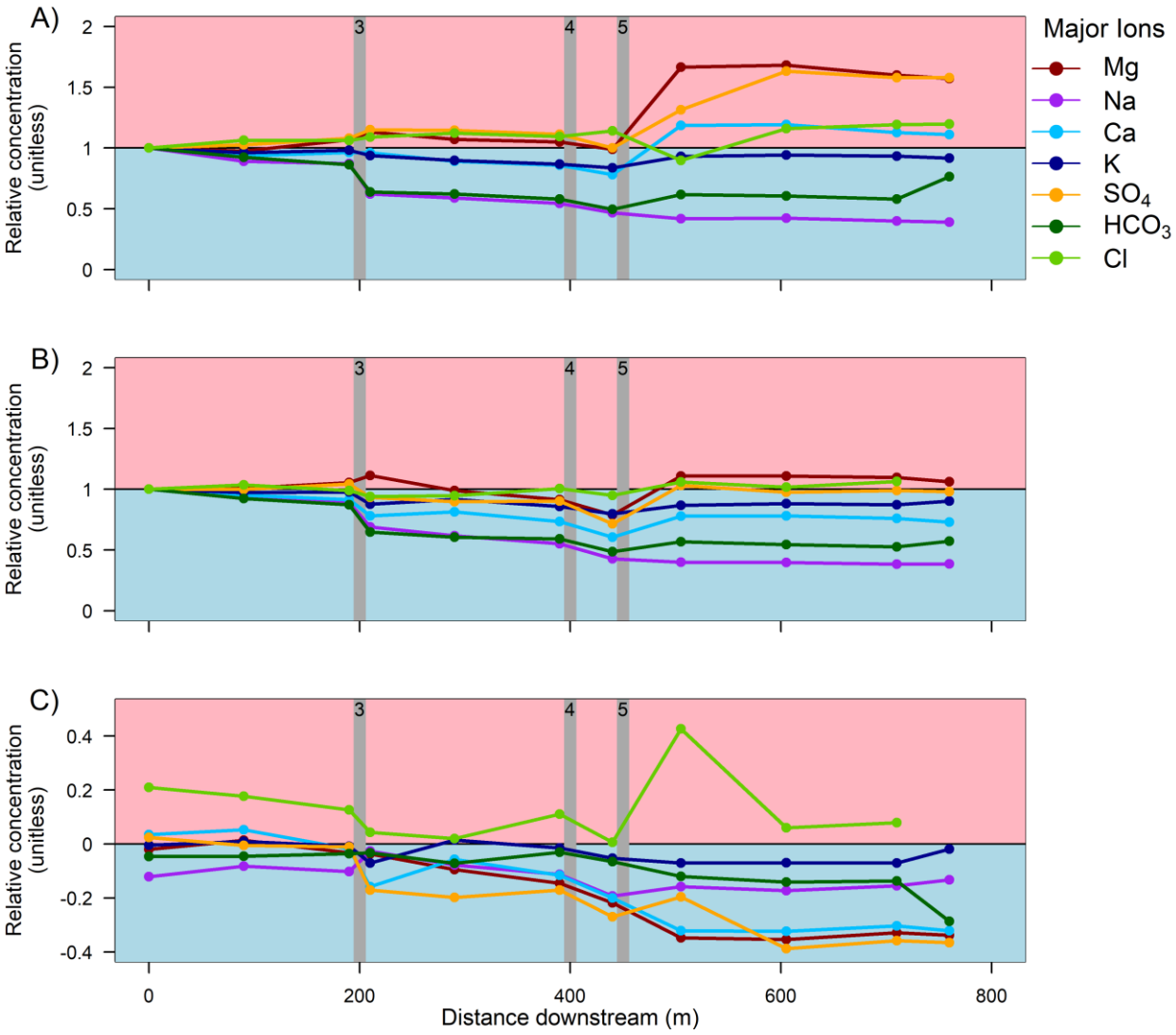

Figure C-1: Relative concentrations of major ions in Hurricane Branch, VA. A) Proportion of concentration at sampling location to concentration at origin under baseflow and B) highflow. C) Relative change in concentrations of major ions under highflow compared to baseflow. Shaded red areas symbolize enriched relative concentrations. Shaded blue areas symbolize diluted relative concentrations.

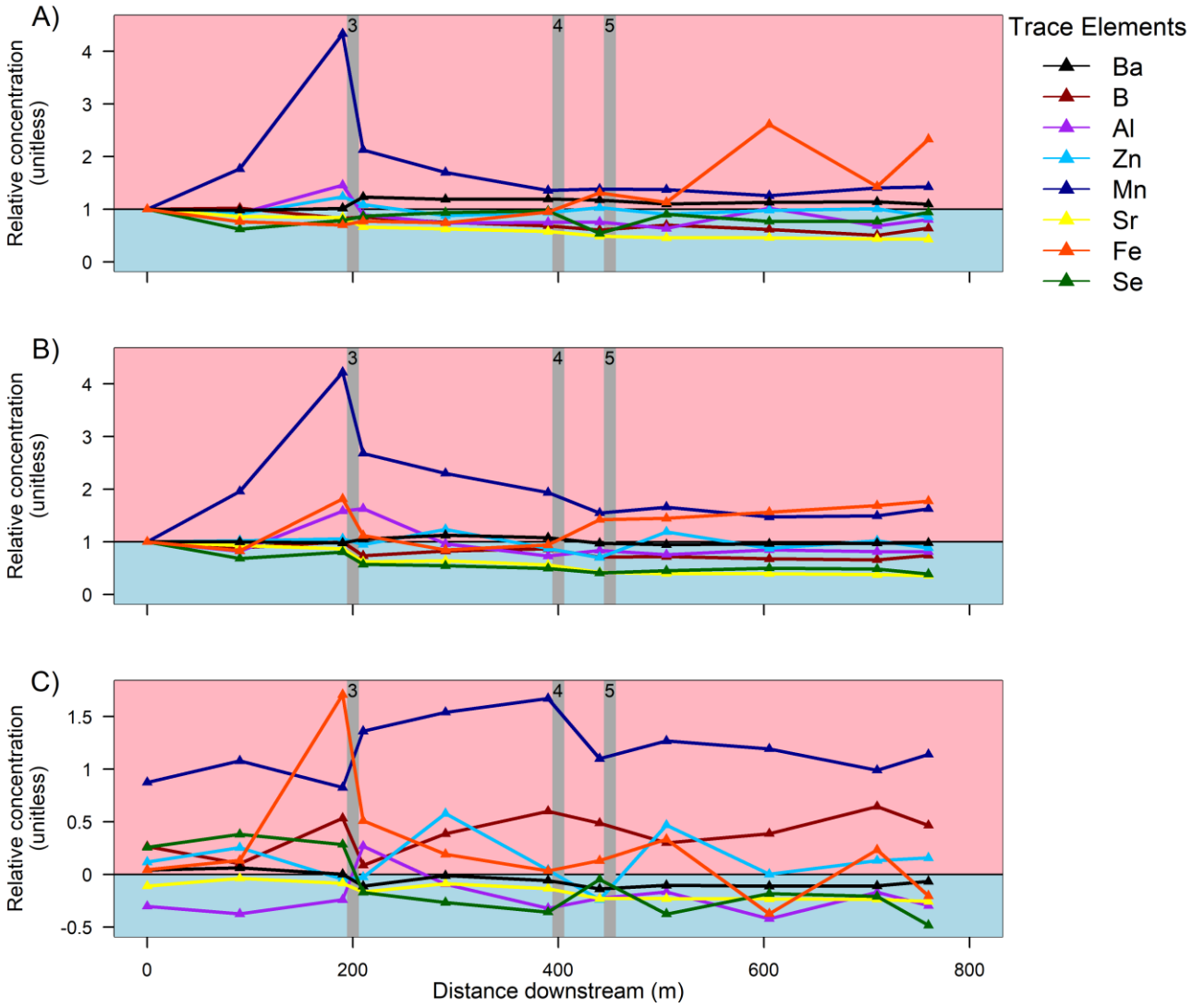

Figure C-2: Relative concentrations of trace elements in Hurricane Branch, VA. A) Proportion of concentration at sampling location to concentration at origin under baseflow and B) highflow. C) Relative change in concentrations of major ions under highflow compared to baseflow. Shaded red areas symbolize enriched relative concentrations. Shaded blue areas symbolize diluted relative concentrations.

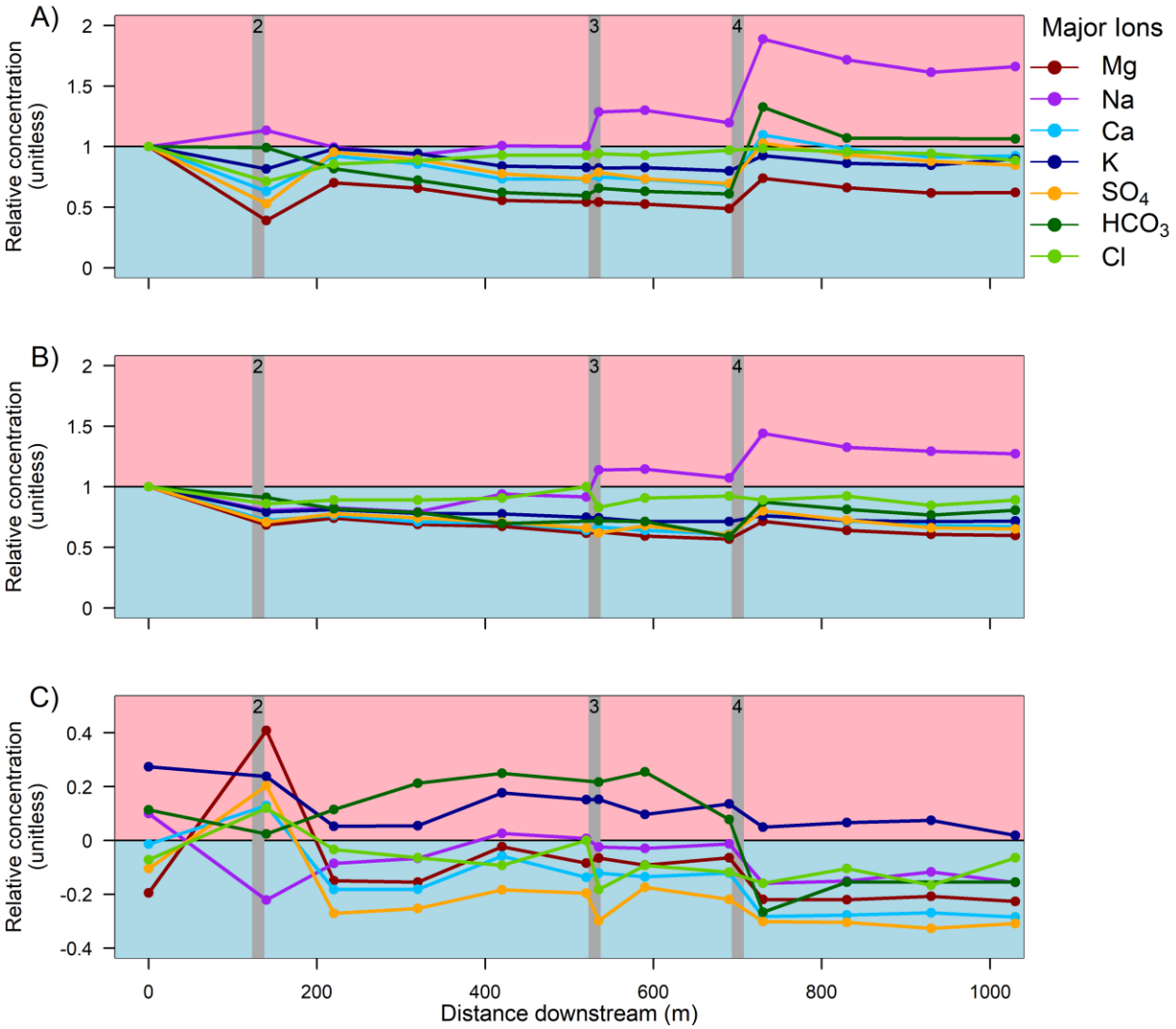

Figure C-3: Relative concentrations of major ions in Longlick Branch East Fork, WV. A) Proportion of concentration at sampling location to concentration at origin under baseflow and B) highflow. C) Relative change in concentrations of major ions under highflow compared to baseflow. Shaded red areas symbolize enriched relative concentrations. Shaded blue areas symbolize diluted relative concentrations.

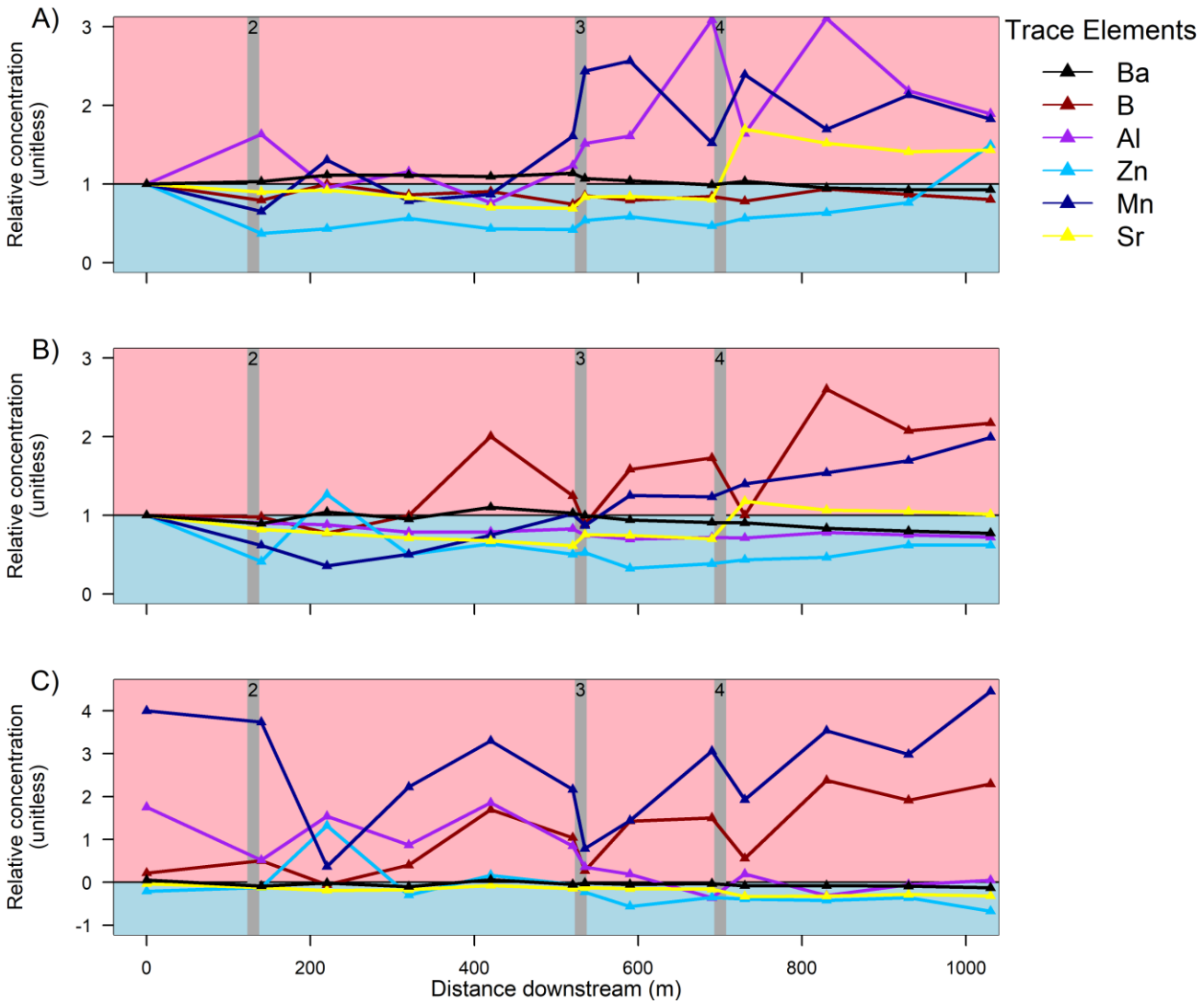

Figure C-4: Relative concentrations of trace elements in Longlick Branch East Fork, WV. A) Proportion of concentration at sampling location to concentration at origin under baseflow and B) highflow. C) Relative change in concentrations of major ions under highflow compared to baseflow. Shaded red areas symbolize enriched relative concentrations. Shaded blue areas symbolize diluted relative concentrations.

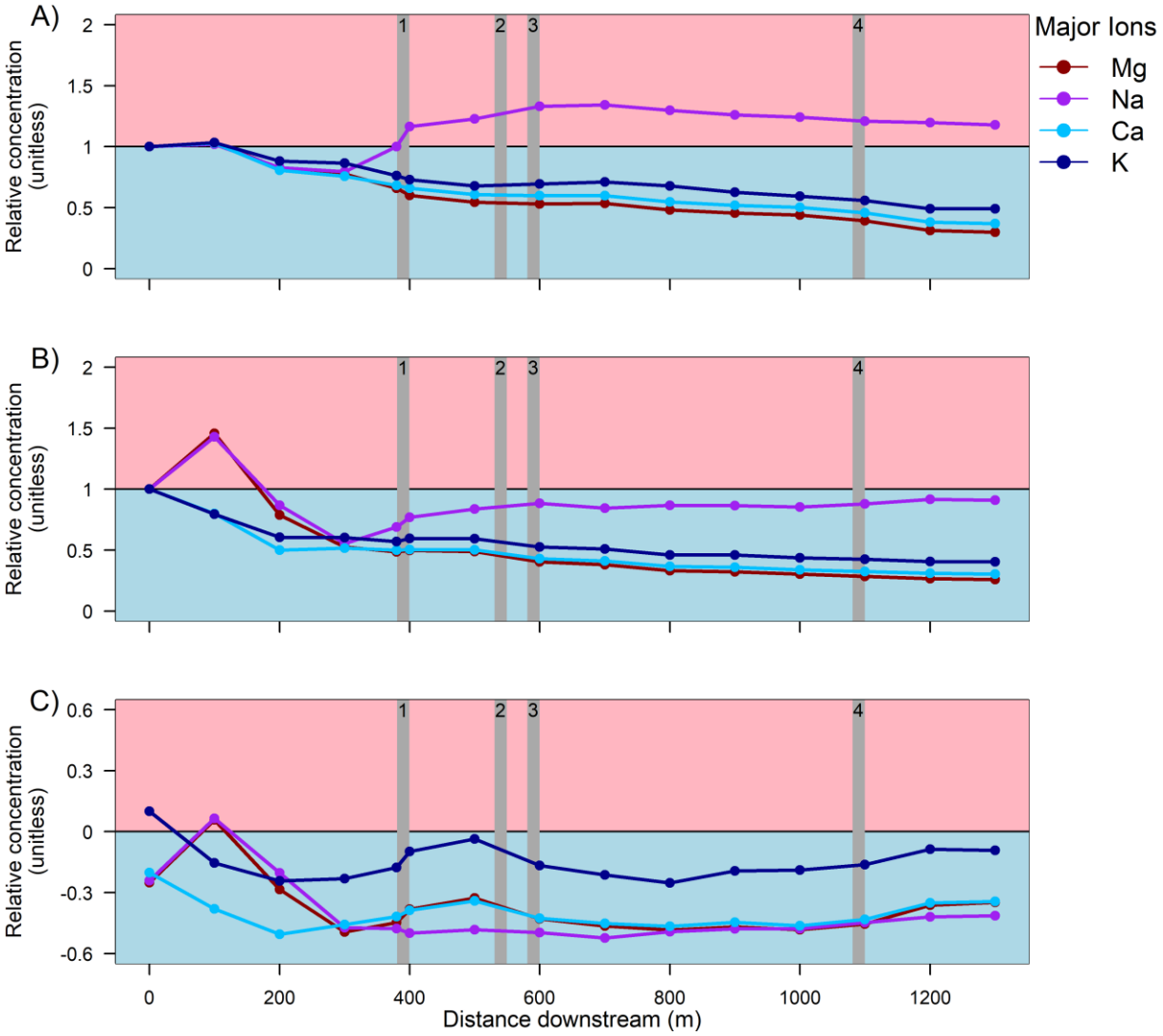

Figure C-5: Relative concentrations of major ions in Roll Pone Branch, VA. A) Proportion of concentration at sampling location to concentration at origin under baseflow and B) highflow. C) Relative change in concentrations of major ions under highflow compared to baseflow. Shaded red areas symbolize enriched relative concentrations. Shaded blue areas symbolize diluted relative concentrations.

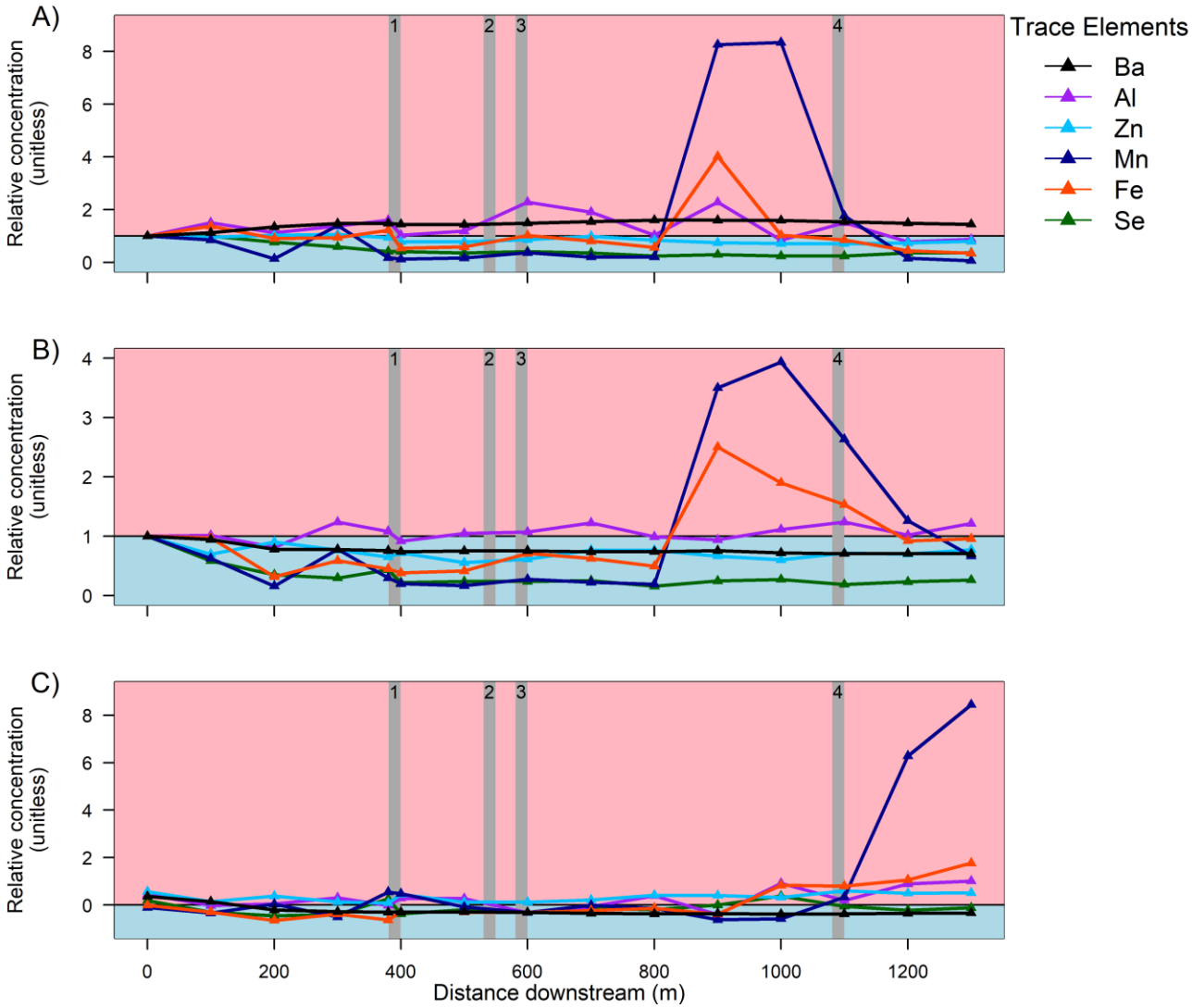

Figure C-6: Relative concentrations of trace elements in Roll Pone Branch, VA. A) Proportion of concentration at sampling location to concentration at origin under baseflow and B) highflow. C) Relative change in concentrations of major ions under highflow compared to baseflow. Shaded red areas symbolize enriched relative concentrations. Shaded blue areas symbolize diluted relative concentrations.

Table C-1: Concentrations of major ions and trace elements at the flow origin under baseflow and highflow conditions.

			Flow origin major ion and trace element concentrations (µg/L)														
Site Id	flow type	SC[1]	HCO_3	Cl	SO_4	Na	Mg	K	Ca	B	Al	Mn	Fe	Zn	Se	Sr	Ba
HUR	high	284	67.26	0.65	81.94	15.51	11.05	2.27	27.09	14.15	18.62	6.56	11.62	14.98	1.96	559.71	26.13
HUR	base	290	70.53	0.54	80.02	17.64	11.27	2.28	26.19	11.19	26.69	3.50	11.13	13.40	1.56	628.99	25.07
LLE	high	314	26.98	0.65	119.00	2.85	18.79	2.23	30.24	8.61	10.57	1.15	<MRL[3]	15.42	<MRL[4]	452.63	41.27
LLE	base	419	24.24	0.70	132.86	2.59	23.33	1.75	30.67	7.08	3.84	0.23	<MRL	19.51	<MRL	468.93	39.24
ROL	high	1111	ND[2]	ND	ND	11.92	95.49	6.50	161.26	ND	4.63	15.57	10.84	16.93	2.03	ND	50.65
ROL	base	1741	ND	ND	ND	15.70	127.40	5.90	202.10	ND	3.20	17.40	10.90	10.80	1.70	ND	37.20

[1]SC- specific conductance (µs/cm). [2]ND- no data collected. [3]Iron (Fe) MRL – 10.0 µg/L. [4]Selenium (Se) MRL – 0.5 µg/L.

APPENDIX D - SUPPLEMENTARY DATA OF PROCESSED MATERIAL FOR SELENIUM BIOACCUMULATION STUDY

Table D-1: Count and identification of leaf material collected at all six study streams in summer 2018.

Site ID	Date of collection	Acer saccharum	Aesculus octandra	Betula lenta	Carpinus caroliniana	Fagus grandifolia	Liriodendron tulipifera	Platanus occidentalis	Quercus alba	Quercus prinus	Quercus rubra	Tilia americana
CRA1	7/12/2018		24			2	1	10				
CRA2	7/12/2018		8				3	6				
CRA3	7/12/2018		29				1	9				
CRA4	7/13/2018		20				3	10			1	
CRA5	7/13/2018		16				1	8				
EAS1	6/4/2018		13							2		5
EAS2	6/4/2018		8	3							5	
EAS3	6/5/2018	1	6							1	9	4
EAS4	6/5/2018		20								4	
FRY1	6/5/2018	1				5	3					
FRY2	6/6/2018			7		7	2		1			
FRY3	6/6/2018	1					5				1	
FRY4	6/6/2018	2		2		1	1		1			
HCN1	7/25/2018			5		2	4					1
HCN2	7/25/2018	1				6	13				4	
HCN3	7/25/2018			6		4	20					
HCN4	7/26/2018					11	7	2				
HCN5	7/26/2018			2		6	17	5				
LLC1	7/18/2018		4				7	12				
LLC2	7/18/2018		38					6				3
LLC3	7/18/2018		28				1					
LLC4	7/19/2018		9		5	2	3					1
LLC5	7/19/2018		10					5				
ROC1	7/10/2018		6				4	11				
ROC2	7/10/2018		13		3	1	3	9				1
ROC3	7/10/2018			9			11	1				
ROC4	7/11/2018		6	6		2	8	3				1
ROC5	7/11/2018			12		7	1	4	4			

Table D-2: Identification and length of salamanders collected at reference streams in summer 2018.

Site ID	species	length (mm)
EAS1	Desmognathus monticola	117
EAS1	Desmognathus monticola	54
EAS1	Desmognathus monticola	122
EAS2	Desmognathus monticola	100
EAS2	Desmognathus monticola	112
EAS2	Desmognathus monticola	125
EAS2	Desmognathus monticola	59
EAS2	Desmognathus monticola	50
EAS3	Desmognathus monticola	110
EAS3	Desmognathus monticola	100
EAS3	Desmognathus monticola	128
EAS3	Desmognathus monticola	108
EAS3	Desmognathus monticola	121
EAS4	Desmognathus monticola	124
EAS4	Desmognathus monticola	116
EAS4	Desmognathus monticola	119
EAS4	Desmognathus monticola	117
EAS4	Desmognathus monticola	142

Site ID	species	length (mm)
HCN1	Desmognathus fuscus	80
HCN1	Desmognathus fuscus	94
HCN1	Desmognathus fuscus	114
HCN2	Desmognathus monticola	125
HCN2	Desmognathus monticola	75
HCN2	Desmognathus monticola	72
HCN3	Desmognathus monticola	70
HCN3	Desmognathus monticola	67
HCN3	Desmognathus monticola	101
HCN4	Desmognathus fuscus	110
HCN4	Desmognathus fuscus	92
HCN4	Desmognathus monticola	96
HCN4	Desmognathus monticola	120
HCN4	Desmognathus monticola	114
HCN4	Desmognathus monticola	72
HCN5	Desmognathus monticola	123
HCN5	Desmognathus monticola	94
HCN5	Desmognathus monticola	54

Table D-3: Identification and length of salamanders collected at low-Se streams in summer 2018.

Site ID	species	length (mm)
CRA1	Desmognathus fuscus	98
CRA1	Desmognathus fuscus	79
CRA1	Desmognathus fuscus	86
CRA2	Desmognathus monticola	123
CRA2	Desmognathus monticola	130
CRA2	Desmognathus monticola	97
CRA2	Desmognathus monticola	120
CRA3	Desmognathus fuscus	87
CRA3	Desmognathus fuscus	115
CRA3	Desmognathus monticola	129
CRA3	Desmognathus monticola	73
CRA4	Desmognathus fuscus	85
CRA4	Desmognathus fuscus	60
CRA4	Desmognathus monticola	122
CRA4	Desmognathus monticola	129
CRA5	Desmognathus monticola	87
CRA5	Desmognathus monticola	94
CRA5	Desmognathus monticola	120

Site ID	species	length (mm)
FRY1	Desmognathus fuscus	114
FRY1	Desmognathus fuscus	110
FRY1	Desmognathus fuscus	95
FRY2	Desmognathus fuscus	89
FRY2	Desmognathus fuscus	119
FRY2	Desmognathus fuscus	117
FRY2	Desmognathus fuscus	116
FRY2	Desmognathus monticola	102
FRY3	Desmognathus fuscus	113
FRY3	Desmognathus fuscus	97
FRY3	Desmognathus fuscus	85
FRY3	Desmognathus monticola	94
FRY3	Desmognathus monticola	133
FRY4	Desmognathus fuscus	105
FRY4	Desmognathus fuscus	92
FRY4	Desmognathus fuscus	115
FRY4	Desmognathus monticola	99
FRY4	Desmognathus monticola	127

Table D-4: Count and identification of salamanders collected at high-Se streams in summer 2018.

Site ID	species	length (mm)
LLC2	Desmognathus fuscus	94
LLC2	Desmognathus fuscus	80
LLC2	Desmognathus monticola	52
LLC2	Desmognathus monticola	135
LLC2	Desmognathus monticola	81
LLC3	Desmognathus monticola	76
LLC3	Desmognathus monticola	94
LLC3	Desmognathus monticola	127
LLC3	Desmognathus monticola	122
LLC3	Desmognathus monticola	125
LLC4	Desmognathus fuscus	97
LLC4	Desmognathus fuscus	90
LLC5	Desmognathus monticola	108
LLC5	Desmognathus monticola	97
LLC5	Desmognathus monticola	68

Site ID	species	length (mm)
ROC1	Desmognathus fuscus	83
ROC1	Desmognathus fuscus	108
ROC1	Desmognathus monticola	103
ROC1	Desmognathus monticola	90
ROC2	Desmognathus monticola	92
ROC2	Desmognathus monticola	95
ROC2	Desmognathus monticola	98
ROC3	Desmognathus fuscus	83
ROC3	Desmognathus monticola	97
ROC3	Desmognathus monticola	80
ROC3	Desmognathus monticola	114
ROC3	Desmognathus monticola	74
ROC4	Desmognathus fuscus	94
ROC4	Desmognathus monticola	98
ROC4	Desmognathus monticola	105
ROC4	Desmognathus monticola	115
ROC5	Desmognathus fuscus	109
ROC5	Desmognathus monticola	130
ROC5	Desmognathus monticola	116

Table D-5: Count and identification of benthic macroinvertebrate predators collected at all six study streams in summer 2018.

Family (Genus)[1]	Aeshnidae		Calopterygidae		Chloroperlidae (Suwallia)		Corydalidae		Cordulegastridae		Ephemerellidae (Drunella)		Gerridae		Gomphidae		Hydrophilidae (larvae)		Perlidae		Perlodidae		Polycentropodidae (polycentropus)		Rhyacophilidae		Tipulidae (Hexatoma)		vellidae	
FFG[2]	PR		PR		PR		PR		PR		PR		PR		PR		PR		PR		PR		PR		PR		PR		PR	
EAS1							1		1		53				6				16		13		3		1					
EAS2							2				22				4				23		7				3					
EAS3							1								14				7		23								1	
EAS4					5		1								14				10		26		4						1	
FRY1							9				31		2		1				113				9		23					
FRY2							3		1		37		21		3				77		5				20					
FRY3							6				20				4				47		3		1		22					
FRY4							12		1		4				9				52		5		1		23					
CRA1									1				2		1				18		18				4		2		15	
CRA2			1										30						6		10				5		3		13	
CRA3													20		1				6		28		2		20		3		2	
CRA4													11				1				8		2		20		2		7	
CRA5																			1		4		1		2				1	
LLC1			4				10								36				50										5	
LLC2							3								16				46				4				1			
LLC3	1						6								21				37										8	
LLC4	3						8								19				21										4	
LLC5	5						8								8				10				1		1				8	
ROC1	1						2								9				12		9				11				18	
ROC2	1						1								4				18		7		4		7				40	
ROC3	1						6								8				32		9		8		34				19	
ROC4							3								10				5		7		7		29				6	
ROC5							2								5				4				2		7				27	
HCN1	2						1								5				12		1		1				1		4	
HCN2	1														1				11		2						2		2	
HCN3	2												1		10				9		9		1				2		2	
HCN4	3								1						5				39		4						16		9	
HCN5	1						1								4				37		2						20		8	

[1]Benthic macroinvertebrates were identified to the family level. Individuals were further identified to genus if family contained taxa with multiple feeding habits. [2]Functional Feeding Groups (FFG). Primary source for classification: Poff, N. LeRoy, et al. J. of the North Am. Benthological Soc. 25.4 2006: 730-755.

Table D-6: Count and identification of primary-consumer benthic macroinvertebrates collected at all six study streams in summer 2018.

Family (Genus)[1]	Ameletidae	Baetidae	Chironomidae	Dryopidae (adults)	Elmidae (adults)	Elmidae (larva)	Ephemerellidae (Ephemerella)	Ephemeridae	Lepidostomatidae	Leptophlebiidae	Leuctridae	Limnephilidae	Heptageniidae	Hydropsychidae	Isonychiidae	Nemouridae	Peltoperlidae	Philopotamidae	Psephenidae	Pteronarcyidae	Simuliidae	Taeniopterygidae	Tipulidae (Tipula)
FFG[2]	SC/CG	CG	CG	SC/H	CG	CG	CG	CG	SD	CG	SD	SH	SC	CF	CF	H	SD	CF	SC	SD	CF	SD	SD
EAS1	2	44					14			5	3		69	95	4		7	30		6	7		2
EAS2	8	25					5		1	5			64	126		4	7	50		4	3		1
EAS3	1	3					1			3	6		29	122			46	47	1	18			1
EAS4	2	6					13			3			44	105			96	24		18		1	1
FRY1			49			1		4			4		47	88				34		47			6
FRY2		1	61			1					10		36	150				26		52			1
FRY3		1	89	2			1	1		1	13		25	153				24		41	2		7
FRY4		7	103	2							20		9	134				37		55	3		5
CRA1			8	8							93			192			13	11				1	4
CRA2			4	9	4						80			154			5	2				2	
CRA3		2	16	11							42			174			12				1	1	1
CRA4		10	33	9	6						102			133			17	1			3		1
CRA5		3	2	2	1						3			61			80				1	1	6
LLC1			6	17	7						29			189				18		10	1		1
LLC2			2	10	13						11			326				88		7			1
LLC3			3	12	7						4			238			1	65		4			1
LLC4			3	5	1									248			1	136	1	3			1
LLC5			12	2							2			324				97	1	1	1		2
ROC1		3	7	1	15						174			197			1	45			2		5
ROC2		2	1	32	3						110	1		138			2	42					9
ROC3		7	9	21	36						176			162			4	37	1		2		3
ROC4		6	3	6	7						155			106			1	37			8		3
ROC5		12	5	12	3						85			88				30					
HCN1		4		2	3						154		150	135	7			2	2	19			
HCN2		1			4	2	1	1			42		28	191	22			19	11	50			
HCN3				2	1			5			51		25	115	18		14	15	5	56			2
HCN4		7		12	11						47		36	62	8		1	14	19	23			
HCN5		3		20	3			1			53	1	24	68	4		6	5	7	30			2

[1]Benthic macroinvertebrates were identified to the family level. Individuals were further identified to genus if family contained taxa with multiple feeding habits. [2]Functional Feeding Groups (FFG). Primary source for classification: Poff, N. LeRoy, et al. J. of the North Am. Benthological Soc. 25.4 2006: 730-755.

Table D-7: Identification and length of fish collected at the reference stream, HCN, in summer 2018. No fish were collected from the reference stream, EAS.

Site ID	species	length (mm)
HCN1	Rhinichthys atratulus	60
HCN1	Rhinichthys atratulus	68
HCN1	Rhinichthys atratulus	72
HCN1	Rhinichthys atratulus	66
HCN1	Rhinichthys atratulus	70
HCN1	Cottus bairdi	87
HCN2	Semotilus atromaculatus	92
HCN2	Semotilus atromaculatus	55
HCN2	Rhinichthys atratulus	79
HCN2	Rhinichthys atratulus	62
HCN2	Rhinichthys atratulus	64
HCN2	Rhinichthys atratulus	62
HCN3	Semotilus atromaculatus	102
HCN3	Semotilus atromaculatus	82
HCN3	Semotilus atromaculatus	59
HCN3	Rhinichthys atratulus	70
HCN3	Rhinichthys atratulus	70
HCN3	Rhinichthys atratulus	66
HCN3	Rhinichthys atratulus	64
HCN3	Cottus bairdi	49
HCN4	Semotilus atromaculatus	127
HCN4	Semotilus atromaculatus	75
HCN4	Rhinichthys atratulus	73
HCN4	Rhinichthys atratulus	70
HCN4	Rhinichthys atratulus	70
HCN4	Rhinichthys atratulus	76
HCN4	Cottus bairdi	52
HCN5	Semotilus atromaculatus	102
HCN5	Rhinichthys atratulus	70
HCN5	Rhinichthys atratulus	65
HCN5	Rhinichthys atratulus	63
HCN5	Rhinichthys atratulus	52
HCN5	Rhinichthys atratulus	55
HCN5	Cottus bairdi	60

Table D-8: Identification and length of fish collected at low-Se streams in summer 2018.

Site ID	species	length (mm)
FRY1	Rhinichthys atratulus	38
FRY1	Rhinichthys atratulus	46
FRY1	Rhinichthys atratulus	49
FRY2	Rhinichthys atratulus	75
FRY2	Rhinichthys atratulus	75
FRY2	Rhinichthys atratulus	64
FRY2	Rhinichthys atratulus	84
FRY3	Rhinichthys atratulus	77
FRY3	Rhinichthys atratulus	80
FRY3	Rhinichthys atratulus	83
FRY3	Rhinichthys atratulus	48
FRY3	Rhinichthys atratulus	64
FRY3	Rhinichthys atratulus	65
FRY3	Rhinichthys atratulus	60
FRY4	Rhinichthys atratulus	68
FRY4	Rhinichthys atratulus	71
FRY4	Rhinichthys atratulus	72
FRY4	Rhinichthys atratulus	72
FRY4	Rhinichthys atratulus	68
CRA1	Rhinichthys atratulus	85
CRA1	Rhinichthys atratulus	54
CRA1	Rhinichthys atratulus	65
CRA1	Rhinichthys atratulus	57
CRA1	Rhinichthys atratulus	66
CRA2	Rhinichthys atratulus	66
CRA2	Rhinichthys atratulus	64
CRA2	Rhinichthys atratulus	70
CRA2	Rhinichthys atratulus	68
CRA2	Rhinichthys atratulus	63
CRA2	Rhinichthys atratulus	64
CRA3	Rhinichthys atratulus	75
CRA3	Rhinichthys atratulus	70
CRA3	Rhinichthys atratulus	72
CRA3	Rhinichthys atratulus	68
CRA3	Rhinichthys atratulus	74
CRA4	Rhinichthys atratulus	75

Table D-9: Identification and length of fish collected at high-Se streams in summer 2018.

Site ID	species	length (mm)
LLC1	Rhinichthys atratulus	62
LLC1	Rhinichthys atratulus	59
LLC1	Rhinichthys atratulus	66
LLC1	Rhinichthys atratulus	58
LLC1	Rhinichthys atratulus	52
LLC1	Cottus bairdi	65
LLC2	Rhinichthys atratulus	54
LLC2	Rhinichthys atratulus	58
LLC2	Cottus bairdi	63
LLC3	Semotilus atromaculatus	70
LLC3	Semotilus atromaculatus	66
LLC3	Semotilus atromaculatus	61
LLC3	Semotilus atromaculatus	119
LLC3	Semotilus atromaculatus	120
LLC3	Semotilus atromaculatus	128
LLC3	Semotilus atromaculatus	108
LLC3	Semotilus atromaculatus	131
LLC3	Semotilus atromaculatus	125
LLC3	Semotilus atromaculatus	115
LLC3	Rhinichthys atratulus	82
LLC3	Cottus bairdi	80
LLC4	Rhinichthys atratulus	72
LLC4	Rhinichthys atratulus	70
LLC4	Rhinichthys atratulus	74
LLC4	Rhinichthys atratulus	69
LLC4	Rhinichthys atratulus	82
LLC4	Cottus bairdi	52

Site ID	species	length (mm)
ROC1	Luxilus albeolus	60
ROC1	Luxilus albeolus	76
ROC1	Luxilus albeolus	76
ROC1	Luxilus albeolus	73
ROC1	Luxilus albeolus	76
ROC1	Luxilus albeolus	79
ROC1	Luxilus albeolus	98
ROC2	Semotilus atromaculatus	100
ROC2	Semotilus atromaculatus	131
ROC2	Semotilus atromaculatus	142
ROC2	Lepomis macrochirus	73
ROC2	Lepomis macrochirus	99
ROC2	Cottus bairdi	77
ROC3	Semotilus atromaculatus	129
ROC3	Semotilus atromaculatus	100
ROC3	Semotilus atromaculatus	119
ROC3	Rhinichthys atratulus	76

APPENDIX E - TRACE ELEMENT BIOACCUMULATION RESULTS

Table E-1: Media trace element concentrations at the reference stream, EAS.

		Distance		Trace element concentrations (µg/g dry wt)								
Site ID	Site Type	downstream (m)	media type	Cr	Co	Ni	Cu	Zn	As	Se	Sr	Cd
EAS	Ref	0	biofilm	22.93	8.43	29.42	13.71	77.15	6.77	2.62	166.96	0.67
EAS	Ref	400	biofilm	15.53	5.49	27.56	10.19	51.44	6.06	1.36	163.32	0.38
EAS	Ref	800	biofilm	16.95	5.97	22.74	9.81	51.19	5.32	1.39	28.67	0.38
EAS	Ref	1200	biofilm	20.44	8.68	24.98	11.13	65.72	5.97	1.78	54.66	0.41
EAS	Ref	0	*Desmognathus monticola*	0.32	0.03	0.12	1.58	48.67	0.06	1.25	16.16	0.05
EAS	Ref	0	*Desmognathus monticola*	0.27	0.05	0.10	2.71	55.58	0.07	1.16	20.86	0.04
EAS	Ref	0	*Desmognathus monticola*	0.39	0.08	0.42	4.74	79.94	0.10	1.21	21.34	0.05
EAS	Ref	0	*Desmognathus monticola*	0.68	0.03	0.07	1.14	62.38	0.05	1.22	32.90	0.03
EAS	Ref	0	*Desmognathus monticola*	2.10	1.16	1.98	6.54	91.34	1.16	3.13	46.46	0.18
EAS	Ref	0	*Desmognathus monticola*	0.46	0.03	0.16	2.20	52.68	0.10	0.90	29.25	0.01
EAS	Ref	400	*Desmognathus monticola*	0.78	0.13	0.35	3.06	70.09	0.11	1.61	25.36	0.11
EAS	Ref	400	*Desmognathus monticola*	0.37	0.05	0.22	3.71	60.68	0.08	1.21	19.46	0.07
EAS	Ref	400	*Desmognathus monticola*	0.52	0.01	0.07	1.87	58.26	0.06	1.04	20.54	0.03
EAS	Ref	400	*Desmognathus monticola*	0.56	0.07	0.20	2.03	47.76	0.08	1.08	16.40	0.06
EAS	Ref	400	*Desmognathus monticola*	0.42	0.06	0.17	1.78	54.93	0.09	1.34	26.59	0.06
EAS	Ref	800	*Desmognathus monticola*	0.39	0.08	0.23	6.14	81.53	0.12	1.70	18.59	0.14
EAS	Ref	800	*Desmognathus monticola*	0.72	0.09	0.26	2.99	69.50	0.09	1.11	36.75	0.12
EAS	Ref	800	*Desmognathus monticola*	0.49	0.05	0.16	2.30	60.72	0.13	1.44	31.57	0.03
EAS	Ref	800	*Desmognathus monticola*	0.82	0.29	0.51	3.52	101.13	0.21	1.22	22.25	0.13
EAS	Ref	1200	*Desmognathus monticola*	0.57	0.06	0.17	3.60	68.06	0.14	2.01	16.91	0.08
EAS	Ref	1200	*Desmognathus monticola*	1.93	0.49	0.47	3.71	81.57	0.24	1.78	18.30	0.56
EAS	Ref	1200	*Desmognathus monticola*	0.50	0.06	0.14	3.29	98.41	0.05	1.34	53.27	0.11
EAS	Ref	1200	*Eurycea cirrigera*	0.39	0.16	0.52	2.69	101.06	0.75	1.55	62.92	0.18
EAS	Ref	1200	*Eurycea cirrigera*	0.73	0.17	0.46	3.65	116.62	0.10	1.77	55.90	0.14
EAS	Ref	0	leaf detritus	154.42	2.43	12.31	9.53	36.39	1.37	0.61	65.04	0.27
EAS	Ref	400	leaf detritus	112.46	3.16	13.92	10.34	44.07	1.68	1.06	67.50	0.34
EAS	Ref	800	leaf detritus	74.50	2.33	12.07	9.51	44.11	1.06	0.63	64.93	0.40
EAS	Ref	1200	leaf detritus	39.93	1.21	6.24	5.63	29.71	0.33	0.28	65.09	0.17
EAS	Ref	0	predator BMI	1.16	1.02	1.18	20.38	187.10	0.39	2.21	7.01	1.07
EAS	Ref	400	predator BMI	1.41	0.97	1.38	22.98	209.12	0.40	2.36	15.49	1.16
EAS	Ref	800	predator BMI	1.31	1.61	1.65	23.71	193.65	0.52	2.74	11.60	1.59
EAS	Ref	1200	predator BMI	1.20	4.49	1.72	21.65	197.54	0.55	1.85	10.67	1.90
EAS	Ref	0	primary consumer BMI	2.63	1.41	3.35	24.88	593.38	0.75	1.22	10.26	1.56
EAS	Ref	400	primary consumer BMI	2.81	1.37	3.25	22.70	383.59	0.79	1.11	9.04	1.29
EAS	Ref	800	primary consumer BMI	2.77	2.04	3.39	27.20	240.25	0.95	1.59	7.40	2.04
EAS	Ref	1200	primary consumer BMI	2.52	2.84	3.72	26.54	268.14	0.90	1.28	8.56	1.77
EAS	Ref	0	*Pteronarcys*	1.05	0.61	6.10	30.39	636.55	0.36	0.51	30.77	0.41
EAS	Ref	400	*Pteronarcys*	1.93	0.88	5.85	36.03	554.18	0.46	0.58	26.60	0.34
EAS	Ref	800	*Pteronarcys*	1.49	0.91	5.19	23.61	420.29	0.54	0.57	27.86	0.47
EAS	Ref	1200	*Pteronarcys*	0.96	1.21	6.97	28.61	484.70	0.54	0.56	29.59	0.48
EAS	Ref	0	sediment	12.04	5.49	9.72	5.12	29.54	3.63	0.97	7.28	0.14
EAS	Ref	400	sediment	13.35	5.20	9.66	5.11	29.96	3.61	0.84	8.01	0.12
EAS	Ref	800	sediment	9.61	4.56	7.95	3.89	22.75	3.52	0.54	2.96	0.09
EAS	Ref	1200	sediment	9.29	4.47	8.33	4.07	23.05	3.37	0.56	4.34	0.10

Table E-2: Media trace element concentrations at the reference stream, HCN.

		Distance		Trace element concentrations (µg/g dry wt)								
Site ID	Site Type	downstream (m)	media type	Cr	Co	Ni	Cu	Zn	As	Se	Sr	Cd
HCN	Ref	0	biofilm	18.46	12.78	23.17	19.51	76.38	5.16	2.12	19.49	0.12
HCN	Ref	800	biofilm	19.56	12.36	26.07	19.76	78.47	5.19	2.59	25.37	0.18
HCN	Ref	1200	biofilm	19.08	11.91	22.71	17.37	71.23	5.07	2.14	21.18	0.14
HCN	Ref	1600	biofilm	22.12	10.11	27.47	17.95	83.04	6.53	2.64	32.18	0.15
HCN	Ref	0	*Cottus bairdi*	0.15	0.75	0.27	4.21	109.36	0.17	1.80	160.36	0.10
HCN	Ref	400	*Cottus bairdi*	0.33	0.46	0.13	4.58	101.65	0.43	1.35	121.79	0.08
HCN	Ref	800	*Cottus bairdi*	1.08	1.21	1.76	4.35	106.77	0.39	1.58	143.00	0.12
HCN	Ref	1600	*Cottus bairdi*	0.11	0.12	0.14	3.25	140.43	0.12	1.27	184.85	0.03
HCN	Ref	400	*Desmognathus fuscus*	0.55	0.14	0.09	4.08	99.61	0.26	0.79	45.37	0.04
HCN	Ref	400	*Desmognathus fuscus*	0.35	0.08	0.22	3.39	75.53	0.03	1.21	45.82	0.06
HCN	Ref	1600	*Desmognathus fuscus*	0.25	0.11	0.22	4.00	77.12	0.12	1.18	26.81	0.15
HCN	Ref	1600	*Desmognathus fuscus*	1.62	0.30	1.09	4.59	86.40	0.41	0.89	26.39	0.06
HCN	Ref	1600	*Desmognathus fuscus*	0.22	0.06	0.21	5.62	93.10	0.07	0.71	23.37	0.50
HCN	Ref	0	*Desmognathus monticola*	0.44	0.17	0.39	4.88	58.74	0.13	0.50	24.24	0.03
HCN	Ref	0	*Desmognathus monticola*	0.21	0.09	0.21	6.22	80.39	0.14	1.14	24.95	0.08
HCN	Ref	0	*Desmognathus monticola*	0.15	0.07	0.17	2.61	75.54	0.10	0.73	19.79	0.07
HCN	Ref	400	*Desmognathus monticola*	0.65	0.31	0.25	5.56	94.29	0.26	1.06	32.97	0.09
HCN	Ref	400	*Desmognathus monticola*	0.98	0.55	1.13	12.89	184.34	0.42	1.88	67.38	0.38
HCN	Ref	400	*Desmognathus monticola*	1.86	0.98	1.82	6.68	119.91	0.70	1.88	47.27	0.53
HCN	Ref	400	*Desmognathus monticola*	0.07	0.08	0.15	3.15	54.98	0.05	0.68	23.53	0.00
HCN	Ref	800	*Desmognathus monticola*	0.41	0.23	0.37	4.34	105.88	0.25	1.71	31.19	0.07
HCN	Ref	800	*Desmognathus monticola*	2.61	1.49	2.45	10.15	191.39	1.45	2.54	50.09	0.14
HCN	Ref	800	*Desmognathus monticola*	0.29	0.14	0.28	4.48	73.59	0.14	1.08	17.56	0.05
HCN	Ref	1200	*Desmognathus monticola*	0.23	0.05	0.32	4.41	68.93	0.07	0.82	35.58	0.03
HCN	Ref	1200	*Desmognathus monticola*	0.82	0.26	3.57	5.20	92.54	0.37	1.14	23.72	0.12
HCN	Ref	1200	*Desmognathus monticola*	0.53	0.29	0.59	4.67	99.65	0.33	1.39	23.80	0.14
HCN	Ref	0	*Eurycea cirrigera*	0.18	0.11	0.37	4.37	95.47	0.06	0.79	49.32	0.32
HCN	Ref	0	leaf detritus	25.17	2.76	7.75	10.39	32.91	0.80	0.24	79.16	0.08
HCN	Ref	400	leaf detritus	13.08	3.30	9.23	12.41	35.33	1.12	0.35	72.68	0.09
HCN	Ref	800	leaf detritus	12.07	1.07	6.00	22.92	46.88	0.51	0.17	86.62	0.06
HCN	Ref	1200	leaf detritus	16.09	1.26	5.12	11.22	37.99	0.70	0.20	76.96	0.05
HCN	Ref	1600	leaf detritus	16.55	1.89	5.95	12.09	67.33	0.86	0.35	98.42	0.52
HCN	Ref	0	predator BMI	1.42	2.35	2.01	24.75	214.11	0.51	2.11	9.12	0.86
HCN	Ref	400	predator BMI	0.51	1.02	0.55	12.95	96.23	0.34	0.79	3.01	0.40
HCN	Ref	800	predator BMI	0.68	0.93	1.09	28.24	240.47	0.35	1.93	6.22	0.63
HCN	Ref	1200	predator BMI	0.73	1.33	1.40	28.34	196.28	0.85	2.61	9.50	1.10
HCN	Ref	1600	predator BMI	1.90	1.75	2.29	23.79	174.06	1.04	1.42	13.08	0.24
HCN	Ref	0	primary consumer BMI	3.14	3.86	4.48	21.76	144.10	1.75	1.92	7.59	0.60
HCN	Ref	400	primary consumer BMI	4.90	4.48	5.84	24.59	115.32	2.26	1.91	8.66	0.81
HCN	Ref	800	primary consumer BMI	2.64	2.23	3.32	12.02	90.22	1.13	1.02	5.68	0.57
HCN	Ref	1200	primary consumer BMI	5.85	4.21	7.29	24.99	157.90	2.44	2.54	12.92	1.22
HCN	Ref	1600	primary consumer BMI	3.75	2.97	4.96	25.05	102.49	2.60	1.78	12.75	0.52

Site ID	Site Type	Distance downstream (m)	media type	Trace element concentrations (µg/g dry wt) Cr	Co	Ni	Cu	Zn	As	Se	Sr	Cd
HCN	Ref	0	*Pteronarcys*	2.19	6.06	9.54	32.34	474.37	0.83	0.63	29.18	0.27
HCN	Ref	400	*Pteronarcys*	2.01	6.33	9.75	36.99	509.47	0.95	0.69	32.57	0.23
HCN	Ref	800	*Pteronarcys*	2.23	2.71	6.15	31.84	397.33	0.84	0.77	29.44	0.19
HCN	Ref	1200	*Pteronarcys*	1.71	2.12	5.48	36.51	555.80	0.75	0.66	28.59	0.25
HCN	Ref	1600	*Pteronarcys*	2.61	4.41	7.84	35.28	315.34	1.79	0.55	28.83	0.25
HCN	Ref	0	*Rhinichthys atratulus*	0.06	0.07	0.11	3.26	181.18	0.05	1.62	82.50	0.24
HCN	Ref	0	*Rhinichthys atratulus*	0.05	0.04	0.12	2.53	255.54	0.07	2.00	86.87	0.11
HCN	Ref	0	*Rhinichthys atratulus*	0.04	0.09	0.10	1.95	228.23	0.13	1.92	88.40	0.04
HCN	Ref	0	*Rhinichthys atratulus*	0.13	0.08	0.21	2.06	193.56	0.21	1.50	86.85	0.06
HCN	Ref	0	*Rhinichthys atratulus*	0.26	0.18	0.27	2.84	163.95	0.17	1.41	67.20	0.05
HCN	Ref	400	*Rhinichthys atratulus*	0.01	0.01	0.02	2.61	243.79	0.01	1.45	80.92	0.07
HCN	Ref	400	*Rhinichthys atratulus*	0.04	0.01	0.05	2.47	170.82	0.01	1.86	55.64	0.05
HCN	Ref	400	*Rhinichthys atratulus*	0.11	0.06	0.00	2.24	187.54	0.13	1.26	72.73	0.06
HCN	Ref	400	*Rhinichthys atratulus*	0.01	0.01	0.15	1.99	176.46	0.04	1.09	73.53	0.06
HCN	Ref	800	*Rhinichthys atratulus*	0.07	0.02	0.03	3.44	271.00	0.01	1.54	98.46	0.17
HCN	Ref	800	*Rhinichthys atratulus*	0.03	0.03	0.09	2.24	156.49	0.07	1.61	53.46	0.07
HCN	Ref	800	*Rhinichthys atratulus*	0.05	0.08	0.14	3.26	307.52	0.04	2.09	124.96	0.12
HCN	Ref	800	*Rhinichthys atratulus*	0.02	0.04	0.05	2.59	258.50	0.01	1.68	124.75	0.07
HCN	Ref	1200	*Rhinichthys atratulus*	0.04	0.03	0.10	2.48	238.71	0.08	1.42	79.62	0.06
HCN	Ref	1200	*Rhinichthys atratulus*	0.04	0.02	0.11	1.77	198.40	0.05	1.59	60.67	0.04
HCN	Ref	1200	*Rhinichthys atratulus*	0.07	0.06	0.12	2.16	265.54	0.14	1.97	97.37	0.09
HCN	Ref	1200	*Rhinichthys atratulus*	0.06	0.03	0.06	1.82	198.29	0.08	1.83	81.48	0.06
HCN	Ref	1600	*Rhinichthys atratulus*	0.16	0.05	0.97	2.50	245.53	0.07	1.63	99.42	0.04
HCN	Ref	1600	*Rhinichthys atratulus*	0.08	0.04	0.17	2.18	167.01	0.07	1.19	56.62	0.06
HCN	Ref	1600	*Rhinichthys atratulus*	0.08	0.05	0.08	2.14	189.78	0.04	1.27	82.12	0.06
HCN	Ref	1600	*Rhinichthys atratulus*	0.09	0.03	0.08	2.96	208.97	0.07	1.00	121.34	0.03
HCN	Ref	1600	*Rhinichthys atratulus*	0.12	0.06	0.79	2.90	236.71	0.09	1.58	81.82	0.11
HCN	Ref	0	sediment	6.54	4.89	8.12	5.04	25.86	2.32	0.66	5.17	0.08
HCN	Ref	400	sediment	6.31	4.71	7.75	5.20	25.79	2.41	0.67	4.72	0.04
HCN	Ref	800	sediment	5.87	4.32	7.28	4.32	24.73	2.19	0.44	4.26	0.03
HCN	Ref	1200	sediment	5.47	3.72	6.23	3.77	22.19	2.02	0.45	3.55	0.03
HCN	Ref	1600	sediment	5.79	4.14	7.33	4.17	24.26	2.22	0.55	5.15	0.04
HCN	Ref	0	*Semotilus atromaculatus*	3.72	0.26	0.23	4.08	99.85	0.02	1.14	100.73	0.06
HCN	Ref	400	*Semotilus atromaculatus*	0.11	0.03	0.18	2.31	106.30	0.04	0.77	140.79	0.03
HCN	Ref	400	*Semotilus atromaculatus*	0.03	0.01	0.01	3.86	107.22	0.01	1.30	59.79	0.05
HCN	Ref	800	*Semotilus atromaculatus*	0.06	0.01	0.11	2.62	146.71	0.00	0.84	175.61	0.00
HCN	Ref	800	*Semotilus atromaculatus*	0.04	0.01	0.11	3.11	167.45	0.00	0.99	111.35	0.01
HCN	Ref	800	*Semotilus atromaculatus*	0.02	0.00	0.08	4.52	151.13	0.00	0.99	88.39	0.00
HCN	Ref	1200	*Semotilus atromaculatus*	0.35	0.03	0.13	3.00	121.08	0.02	1.15	147.06	0.02
HCN	Ref	1200	*Semotilus atromaculatus*	0.03	0.00	0.03	3.01	187.49	0.00	1.06	94.46	0.00

Table E-3: Media trace element concentrations at the low-Se stream, CRA.

		Distance		Trace element concentrations (µg/g dry wt)								
Site ID	Site Type	downstream (m)	media type	Cr	Co	Ni	Cu	Zn	As	Se	Sr	Cd
CRA	Low-Se	0	biofilm	23.74	31.34	63.67	37.95	182.99	8.39	5.21	85.05	0.45
CRA	Low-Se	400	biofilm	22.53	25.66	55.12	32.10	170.73	7.49	4.49	77.89	0.37
CRA	Low-Se	800	biofilm	20.29	24.92	53.57	31.09	178.75	6.94	4.09	64.00	0.35
CRA	Low-Se	1200	biofilm	21.92	37.29	79.04	38.62	261.96	7.96	5.53	69.15	0.53
CRA	Low-Se	400	*Desmognathus fuscus*	0.53	0.20	0.00	2.95	72.90	0.12	1.57	68.43	0.09
CRA	Low-Se	400	*Desmognathus fuscus*	1.14	0.92	1.76	5.27	100.05	0.44	2.58	80.65	0.28
CRA	Low-Se	800	*Desmognathus fuscus*	0.63	0.79	1.46	3.72	79.36	0.17	1.65	64.06	0.09
CRA	Low-Se	800	*Desmognathus fuscus*	0.33	0.49	1.34	5.55	75.82	0.17	2.22	85.00	0.16
CRA	Low-Se	1600	*Desmognathus fuscus*	0.68	0.89	1.29	4.13	81.12	0.35	2.91	23.54	0.15
CRA	Low-Se	1600	*Desmognathus fuscus*	0.10	0.07	0.27	2.48	90.57	0.08	2.06	83.17	0.16
CRA	Low-Se	1600	*Desmognathus fuscus*	0.19	0.16	0.37	4.27	61.69	0.13	1.87	48.13	0.25
CRA	Low-Se	0	*Desmognathus monticola*	0.93	0.31	0.31	16.51	91.38	0.22	1.95	77.64	0.54
CRA	Low-Se	0	*Desmognathus monticola*	0.19	0.27	0.29	12.88	122.71	0.10	2.18	189.84	0.35
CRA	Low-Se	0	*Desmognathus monticola*	1.74	1.58	3.19	7.23	112.77	0.80	2.53	70.92	1.30
CRA	Low-Se	400	*Desmognathus monticola*	0.25	0.09	0.14	4.17	82.43	0.08	1.61	99.36	0.08
CRA	Low-Se	400	*Desmognathus monticola*	0.87	0.14	0.24	6.57	87.93	0.05	1.18	112.27	0.25
CRA	Low-Se	800	*Desmognathus monticola*	0.36	0.08	0.29	5.99	99.94	0.08	1.80	93.12	0.06
CRA	Low-Se	800	*Desmognathus monticola*	0.71	0.45	1.57	5.22	70.82	0.27	3.21	26.79	0.18
CRA	Low-Se	1200	*Desmognathus monticola*	0.25	0.10	0.12	4.79	52.84	0.08	1.12	45.00	0.02
CRA	Low-Se	1200	*Desmognathus monticola*	1.73	1.44	3.99	12.54	87.09	0.92	1.54	120.94	0.56
CRA	Low-Se	1200	*Desmognathus monticola*	1.25	1.87	2.33	6.89	80.35	0.44	2.18	40.28	0.95
CRA	Low-Se	1200	*Desmognathus monticola*	0.33	0.31	0.51	4.56	63.87	0.22	1.85	46.55	0.07
CRA	Low-Se	0	leaf detritus	17.84	13.16	34.76	15.03	139.52	1.26	2.11	289.33	0.43
CRA	Low-Se	400	leaf detritus	43.36	6.02	18.47	11.64	62.12	1.01	1.53	242.61	0.16
CRA	Low-Se	800	leaf detritus	31.12	4.66	17.09	12.97	50.71	0.97	1.43	246.18	0.13
CRA	Low-Se	1200	leaf detritus	14.27	5.46	24.84	22.20	87.78	0.92	1.37	223.76	0.29
CRA	Low-Se	1600	leaf detritus	33.93	2.11	12.35	13.56	41.15	0.86	0.86	243.43	0.12
CRA	Low-Se	0	predator BMI	4.17	2.01	0.47	26.09	293.65	0.48	6.56	26.41	0.36
CRA	Low-Se	400	predator BMI	0.86	1.98	1.40	18.97	319.75	0.26	6.21	33.04	0.19
CRA	Low-Se	800	predator BMI	0.61	3.12	2.28	29.29	292.76	0.34	7.39	40.97	0.84
CRA	Low-Se	1200	predator BMI	1.21	1.11	2.96	21.98	275.50	0.28	5.35	37.06	0.28
CRA	Low-Se	0	primary consumer BMI	2.55	5.12	7.07	30.43	601.09	0.60	4.36	37.14	0.57
CRA	Low-Se	400	primary consumer BMI	2.50	15.20	13.18	39.31	363.06	1.06	5.47	41.23	0.90
CRA	Low-Se	800	primary consumer BMI	2.14	7.37	10.51	33.24	273.17	1.06	4.54	32.89	1.04
CRA	Low-Se	1200	primary consumer BMI	2.65	8.50	14.43	36.23	307.25	1.33	6.17	43.52	1.13
CRA	Low-Se	1600	primary consumer BMI	3.40	4.47	10.12	36.86	265.79	1.41	6.03	45.17	0.79
CRA	Low-Se	400	*Rhinichthys atratulus*	0.21	0.27	0.36	4.24	312.78	0.05	4.45	358.49	0.08
CRA	Low-Se	800	*Rhinichthys atratulus*	0.09	0.10	0.25	4.47	242.28	0.02	4.73	193.71	0.17
CRA	Low-Se	800	*Rhinichthys atratulus*	0.09	0.24	0.22	3.91	264.25	0.09	7.07	309.27	0.15
CRA	Low-Se	800	*Rhinichthys atratulus*	0.10	0.08	0.20	2.89	186.05	0.05	4.74	302.60	0.02
CRA	Low-Se	800	*Rhinichthys atratulus*	0.10	0.09	0.22	2.90	272.77	0.02	2.53	162.75	0.09
CRA	Low-Se	800	*Rhinichthys atratulus*	0.28	0.07	0.23	4.12	190.44	0.01	2.45	191.53	0.16
CRA	Low-Se	1200	*Rhinichthys atratulus*	0.11	0.12	0.19	4.59	268.09	0.05	6.10	261.46	0.09
CRA	Low-Se	1200	*Rhinichthys atratulus*	0.09	0.06	0.16	2.23	184.01	0.04	4.23	226.44	0.06
CRA	Low-Se	1200	*Rhinichthys atratulus*	0.15	0.05	0.14	3.06	245.60	0.02	4.23	183.57	0.14
CRA	Low-Se	1200	*Rhinichthys atratulus*	0.07	0.09	0.22	3.86	265.09	0.04	8.32	185.25	0.22
CRA	Low-Se	1200	*Rhinichthys atratulus*	0.10	0.20	0.23	3.24	213.65	0.16	7.79	192.37	0.33
CRA	Low-Se	1200	*Rhinichthys atratulus*	0.08	0.03	0.13	2.70	213.81	0.03	2.77	196.48	0.06
CRA	Low-Se	1600	*Rhinichthys atratulus*	0.08	0.03	0.24	5.79	183.63	0.04	1.92	221.79	0.05
CRA	Low-Se	1600	*Rhinichthys atratulus*	0.09	0.05	0.13	2.17	247.34	0.13	4.67	254.11	0.05
CRA	Low-Se	1600	*Rhinichthys atratulus*	0.66	0.08	0.28	1.97	153.73	0.17	7.24	121.00	0.20
CRA	Low-Se	1600	*Rhinichthys atratulus*	0.07	0.03	0.07	2.46	196.26	0.06	3.32	179.66	0.03
CRA	Low-Se	1600	*Rhinichthys atratulus*	0.08	0.04	2.43	2.22	192.47	0.09	6.02	241.59	0.04
CRA	Low-Se	0	sediment	15.93	20.44	47.46	22.96	128.28	6.15	2.73	36.92	0.24
CRA	Low-Se	400	sediment	16.12	22.76	52.81	24.00	146.49	5.64	3.20	43.23	0.28
CRA	Low-Se	800	sediment	16.95	21.18	50.80	24.63	135.88	6.35	3.23	43.68	0.28
CRA	Low-Se	1200	sediment	15.60	19.68	47.37	21.95	125.49	5.67	2.79	37.25	0.26
CRA	Low-Se	1600	sediment	13.19	16.64	39.65	20.99	104.28	6.39	2.46	31.07	0.22
CRA	Low-Se	1200	*Semotilus atromaculatus*	0.09	0.07	0.48	2.94	146.58	0.01	2.40	233.50	0.06
CRA	Low-Se	400	*Tipula*	2.43	20.12	35.33	31.39	166.35	1.44	4.90	52.50	0.31
CRA	Low-Se	800	*Tipula*	2.64	15.04	30.01	32.65	155.47	1.02	4.93	40.04	0.22
CRA	Low-Se	1600	*Tipula*	3.46	11.29	23.50	24.51	118.25	1.40	5.15	28.12	0.57

Table E-4: Media trace element concentrations at the low-Se stream, FRY.

Site ID	Site Type	Distance downstream (m)	media type	Trace element concentrations (µg/g dry wt) Cr	Co	Ni	Cu	Zn	As	Se	Sr	Cd
FRY	Low-Se	0	biofilm	4.49	2.73	5.27	8.58	36.63	2.97	2.01	97.24	0.22
FRY	Low-Se	400	biofilm	47.99	30.80	57.13	48.76	257.98	17.07	7.05	97.41	0.36
FRY	Low-Se	800	biofilm	3.88	2.59	5.10	8.05	37.94	2.56	2.13	98.91	0.30
FRY	Low-Se	1200	biofilm	7.36	4.44	8.75	10.89	52.28	3.48	2.43	82.90	0.30
FRY	Low-Se	0	*Desmognathus fuscus*	0.07	0.03	0.06	2.96	84.78	0.11	1.71	75.77	0.02
FRY	Low-Se	0	*Desmognathus fuscus*	1.14	0.67	1.13	4.23	91.87	0.93	2.50	87.23	0.17
FRY	Low-Se	0	*Desmognathus fuscus*	0.11	0.07	0.11	2.42	101.06	0.11	1.12	89.97	0.04
FRY	Low-Se	400	*Desmognathus fuscus*	0.36	0.20	0.42	4.35	67.40	0.17	1.99	56.19	0.04
FRY	Low-Se	400	*Desmognathus fuscus*	0.20	0.07	0.22	5.92	76.01	0.18	1.76	41.56	0.07
FRY	Low-Se	400	*Desmognathus fuscus*	0.15	0.08	0.16	4.84	90.58	0.14	2.24	23.55	0.23
FRY	Low-Se	800	*Desmognathus fuscus*	2.10	0.80	1.90	5.21	87.98	1.06	2.84	35.07	0.16
FRY	Low-Se	800	*Desmognathus fuscus*	2.04	1.27	2.15	5.08	80.40	1.00	3.69	63.31	0.21
FRY	Low-Se	800	*Desmognathus fuscus*	0.52	0.38	0.69	4.99	80.63	0.46	4.25	77.09	0.07
FRY	Low-Se	800	*Desmognathus fuscus*	0.80	0.41	0.88	5.04	99.60	0.45	1.60	61.61	0.09
FRY	Low-Se	1200	*Desmognathus fuscus*	0.51	0.38	0.69	3.51	71.42	0.42	4.14	47.69	0.11
FRY	Low-Se	1200	*Desmognathus fuscus*	0.37	0.19	0.37	3.13	52.23	0.20	1.68	33.80	0.05
FRY	Low-Se	1200	*Desmognathus fuscus*	0.20	0.26	0.26	3.69	86.04	0.18	1.95	28.47	0.04
FRY	Low-Se	0	*Desmognathus monticola*	0.96	0.54	0.95	5.61	92.34	0.42	2.07	60.66	0.05
FRY	Low-Se	400	*Desmognathus monticola*	1.24	0.54	1.11	7.16	97.38	0.66	2.45	52.43	0.20
FRY	Low-Se	800	*Desmognathus monticola*	1.65	1.01	1.86	4.37	73.11	0.87	2.54	66.07	0.05
FRY	Low-Se	400	*Eurycea cirrigera*	1.11	0.26	0.63	1.66	54.53	0.17	0.38	30.84	0.03
FRY	Low-Se	0	leaf detritus	27.31	2.28	7.10	9.54	35.67	1.17	1.59	141.43	0.09
FRY	Low-Se	400	leaf detritus	11.89	2.94	6.61	9.92	79.64	1.02	2.37	151.41	0.11
FRY	Low-Se	800	leaf detritus	37.44	2.64	7.91	12.05	53.02	1.19	4.41	141.78	0.14
FRY	Low-Se	1200	leaf detritus	37.25	2.09	6.88	10.61	39.09	1.12	2.17	166.06	0.09
FRY	Low-Se	0	predator BMI	0.66	0.61	1.07	18.65	161.52	0.32	4.28	10.54	0.17
FRY	Low-Se	400	predator BMI	0.88	1.15	1.19	24.73	237.03	0.52	5.06	16.28	0.20
FRY	Low-Se	800	predator BMI	1.60	1.24	1.22	23.26	233.61	0.53	5.49	20.09	0.36
FRY	Low-Se	1200	predator BMI	0.91	1.03	1.37	19.70	178.42	0.58	5.28	22.87	0.25
FRY	Low-Se	0	primary consumer BMI	1.97	1.57	2.46	32.20	165.57	0.92	4.44	17.41	0.54
FRY	Low-Se	400	primary consumer BMI	3.96	2.60	3.87	31.90	236.46	1.96	5.06	21.24	0.47
FRY	Low-Se	800	primary consumer BMI	3.22	2.44	3.82	39.37	234.93	1.83	6.08	22.61	0.75
FRY	Low-Se	1200	primary consumer BMI	3.33	2.21	3.78	40.71	217.75	1.68	5.70	21.68	0.76
FRY	Low-Se	0	*Pteronarcys*	1.37	1.03	4.12	27.53	294.84	0.70	2.15	35.97	0.17
FRY	Low-Se	400	*Pteronarcys*	1.72	1.82	4.54	28.03	528.98	1.05	1.75	35.32	0.06
FRY	Low-Se	800	*Pteronarcys*	1.53	1.34	3.10	29.51	424.54	0.95	2.91	32.89	0.13
FRY	Low-Se	1200	*Pteronarcys*	1.05	0.80	2.46	27.29	370.69	0.77	2.06	26.76	0.10
FRY	Low-Se	0	*Rhinichthys atratulus*	0.14	0.07	0.13	2.90	128.44	0.11	3.06	51.73	0.05
FRY	Low-Se	0	*Rhinichthys atratulus*	0.10	0.02	0.38	3.28	109.43	0.11	3.14	49.93	0.01
FRY	Low-Se	0	*Rhinichthys atratulus*	0.12	0.08	0.24	5.87	117.48	0.15	2.40	65.17	0.10
FRY	Low-Se	0	*Rhinichthys atratulus*	0.07	0.03	0.48	3.01	122.07	0.08	2.60	46.82	0.03
FRY	Low-Se	0	*Rhinichthys atratulus*	0.05	0.04	0.08	3.52	113.89	0.08	3.22	46.46	0.02
FRY	Low-Se	400	*Rhinichthys atratulus*	0.09	0.08	0.08	2.57	171.08	0.16	3.25	142.51	0.05
FRY	Low-Se	400	*Rhinichthys atratulus*	0.15	0.08	0.15	3.48	165.44	0.22	2.82	179.55	0.06
FRY	Low-Se	400	*Rhinichthys atratulus*	0.08	0.05	0.05	2.81	169.05	0.10	4.55	62.97	0.03
FRY	Low-Se	400	*Rhinichthys atratulus*	0.15	0.12	0.17	3.22	144.42	0.20	5.10	62.10	0.03
FRY	Low-Se	400	*Rhinichthys atratulus*	0.07	0.04	0.08	2.97	150.01	0.17	3.58	74.15	0.06
FRY	Low-Se	400	*Rhinichthys atratulus*	0.07	0.06	0.06	3.32	159.20	0.19	3.05	91.91	0.02
FRY	Low-Se	400	*Rhinichthys atratulus*	0.09	0.05	0.08	2.00	143.63	0.08	4.54	56.79	0.03
FRY	Low-Se	800	*Rhinichthys atratulus*	0.13	0.06	0.07	2.48	185.02	0.13	3.81	120.72	0.00
FRY	Low-Se	800	*Rhinichthys atratulus*	0.06	0.03	0.06	3.29	151.59	0.17	3.07	91.04	0.06
FRY	Low-Se	800	*Rhinichthys atratulus*	0.21	0.06	0.10	3.11	153.34	0.17	4.16	119.50	0.03
FRY	Low-Se	800	*Rhinichthys atratulus*	0.11	0.02	0.05	3.07	108.16	0.13	3.59	45.78	0.02
FRY	Low-Se	0	sediment	11.09	7.34	13.82	12.35	54.38	3.36	1.24	10.09	0.07
FRY	Low-Se	400	sediment	1.04	0.74	1.22	2.27	13.41	0.76	0.58	23.41	0.04
FRY	Low-Se	800	sediment	9.37	6.37	10.53	7.83	43.11	3.82	1.10	15.58	0.05
FRY	Low-Se	1200	sediment	8.98	6.53	11.06	8.71	46.27	3.80	1.46	17.85	0.07
FRY	Low-Se	0	*Semotilus atromaculatus*	0.07	0.07	0.41	4.06	147.81	0.03	1.98	83.57	0.04
FRY	Low-Se	0	*Tipula*	3.07	2.23	3.75	15.46	86.89	1.11	4.61	22.86	0.08
FRY	Low-Se	400	*Tipula*	3.55	3.81	5.40	18.35	130.67	2.11	6.23	31.69	0.13
FRY	Low-Se	800	*Tipula*	3.64	3.24	5.95	18.97	106.69	1.80	6.38	34.58	0.13
FRY	Low-Se	1200	*Tipula*	4.42	3.22	5.62	16.17	95.59	2.18	6.27	36.60	0.11

Table E-5: Trace element concentrations at the high-Se stream, LLC.

Site ID	Site Type	Distance downstream (m)	media type	Trace element concentrations (µg/g dry wt) Cr	Co	Ni	Cu	Zn	As	Se	Sr	Cd
LLC	High-Se	400	biofilm	16.22	72.30	174.01	21.33	293.01	4.94	6.92	72.72	1.05
LLC	High-Se	400	biofilm	7.73	20.24	49.91	6.93	93.26	5.15	3.24	98.29	0.69
LLC	High-Se	1200	biofilm	18.13	48.17	114.59	20.43	198.15	4.14	5.33	63.61	0.72
LLC	High-Se	1200	biofilm	15.34	47.30	113.28	22.31	201.23	4.92	6.28	62.38	0.68
LLC	High-Se	1600	biofilm	19.03	39.76	96.81	17.42	219.45	5.24	6.32	68.55	0.41
LLC	High-Se	400	*Cottus bairdi*	0.38	1.45	1.39	4.04	83.81	0.16	9.34	167.80	0.07
LLC	High-Se	800	*Cottus bairdi*	0.19	1.67	1.59	2.57	218.66	0.10	9.39	191.22	0.08
LLC	High-Se	1200	*Cottus bairdi*	0.33	1.64	1.44	2.45	163.86	0.10	11.38	294.05	0.12
LLC	High-Se	1600	*Cottus bairdi*	0.51	1.22	0.92	2.92	160.50	0.23	13.28	235.34	0.07
LLC	High-Se	400	*Desmognathus fuscus*	0.20	0.25	0.51	7.16	85.62	0.04	2.99	80.25	0.11
LLC	High-Se	400	*Desmognathus fuscus*	0.29	0.63	1.27	2.66	74.89	0.11	3.10	74.35	0.23
LLC	High-Se	1200	*Desmognathus fuscus*	0.25	0.17	0.35	8.19	96.01	0.17	2.61	73.96	0.14
LLC	High-Se	1200	*Desmognathus fuscus*	0.78	0.74	1.73	8.83	101.04	0.15	1.95	89.60	0.18
LLC	High-Se	0	*Desmognathus monticola*	0.33	1.73	2.55	7.97	82.00	0.14	2.22	24.72	0.16
LLC	High-Se	0	*Desmognathus monticola*	1.92	3.27	8.27	20.00	122.05	0.41	2.99	92.06	0.70
LLC	High-Se	0	*Desmognathus monticola*	0.31	0.64	1.01	2.98	67.35	0.07	2.03	37.93	0.17
LLC	High-Se	800	*Desmognathus monticola*	1.24	2.06	5.04	11.76	94.19	0.36	2.90	67.13	0.30
LLC	High-Se	800	*Desmognathus monticola*	0.53	0.79	1.57	9.23	86.09	0.10	1.67	58.70	0.22
LLC	High-Se	800	*Desmognathus monticola*	0.87	1.22	2.09	3.19	77.81	0.12	2.99	53.52	0.20
LLC	High-Se	800	*Desmognathus monticola*	0.68	1.04	2.12	12.95	98.69	0.15	3.05	100.71	0.08
LLC	High-Se	800	*Desmognathus monticola*	1.50	1.69	3.59	11.92	124.44	0.21	2.66	81.20	0.15
LLC	High-Se	1200	*Desmognathus monticola*	0.79	0.42	0.75	7.70	91.66	0.12	4.56	62.59	0.26
LLC	High-Se	1200	*Desmognathus monticola*	1.28	2.69	4.07	16.33	110.14	0.18	4.00	86.97	0.38
LLC	High-Se	1200	*Desmognathus monticola*	1.01	0.97	1.91	5.62	82.45	0.15	3.66	60.06	0.23
LLC	High-Se	0	leaf detritus	15.95	70.26	145.80	11.53	182.47	0.89	8.27	206.50	0.88
LLC	High-Se	400	leaf detritus	49.75	16.65	56.05	12.01	80.09	0.80	5.03	173.89	0.40
LLC	High-Se	800	leaf detritus	43.71	13.80	43.42	11.74	59.51	0.56	5.48	153.89	0.34
LLC	High-Se	1200	leaf detritus	27.48	1.49	6.37	10.99	27.09	0.25	0.68	150.77	0.09
LLC	High-Se	1600	leaf detritus	38.44	1.91	10.93	9.96	38.11	0.30	0.96	131.78	0.09
LLC	High-Se	0	predator BMI	0.79	6.20	11.27	13.54	159.20	0.22	10.92	16.51	0.18
LLC	High-Se	400	predator BMI	1.77	19.03	34.32	17.30	278.82	0.51	14.41	23.46	0.58
LLC	High-Se	800	predator BMI	1.04	7.47	11.48	12.20	177.49	0.23	9.88	15.55	0.21
LLC	High-Se	1200	predator BMI	1.27	2.90	6.98	20.77	265.08	0.27	13.93	30.76	0.24
LLC	High-Se	1600	predator BMI	1.73	4.66	10.16	22.48	272.21	0.41	17.12	33.39	0.36

Site ID	Site Type	Distance downstream (m)	media type	Trace element concentrations (µg/g dry wt) Cr	Co	Ni	Cu	Zn	As	Se	Sr	Cd
LLC	High-Se	0	primary consumer BMI	4.00	10.06	24.68	15.31	136.42	1.05	11.11	30.59	0.79
LLC	High-Se	400	primary consumer BMI	8.29	15.31	40.00	25.82	204.98	2.15	15.39	40.34	1.26
LLC	High-Se	800	primary consumer BMI	7.91	10.89	31.00	24.77	203.72	1.61	13.13	32.19	0.96
LLC	High-Se	1200	primary consumer BMI	7.19	10.52	28.14	22.17	182.42	1.71	14.42	32.98	1.18
LLC	High-Se	1600	primary consumer BMI	4.60	8.47	23.11	26.25	216.16	1.44	19.55	33.79	0.80
LLC	High-Se	0	*Pteronarcys*	3.08	12.45	25.31	19.69	264.89	0.84	9.04	61.34	0.45
LLC	High-Se	400	*Pteronarcys*	2.79	10.90	25.97	18.54	945.71	1.02	10.92	59.53	0.40
LLC	High-Se	800	*Pteronarcys*	1.99	7.46	26.34	19.19	277.49	0.64	7.77	48.55	0.28
LLC	High-Se	1200	*Pteronarcys*	1.98	8.04	21.25	16.11	520.40	0.77	9.24	52.79	0.27
LLC	High-Se	1600	*Pteronarcys*	1.69	5.82	18.77	17.89	666.50	0.84	10.21	61.30	0.30
LLC	High-Se	400	*Rhinichthys atratulus*	0.40	0.16	0.00	3.46	259.20	0.13	5.33	132.69	0.16
LLC	High-Se	400	*Rhinichthys atratulus*	0.43	0.05	0.00	2.70	162.90	0.07	5.44	108.29	0.11
LLC	High-Se	400	*Rhinichthys atratulus*	0.41	0.10	0.00	3.45	351.65	0.05	5.11	330.39	0.03
LLC	High-Se	400	*Rhinichthys atratulus*	0.61	0.19	0.13	3.54	383.04	0.04	8.15	216.79	0.15
LLC	High-Se	400	*Rhinichthys atratulus*	0.06	0.04	0.13	1.83	216.55	0.11	4.72	140.99	0.10
LLC	High-Se	1200	*Rhinichthys atratulus*	0.53	0.33	0.92	2.88	244.90	0.13	7.33	169.48	0.10
LLC	High-Se	1200	*Rhinichthys atratulus*	0.98	0.23	0.75	2.61	162.03	0.19	6.67	166.33	0.05
LLC	High-Se	1600	*Rhinichthys atratulus*	0.47	0.06	0.00	3.07	285.42	0.06	6.51	244.73	0.12
LLC	High-Se	1600	*Rhinichthys atratulus*	0.15	0.21	0.12	2.62	177.88	0.06	6.19	192.55	0.06
LLC	High-Se	1600	*Rhinichthys atratulus*	0.35	0.08	0.00	3.07	356.98	0.05	6.16	316.40	0.11
LLC	High-Se	1600	*Rhinichthys atratulus*	0.32	0.06	0.00	3.38	259.63	0.06	4.65	153.67	0.05
LLC	High-Se	1600	*Rhinichthys atratulus*	0.26	1.38	6.97	3.00	109.51	0.14	10.95	150.31	0.05
LLC	High-Se	0	sediment	6.41	29.65	67.33	5.86	94.01	2.26	1.46	17.33	0.39
LLC	High-Se	400	sediment	6.01	32.61	70.67	6.44	97.10	1.92	1.70	19.75	0.42
LLC	High-Se	800	sediment	4.97	27.47	52.49	4.57	66.51	1.90	1.07	12.61	0.30
LLC	High-Se	1200	sediment	6.03	24.71	51.41	4.55	63.03	1.62	1.00	13.28	0.28
LLC	High-Se	1600	sediment	5.83	22.24	44.70	4.41	61.17	1.73	1.33	14.49	0.28
LLC	High-Se	800	*Semotilus atromaculatus*	0.10	0.12	0.36	40.03	144.66	0.04	6.71	201.41	0.05
LLC	High-Se	800	*Semotilus atromaculatus*	0.14	0.10	0.58	25.68	161.51	0.05	4.56	188.39	0.07
LLC	High-Se	800	*Semotilus atromaculatus*	0.34	0.06	0.25	10.61	116.33	0.02	9.91	191.51	0.03
LLC	High-Se	800	*Semotilus atromaculatus*	0.16	0.10	0.48	5.79	102.78	0.04	3.51	73.46	0.13
LLC	High-Se	800	*Semotilus atromaculatus*	0.11	0.03	0.19	2.66	150.69	0.02	3.33	122.38	0.02
LLC	High-Se	800	*Semotilus atromaculatus*	0.17	0.07	0.23	3.23	241.77	0.03	5.53	155.55	0.08
LLC	High-Se	800	*Semotilus atromaculatus*	0.09	0.10	0.68	11.65	171.67	0.03	7.92	201.47	0.06
LLC	High-Se	800	*Semotilus atromaculatus*	0.18	0.08	0.48	35.70	154.59	0.04	6.15	281.12	0.05
LLC	High-Se	800	*Semotilus atromaculatus*	0.14	0.10	0.62	24.40	212.53	0.06	7.98	235.82	0.11
LLC	High-Se	800	*Semotilus atromaculatus*	0.06	0.06	0.42	12.45	133.26	0.01	4.39	190.62	0.03

Table E-6: Media trace element concentrations at the high-Se stream, ROC.

		Distance		Trace element concentrations (µg/g dry wt)								
Site ID	Site Type	downstream (m)	media type	Cr	Co	Ni	Cu	Zn	As	Se	Sr	Cd
ROC	High-Se	400	biofilm	18.73	19.41	38.72	28.97	132.11	7.06	9.00	120.03	0.30
ROC	High-Se	800	biofilm	19.76	19.16	40.13	28.83	131.66	7.59	10.32	141.19	0.32
ROC	High-Se	1200	biofilm	18.96	19.41	47.91	29.59	162.88	7.14	12.59	148.77	0.36
ROC	High-Se	1600	biofilm	23.82	20.46	49.17	36.59	164.87	7.07	12.37	144.45	0.35
ROC	High-Se	1200	*Cottus bairdi*	0.07	0.39	0.35	2.86	127.00	0.14	15.77	543.38	0.05
ROC	High-Se	400	*Desmognathus fuscus*	0.17	0.12	0.00	13.74	85.21	0.12	1.51	148.84	0.15
ROC	High-Se	800	*Desmognathus fuscus*	0.29	0.21	0.00	3.29	118.59	0.25	3.21	80.59	0.14
ROC	High-Se	1600	*Desmognathus fuscus*	0.17	0.10	0.26	4.91	98.59	0.12	3.92	75.39	0.14
ROC	High-Se	1600	*Desmognathus fuscus*	0.29	0.10	0.28	4.64	153.32	0.15	4.01	122.63	0.29
ROC	High-Se	1600	*Desmognathus fuscus*	0.08	0.05	0.23	3.30	77.65	0.09	2.99	115.88	0.10
ROC	High-Se	0	*Desmognathus monticola*	0.14	0.10	0.05	5.13	82.79	0.12	1.73	104.40	0.02
ROC	High-Se	0	*Desmognathus monticola*	36.91	32.30	51.49	41.22	166.03	18.87	7.06	137.29	0.34
ROC	High-Se	400	*Desmognathus monticola*	0.15	0.12	0.00	21.22	99.95	0.15	1.60	220.01	0.11
ROC	High-Se	400	*Desmognathus monticola*	0.20	0.15	0.06	17.03	78.54	0.11	2.96	69.22	0.08
ROC	High-Se	400	*Desmognathus monticola*	0.10	0.05	0.00	3.59	61.83	0.05	4.49	94.66	0.02
ROC	High-Se	800	*Desmognathus monticola*	0.64	0.19	0.31	4.35	81.38	0.22	2.54	58.35	0.17
ROC	High-Se	800	*Desmognathus monticola*	0.22	0.16	0.31	7.13	100.87	0.16	3.85	80.72	0.19
ROC	High-Se	800	*Desmognathus monticola*	0.31	0.21	0.20	6.20	75.16	0.32	4.33	86.28	0.08
ROC	High-Se	800	*Desmognathus monticola*	0.38	0.44	0.61	14.56	120.56	0.17	2.07	95.17	0.13
ROC	High-Se	1200	*Desmognathus monticola*	0.66	0.72	1.27	14.25	112.27	0.56	2.29	177.97	0.18
ROC	High-Se	1200	*Desmognathus monticola*	0.37	0.21	0.43	10.39	108.48	0.42	3.65	153.13	0.07
ROC	High-Se	1200	*Desmognathus monticola*	0.50	0.23	0.60	4.56	99.05	0.19	5.53	86.20	0.38
ROC	High-Se	1600	*Desmognathus monticola*	0.45	0.30	0.55	7.33	92.50	0.31	6.02	122.85	0.10
ROC	High-Se	1600	*Desmognathus monticola*	0.23	0.10	0.36	4.50	87.79	0.17	9.65	122.20	0.13
ROC	High-Se	0	*Eurycea cirrigera*	0.31	0.31	0.28	3.26	146.43	0.11	3.45	277.35	0.10

		Distance		Trace element concentrations (µg/g dry wt)								
Site ID	Site Type	downstream (m)	media type	Cr	Co	Ni	Cu	Zn	As	Se	Sr	Cd
ROC	High-Se	0	leaf detritus	27.21	1.5	7.33	10.13	53.1	0.65	11.91	316.92	0.23
ROC	High-Se	400	leaf detritus	8.16	1.02	4.93	10.6	27.93	0.65	13.53	312.25	0.11
ROC	High-Se	800	leaf detritus	7.29	1.16	6.26	11.48	42.31	0.47	12.13	305.83	0.13
ROC	High-Se	1200	leaf detritus	32.08	1.33	10.9	12.57	44.08	0.41	13.18	298.6	0.11
ROC	High-Se	1600	leaf detritus	25.56	1.34	15.51	13.45	83.46	0.46	15.09	327.17	0.22
ROC	High-Se	1200	Lepomis macrochirus	0.08	0.16	0.55	3.25	127.5	0.07	7.91	284.97	0.11
ROC	High-Se	1200	Lepomis macrochirus	0.18	0.28	0.26	5.5	100.14	0.05	11.77	185.46	0.02
ROC	High-Se	1600	Luxilus albeolus	0.08	0.04	0.15	1.85	287.23	0.07	6.92	245.43	0.06
ROC	High-Se	1600	Luxilus albeolus	0.14	0.08	0.34	4.35	273.99	0.09	9.7	186.88	0.16
ROC	High-Se	1600	Luxilus albeolus	0.1	0.05	0.16	2.13	377.9	0.03	7.75	220.82	0.14
ROC	High-Se	1600	Luxilus albeolus	0.11	0.13	0.26	4.73	417.22	0.13	9.35	429.8	0.13
ROC	High-Se	1600	Luxilus albeolus	0.1	0.12	0.27	3.22	516.66	0.18	10.63	402.86	0.12
ROC	High-Se	1600	Luxilus albeolus	0.07	0.13	0.34	6.5	320.73	0.16	11.44	187.64	0.26
ROC	High-Se	1600	Luxilus albeolus	0.18	0.1	0.24	3.2	349.9	0.12	7.38	425.68	0.09
ROC	High-Se	0	predator BMI	0.53	0.8	1.84	27.41	211.5	0.36	18.74	38.78	0.28
ROC	High-Se	400	predator BMI	0.45	0.41	0.56	21.77	211.74	0.25	13.58	33.1	0.12
ROC	High-Se	800	predator BMI	0.84	0.68	1.92	23.69	262.43	0.31	16.94	45.21	0.24
ROC	High-Se	1200	predator BMI	0.75	0.79	2.55	31.64	377.37	0.28	22.14	103.19	0.4
ROC	High-Se	1600	predator BMI	0.92	0.7	2.08	25.19	236.71	0.3	17.35	60.67	0.23
ROC	High-Se	400	primary consumer BMI	4.38	3.1	6.14	35.64	180.76	1.6	20.85	78.06	0.57
ROC	High-Se	800	primary consumer BMI	2.8	2.54	6.1	33.36	185.25	1.25	23.32	80.73	0.49
ROC	High-Se	1200	primary consumer BMI	2.2	2.37	7.65	31.36	207.98	1.14	28.63	74.23	0.42
ROC	High-Se	1600	primary consumer BMI	3.47	3.03	9.4	43.79	216.59	1.3	26.01	79.8	0.63
ROC	High-Se	1200	Rhinichthys atratulus	0.1	0.05	4.5	3.24	190.11	0.1	10.56	317.78	0.12
ROC	High-Se	0	sediment	0.07	0.03	0.1	1.05	16.92	0.02	0.73	16.56	0.01
ROC	High-Se	400	sediment	7.51	7.83	13.5	9.69	50.33	4.48	1.81	30.85	0.09
ROC	High-Se	800	sediment	9.48	8.1	14.82	10.49	50.87	5.07	1.94	32.54	0.1
ROC	High-Se	1200	sediment	10.73	9.38	19.9	12.28	70.38	3.86	2.26	19.68	0.11
ROC	High-Se	1600	sediment	7.91	6.83	13.82	9.46	47.63	3.53	1.38	13.55	0.07
ROC	High-Se	800	Semotilus atromaculatus	0.07	0.04	0.45	16.11	140.47	0.03	9.26	326.98	0.08
ROC	High-Se	800	Semotilus atromaculatus	0.21	0.08	0.06	30.88	103.24	0.01	16.36	213.99	0.34
ROC	High-Se	800	Semotilus atromaculatus	0.05	0.04	0.48	3.94	121.66	0.03	7.95	307.68	0.03
ROC	High-Se	800	Semotilus atromaculatus	0.1	0.04	0	4.23	150.2	0.02	12.06	263.26	0.03
ROC	High-Se	1200	Semotilus atromaculatus	0.08	0.05	0.39	3.49	113.03	0.03	4.81	186.25	0.02
ROC	High-Se	1200	Semotilus atromaculatus	0.07	0.43	0.08	5.51	120.34	0.04	7.01	252.46	0.04
ROC	High-Se	0	Tipula	2.65	5.36	13.13	22.28	134.76	2.03	29.89	50.11	0.25
ROC	High-Se	400	Tipula	2.28	7.91	16.16	21.17	115.9	1.59	26.67	47.44	0.16
ROC	High-Se	800	Tipula	3.07	6.09	15.16	23.58	119.29	1.5	33.14	45.11	0.19
ROC	High-Se	1200	Tipula	3.41	6.91	29.51	27.21	158.07	1.77	35.69	67.72	0.24
ROC	High-Se	1600	Tipula	3.08	5.02	18.26	27.45	148.89	1.61	28.86	43.83	0.2

Table E-7: Water column trace element concentrations at all study streams.

				Cr	Co	Ni	Cu	Zn	As	Se	Sr	Cd
				µg/L	µg/L	µg/L	µg/L	µg/L	µg/L	µg/L	µg/L	µg/L
		distance	MDL	0.01	0.01	0.12	0.10	0.24	0.02	0.07	0.01	0.01
Site ID	site type	downstream (m)	MRL	0.20	0.10	5.00	2.00	5.00	0.10	0.50	0.10	0.10
EAS	ref	0		0.04	<MDL	0.13	<MDL	9.27	0.03	<MDL	6.06	<MDL
EAS	ref	400		0.04	<MDL	<MDL	<MDL	9.36	0.04	<MDL	7.12	<MDL
EAS	ref	800		0.05	<MDL	<MDL	<MDL	10.12	0.04	<MDL	8.65	<MDL
EAS	ref	1200		0.15	0.02	0.14	0.13	8.41	0.09	<MDL	7.6	<MDL
HCN	ref	0		0.04	0.09	0.17	0.29	8.32	0.18	<MDL	40.19	<MDL
HCN	ref	400		0.04	0.06	0.18	0.34	7.57	0.14	<MDL	26.62	<MDL
HCN	ref	800		0.05	0.04	0.19	0.31	7.88	0.13	<MDL	28.08	<MDL
HCN	ref	1200		0.04	0.05	0.17	0.34	6.75	0.12	<MDL	26.86	<MDL
HCN	ref	1600		0.07	0.08	0.37	0.38	7.13	0.13	<MDL	28.70	<MDL
CRA	low-Se	0		0.06	1.01	4.25	0.36	17.74	0.03	0.45	1124.74	0.03
CRA	low-Se	400		0.05	0.53	2.80	0.21	12.12	0.04	0.36	1056.90	0.02
CRA	low-Se	800		0.03	0.15	1.96	0.16	12.08	0.04	0.39	1003.63	0.01
CRA	low-Se	1200		0.04	0.05	1.40	0.15	13.25	0.04	0.36	939.37	0.01
CRA	low-Se	1600		0.03	0.05	1.02	0.14	10.71	0.06	0.42	874.28	0.01
FRY	low-Se	0		0.04	0.02	0.16	0.22	11.41	0.16	0.37	334.51	<MDL
FRY	low-Se	400		0.06	0.03	0.17	0.22	11.96	0.17	0.30	347.87	<MDL
FRY	low-Se	800		0.05	0.03	<MDL	0.26	13.70	0.20	0.43	390.72	<MDL
FRY	low-Se	1200		0.04	0.03	<MDL	0.16	10.20	0.20	0.43	404.30	<MDL
LLC	high-Se	0		0.04	0.42	3.28	0.16	10.35	0.08	7.05	1890.51	0.02
LLC	high-Se	400		0.04	0.13	2.02	0.12	9.82	0.09	7.06	1876.16	<MDL
LLC	high-Se	800		0.05	0.16	1.42	0.16	12.90	0.08	6.25	1784.01	<MDL
LLC	high-Se	1200		0.05	0.08	1.00	0.16	10.22	0.09	6.61	1761.87	<MDL
LLC	high-Se	1600		0.05	0.08	0.93	0.13	7.22	0.09	6.20	1722.75	<MDL
ROC	high-Se	0		0.07	0.08	0.28	0.41	12.12	0.24	9.11	1954.67	<MDL
ROC	high-Se	400		0.07	0.18	0.38	0.46	10.43	0.24	9.08	1888.01	<MDL
ROC	high-Se	800		0.09	0.09	0.38	0.43	12.25	0.25	8.96	1866.86	<MDL
ROC	high-Se	1200		0.09	0.08	0.48	0.42	8.79	0.25	8.85	1812.39	<MDL
ROC	high-Se	1600		0.08	0.08	0.47	0.44	10.89	0.25	8.30	1725.78	<MDL

APPENDIX F - LONGITUDINAL GRADIENT SELENIUM CONCENTRATION

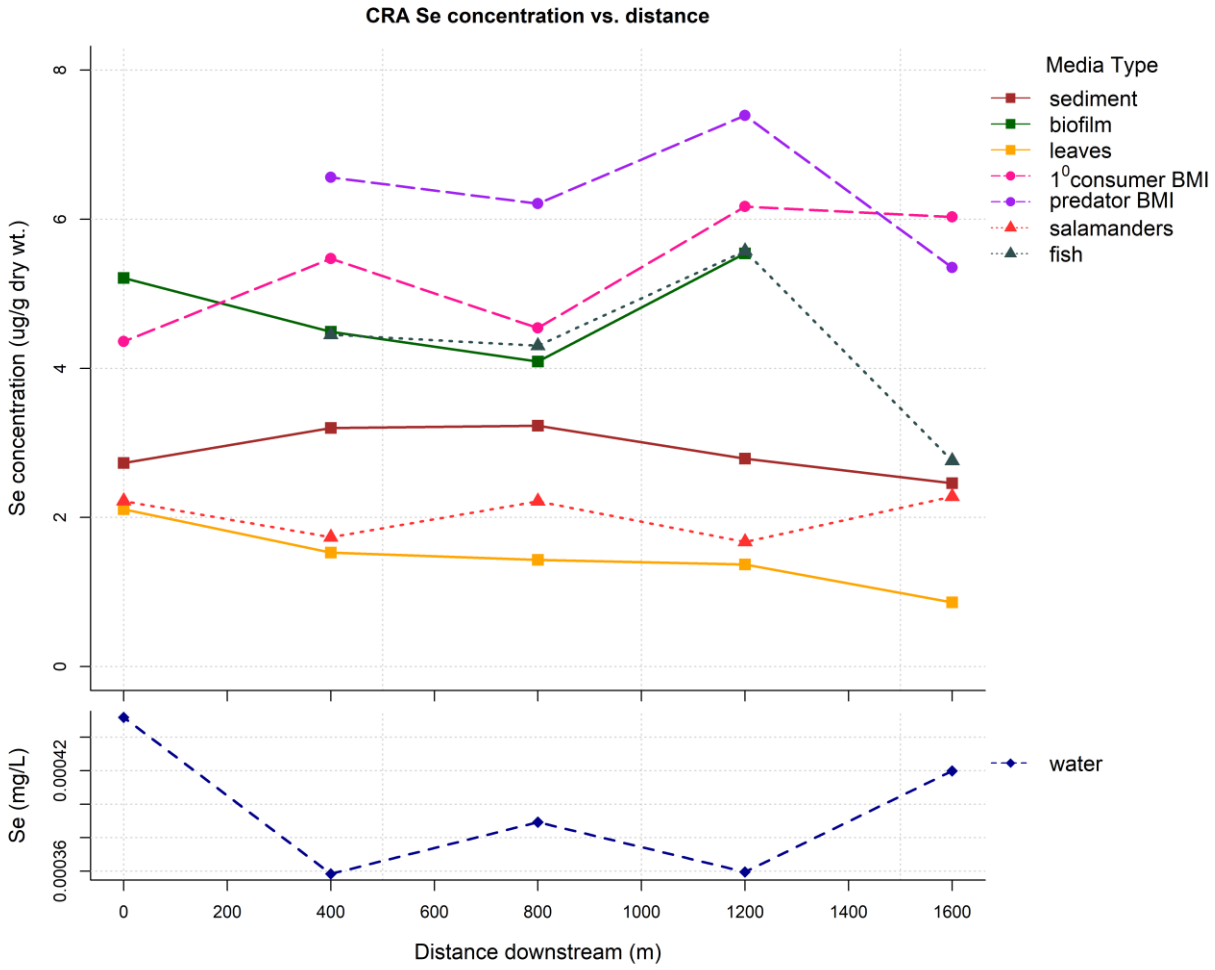

Figure F-1: Selenium concentrations going downstream in the low-Se stream CRA. Top: Selenium concentrations in ecosystem media (particulate-fish). Bottom: Selenium concentration in the water column.

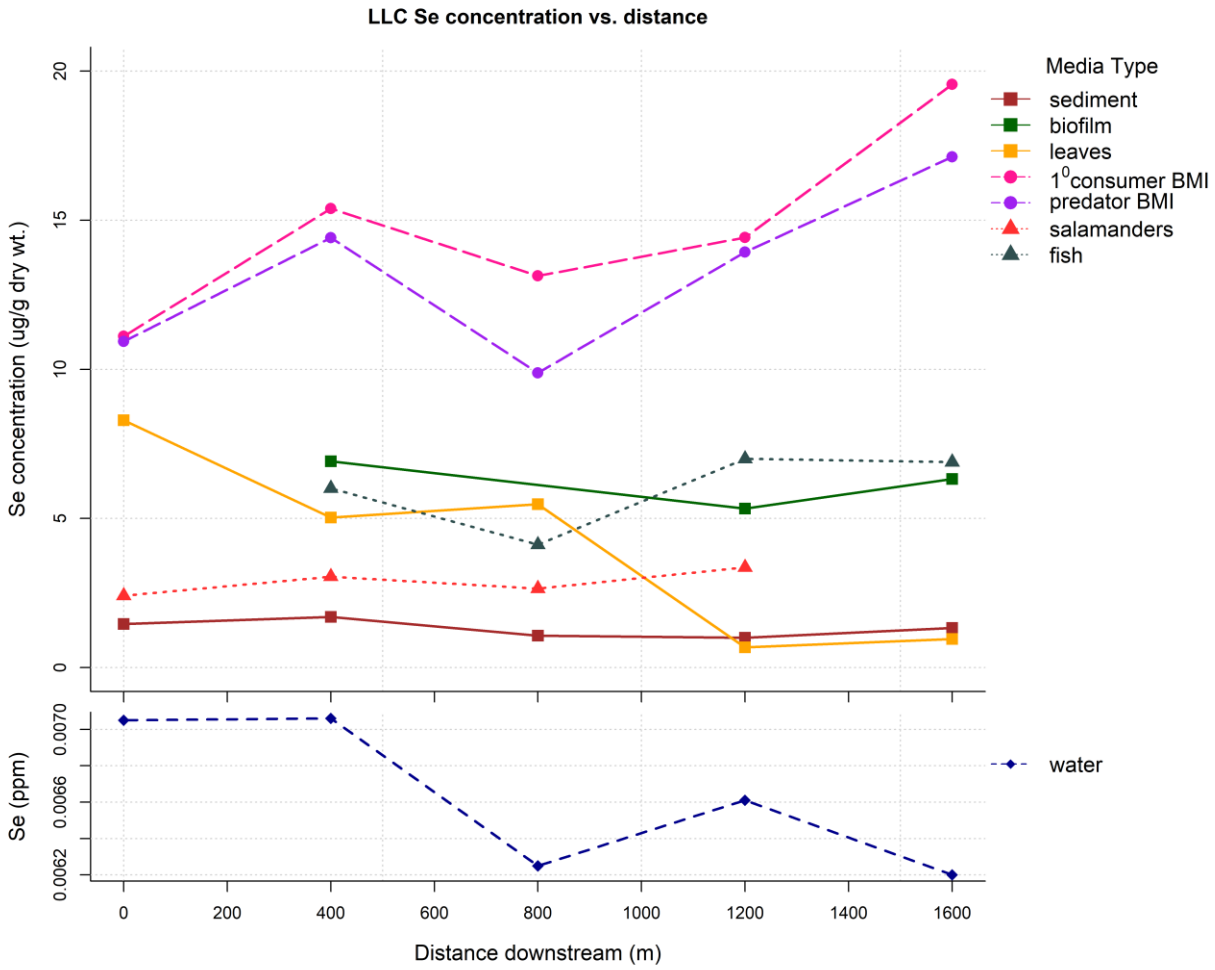

Figure F-2: Selenium concentrations going downstream in the high-Se stream LLC. Top: Selenium concentrations in ecosystem media (particulate-fish). Bottom: Selenium concentration in the water column.

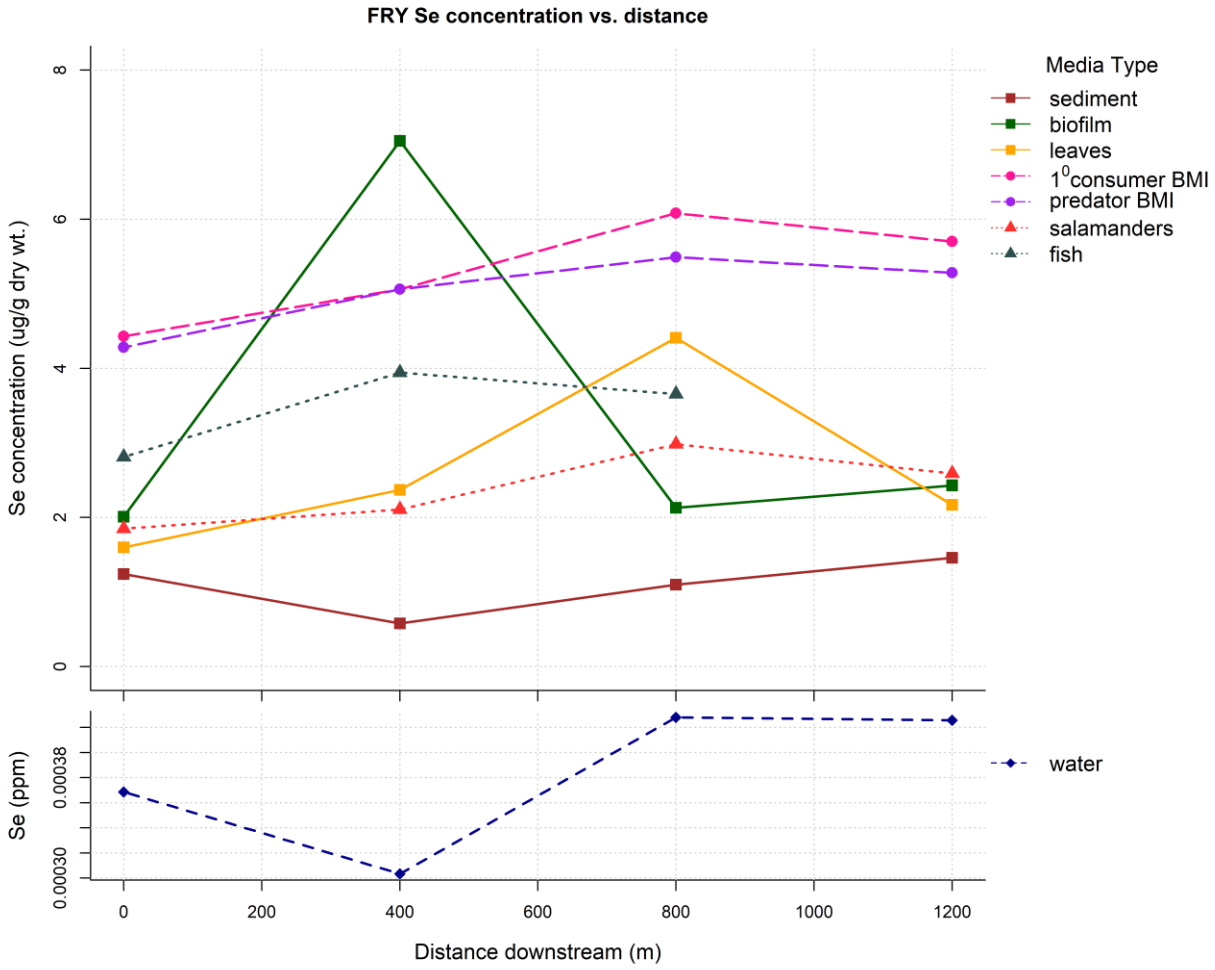

Figure F-3: Selenium concentrations going downstream in the low-Se stream FRY. Top: Selenium concentrations in ecosystem media (particulate-fish). Bottom: Selenium concentration in the water column.

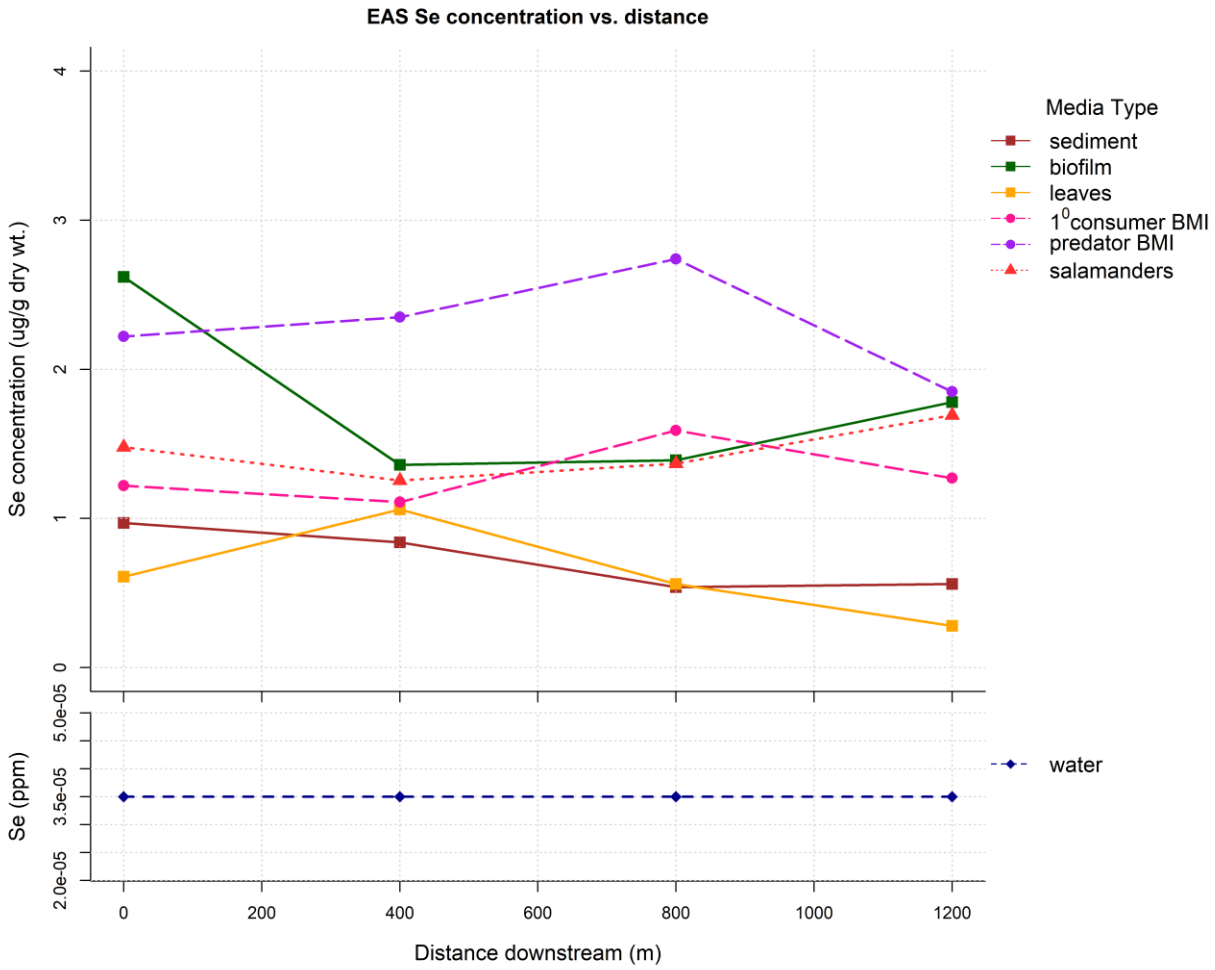

Figure F-4: Selenium concentrations going downstream in the reference stream EAS. Top: Selenium concentrations in ecosystem media (particulate-fish). Bottom: Selenium concentration in the water column.

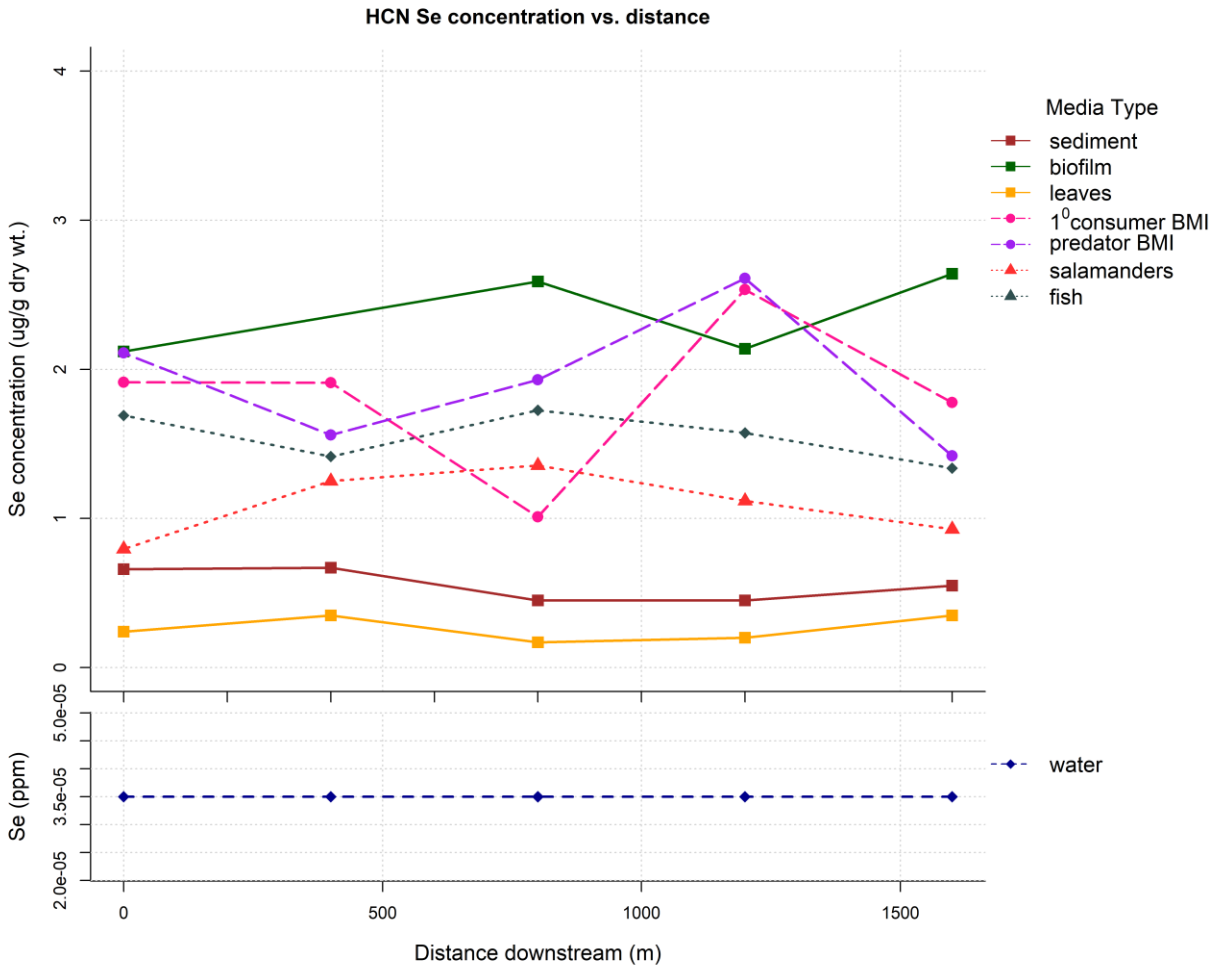

Figure F-5: Selenium concentrations going downstream in the reference stream HCN. Top: Selenium concentrations in ecosystem media (particulate-fish). Bottom: Selenium concentration in the water column.

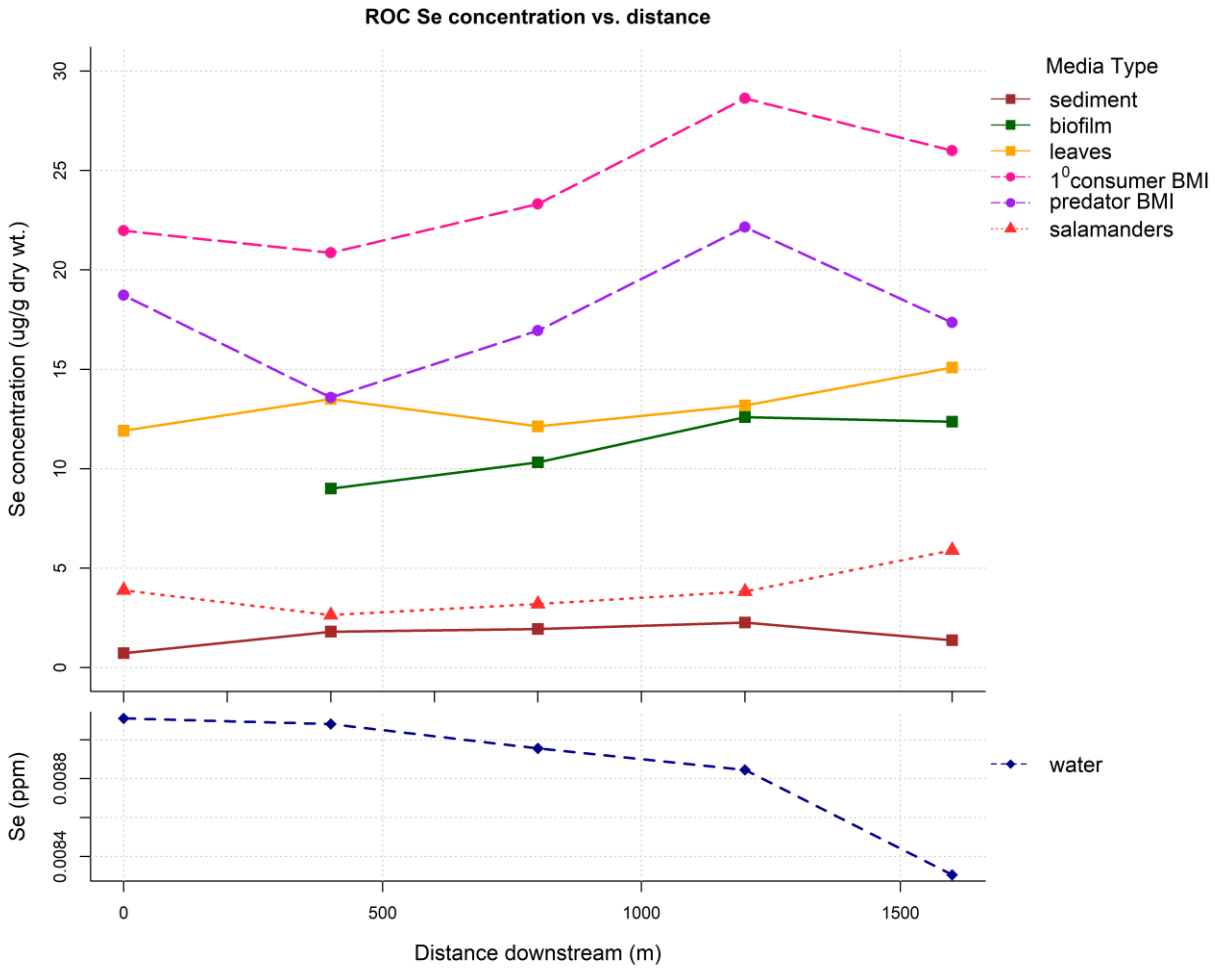

Figure F-6: Selenium concentrations going downstream in the high-Se stream ROC. Top: Selenium concentrations in ecosystem media (particulate-fish). Bottom: Selenium concentration in the water column.

APPENDIX G - TEMPORAL VARIATION IN WATER COLUMN SELENIUM

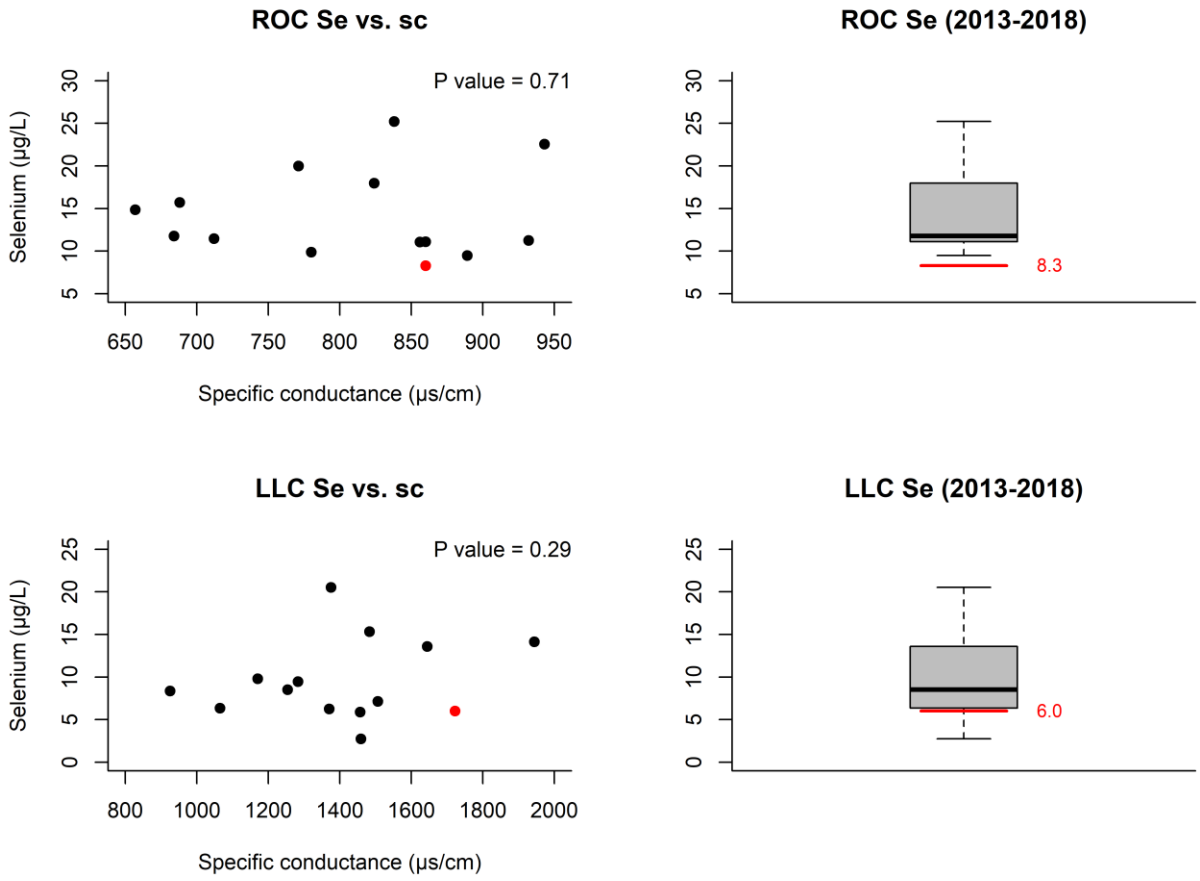

Figure G-1: Water column Se measurements at the two high-Se streams (ROC top; LLC bottom) taken during seasonal sampling (Fall, Spring) of benthic macroinvertebrates, ion matrix, and specific conductance from 2013-2018. Red dots on the left figures and red lines on the right boxplots correspond to measurements taken when media was collected in summer 2018.